Functional and Molecular Characterization of Tolerized Langerhans Cells in Atopic Dermatitis

Mechanistic Insights into the TLR2-NF-κB Signaling Pathway

Doctoral thesis

to obtain a doctorate (MD/PhD)

from the Faculty of Medicine

of the University of Bonn

Yuxuan Deng

from Hunan, PR. China

2025

Written with authorization of

the Faculty of Medicine of the University of Bonn

First reviewer: Prof. Dr. Dr. Prof. h. c. Thomas Bieber

Second reviewer: Prof. Dr. Irmgard Förster

Day of oral examination: 09.25.2025

From the Department of Dermatology and Allergy, University Hospital Bonn, Germany

Table of Contents

List of abbreviations

- APC	Allophycocyanin
7-AAD	7-amino-actinomycin D
Ab	Antibody
AB/AM	Antibiotic-antimycotic
AD	Atopic dermatitis
AhR	The aryl-hydrocarbon receptor
Amp	Amplicon
APC	Antigen presenting cell
ATF3	Activating transcription factor 3
Bcl-3	B-cell CLL/lymphoma 3
BMDCs	Bone marrow-derived dendritic cells
BSA	Bovine serum albumin
CCR6	C-C motif chemokine receptor 6
CCR7	C-C motif chemokine receptor 7
CD34LC	CD34+ hematopoietic stem cell derived LC
cDNA	Complementary DNA
CYLD	Cylindromatosis protein
d	Day
DAMPs	Damage-associated molecular pattern molecules
DC	Dendritic cells
DMSO	Dimethyl sulfoxide
DNA	Deoxyribonucleic acid
dNTP	Deoxyribonucleotide triphosphate
DTT	1,4-dithiothreitol
e.g.	Exempli gratia, for example
EDTA	Ethylenediaminetetraacetic acid
et al.	Et alii, and others
ETA	Exfoliative toxin A
FACS	Fluorescence activated cell sorter

FCS	Fetal calf serum
FcεRI	High affinity IgE receptor
FITC	Fluorescein-5-isothiocyanat
FLG	The filaggrin gene
FLT3L	Fms like tyrosine kinase 3 ligand
FSL-1	Pam2CGDPKHPKSF, lipoprotein
gam	Goat anti-mouse
GM-CSF	Granulocyte-macrophage colony-stimulating factor
h	Hour
H4R	Histamine receptor 4
HCl	Hydrochloric acid
HSV	herpes simplex virus
IDEC	Inflammatory dendritic epidermal cells
IDO	Indoleamine 2,3-dioxygenase
IFN	Interferon
IFN-α	Interferon-alpha
Ig	Immunoglobulin
IgE	Immunoglobulin E
IgG	Immunoglobulin G
IKK	IκB kinase
IL	Interleukin
ILC2s	Group 2 innate lymphoid cells
IRAK	Interleukin-1 receptor-associated kinase
IRFs	Interferon regulatory factors
JAK	Janus kinase
JAKi	Janus kinase inhibitors
KC	Keratinocytes
kDa	Kilo Dalton
L	Liter
LB	Luria broth (complex medium)
LC	Langerhans cell

LPS	Lipopolysaccharides
LTA	Lipoteichoic acid
M	Mol
mAb	Monoclonal antibody
MACS	Magnetic activated cell sorter
max	Maximum
M-CSFR	Macrophage colony-stimulating factor receptor
MFI	Mean fluorescence intensity
MHC II	Major histocompatibility complex class II
Milli-Q	Ultrapure water (type I)
min	Minute
miRNA	Micro-RNA
mRNA	Messenger RNA
n.s.	Not specified
N/A	Not applicable
NLRX1	NLR family member X1
Pam3Cys	Pam3CSK4, Pam3Cys-Ser-(Lys)4 trihydrochloride
PAMP	Pathogen associated molecular pattern
PBMC	Peripheral blood mononuclear cells
PCR	Polymerase chain reaction
PDE4	Phosphodiesterase 4
PE	Phosphatidylethanolamine
PI3K	Phosphatidylinositol 3-kinase
PRRs	Pattern recognition receptors
qPCR	Quantitative polymerase chain reaction
RBP	RNA binding protein
rFI	Relative fluorescence index
RNA	Ribonucleic acid
RT	Room temperature
s	Second
S. a.	Staphylococcus aureus

SCF	Stem cell factor
SCORAD	SCORing AD
SD	Standard deviation
SOCS1	Suppressor of cytokine signaling 1
TCI	Topical calcineurin inhibitor
TCR	T cell receptor
TCS	Topical corticosteroids
TE	Transfection efficiency
TGF-ß	Transforming growth factor beta
Th	T helper
TLR	Toll-like receptor
TNF-α	Tumor necrosis factor alpha
TOLLIP	Toll-interacting protein
TRAF6	Tumour-necrosis factor-receptor-associated factor 6
Treg	Regulatory T cell
Tris	Tris(hydroxymethyl-)aminomethan
Trm	Memory T cells
TSLP	Thymic stromal lymphopoietin
UTR	Untranslated region

1. Introduction

Atopic dermatitis (AD) is the most common chronic inflammatory and recurrent skin disease. The pathogenesis is linked to genetics, immunity, as well as interactions with the environment. Epidermal Langerhans cell (LC), the primary antigen-presenting dendritic cell (DC) in the epidermis, serve as crucial intermediaries between the innate and adaptive immune systems, e.g. by detecting microbial signals through various pattern recognition receptors (PRR). Among these PRRs, Toll-like receptors (TLR) are well-established on antigen-presenting cell (APC), sensing both intracellular and extracellular pathogens. This recognition triggers LC activation, cytokine production, and the subsequent T-cell response. TLR2 has been pinpointed to be sensing *Staphylococcus aureus* (*S. a.*) from the skin microbiota, which is colonized in high proportion in AD skin compared to health, and is suspected to be involved in the complex pathophysiology of this disorder.

This study explores the molecular and functional properties of LC in the context of the TLR2 signaling pathway in AD, shedding light on the associated underlying mechanisms governing these cells.

1.1 Dendritic cells and Langerhans cells

DC are a heterogeneous group of APC with pivotal roles governing innate and adaptive immune responses(Liu and Nussenzweig, 2010; Merad et al., 2013). Langerhans cells are a specialized type of DC that primarily resides in the epidermis, the outermost layer of the skin, which is essential component of the skin's immune system(Deckers et al., 2018; Merad et al., 2008; Romani et al., 2012).

1.1.1 Dendritic cells

DC, as the primary class of APC in the human immune system, play a fundamental role in initiating and regulating immune responses, thereby contributing to the maintenance of immunological balance (Banchereau and Steinman, 1998). Beyond their function in stimulating immune responses, DC also participate in establishing and preserving immune tolerance. This discovery underscored their dual role as central regulators of both protective immune responses and tolerance. Steinman and colleagues in 1973 marked a turning point, as it revealed DC' remarkable ability to activate T lymphocytes. DC phagocytize self and foreign structures such as pathogens and toxic proteins, degrade them into small fragments, and present these antigens on MHC II receptor molecules to naïve T cells. During activation, DC become mature and thereby upregulate CD83 and

other costimulatory receptor molecules, such as CD86, CD80, and CD40, on their cell surface. This maturation process involves the synthesis of various molecules and functional alterations in the DC. Mature DC migrate from peripheral tissues to lymph nodes or the spleen, presenting antigens to T cells and thus activating their differentiation into pro- or anti-inflammatory populations (Cabeza-Cabrerizo et al., 2021; Liu and Nussenzweig, 2010; Merad et al., 2013; Solano-Gálvez et al., 2018).

1.1.1.1. DC's subtypes

DC are a dynamic group of APC crucial to the immune system, and their classification into distinct subsets has unveiled their diverse roles. These subsets encompass two main subgroups: Conventional DC (cDC), also called myeloid DC (mDC), and plasmacytoid DC (pDC), along with further subtypes like monocyte-derived DC (moDC), migratory dermal CD14+ DC, epidermal Langerhans cells (LC) (details in 1.1.2 Langerhans cells), and inflammatory dendritic epidermal cells (IDEC). Each of these subsets exhibits distinct phenotypic and functional characteristics, contributing to the intricacies and adaptability of the immune response(Liu and Nussenzweig, 2010; Merad et al., 2013, 2008; Solano-Gálvez et al., 2018).

Plasmacytoid DC (pDC): pDC are present in circulation and peripheral lymphoid organs, originating from bone marrow hematopoietic stem cells, constituting < 0.4% of PBMC in health. pDC are vital for defending against viral infections and regulating immune responses. Distinguished by substantial IFN-α production upon detecting viral RNA and DNA, they initiate a robust antiviral defense. Despite being relatively scarce in healthy tissues, pDC comprise around 50% of the total DC population in the blood, making them readily available to respond to tissue specific or systemic threats. Based on these, pDC play dual roles in immune responses, either promoting or suppressing reactions based on specific cytokine production. Their interactions with various immune cells, including NK cells, are crucial for coordinating effective immune defenses(Gardner et al., 2020; Merad et al., 2013; Solano-Gálvez et al., 2018).

Conventional DC (cDC)/ Myeloid DC (mDC): cDC are a major subset of DC found in both lymphoid and nonlymphoid tissues. Originating from precursors known as pre-cDC and originating in the bone marrow, cDC subsequently migrate to the bloodstream before seeding various tissues. Their *in-vitro* differentiation hinges on the presence of GM-CSF and Flt3L. Key marker expression includes CD1a, CD11c, CD13, and CD33, while lacking

CD14 or CD16 expression. In tissue, they detect injuries and adeptly capture various environmental and cell-associated antigens, processing and presenting them to T cells, which is a pivotal step in launching adaptive immune responses. cDC diversity extends to two subsets: cDC1 and cDC2, each boasting distinct characteristics and spatial distribution in various tissues. This diversity allows cDC to respond effectively to various immune challenges (Gardner et al., 2020; Merad et al., 2013; Solano-Gálvez et al., 2018).

Monocyte-derived DC (moDC): moDC represent a distinct subset of DC that arise from monocytes and are found in various tissues. A hallmark of moDC is their differentiation from monocytes, particularly under inflammatory conditions involving $CD14^{hi}$ monocytes in humans. Additionally, cells within inflammatory tissues expressing CD11c, CD1a, and CD14 are considered to derive from monocytes as moDC. The difference with cDC is that moDC does not transport antigens to lymph nodes for T cell activation. Their functions are related to inflammatory responses and anti-tumor activities. Moreover, moDC enhance the survival of adoptively transferred T cells and regulate T cell activity by producing TNF-α and NOS2, particularly within tumor immune conditions(Gardner et al., 2020; Liu et al., 2021; Solano-Gálvez et al., 2018).

Dermal CD14+ DC: CD14+ DC represent a distinct subset of DC that are characterized by their expression of CD14, a surface marker typically associated with monocytes. Unlike the moDC with $CD14^{low\ /\ negative}$ expression, CD14+ DC have explicitly been located in the dermal region of various tissues. CD14+ DC exhibit an intermediate phenotype, sharing similarities with both DC and monocytes/macrophages. These specialized DC participate in various critical immunological activities. They are known to contribute to the formation of follicular helper T cells, play a role in the induction of antibody-secreting B cell differentiation, and promote regulatory T cell responses. CD14+ DC have been identified in various tissues, including the skin, lymphoid, and non-lymphoid tissues. Upon stimulation, they secrete cytokines such as IL-1β, IL-6, IL-8, and IL-10, highlighting their involvement in immune responses. While the exact migratory behavior of CD14+ DC to lymph nodes remains under investigation, their presence in lymph node samples suggests potential migration from the blood (Liu and Nussenzweig, 2010; Merad et al., 2013; Solano-Gálvez et al., 2018).

Inflammatory Dendritic Epidermal Cells (IDEC): IDEC have been identified for the first time in inflammatory skin of AD where they play an essential role. They constitute a distinct

subset of DC that tissue response to inflammatory or microbial triggers. Their pivotal role in coordinating immune responses within inflamed tissues, particularly in the skin's immune environment, underscores their significance. IDEC exhibit a unique capacity to generate pro-inflammatory cytokines and chemokines, influencing the local immune milieu during inflammation. Despite sharing phenotypic markers with dermal cDC2 and moDC, the absence of specific surface markers dedicated to IDEC contributes to the challenge of distinguishing them from these related cell populations. The phenotype and characteristics of IDEC prove to be influenced by various factors, including the nature of the inflammatory stimulus, the tissue of origin, and the specific time point of analysis. For instance, IDEC exhibit responsiveness to LPS, undergoing migration and accumulation in lymph nodes. Their involvement in these conditions highlights the diverse and context-dependent functions of IDEC within the intricate network of skin immune responses(Bieber et al., 2011; Kashem et al., 2017; Merad et al., 2013; Novak, 2012; Otsuka et al., 2018; Said and Weindl, 2015).

Tolerogenic DC: DC also contribute significantly to the induction and maintenance of immune tolerance. Tolerogenic DC possess unique characteristics that distinguish them from their immunogenic counterparts. They exhibit a state of immaturity and resistance to maturation signals. This immaturity is evident in their low expression of co-stimulatory molecules, such as CD80 and CD86, which are crucial for T-cell activation. This lower co-stimulatory-to-inhibitory signal ratio is a critical factor in promoting immune tolerance. Additionally, tolerogenic DC reduced to produce pro-inflammatory cytokines like TNF-α,IL-1β, IL-6, IL-12(Mbongue et al., 2017), this diminished cytokine production further underscores their role in immune regulation (Fucikova et al., 2019; Kashem et al., 2017; Mbongue et al., 2017; Morelli and Thomson, 2007; Novak et al., 2010; Solano-Gálvez et al., 2018). Tolerogenic DC also play a central role in the expansion and induction of Tregs, specialized T cells known for their immunosuppressive functions. These DC facilitate the development of Tregs, enabling the suppression of T cells recognizing alloantigens through both direct and indirect pathways. Furthermore, the function of tolerogenic DC can be influenced by the unique microenvironment in specific tissues. DC can acquire tolerogenic properties in certain tissues due to the specified environment. Additionally, *in vitro*, tolerogenic DC can be generated or modulated by exposure to various immunomodulatory agents, including IL-10, TGF-β, and other anti-inflammatory and

immunosuppressive factors (Fucikova et al., 2019; Kashem et al., 2017; Mbongue et al., 2017; Morelli and Thomson, 2007; Novak et al., 2010; Solano-Gálvez et al., 2018).

1.1.1.2. Function of DC

DC have multiple functions in the immune system.

I. Sensing and antigen capture: Sensing is an integral facet of the immune system and encompasses the intricate processes by which specialized immune cells, particularly DC, detect and respond to potential threats within the body. At the forefront of the immune system's defense, DC act as vigilant sentinels strategically positioned in various tissues, ready to sense and respond to any signs of trouble. Their ability to sense is supported by an extensive array of pattern recognition receptors (PRRs), such as TLR. PRRs serve as the immune system's early warning system, detecting a wide range of pathogen-associated molecular patterns (PAMPs) or damage-associated molecular patterns (DAMPs) (Cabeza-Cabrerizo et al., 2021; Mbongue et al., 2017; Solano-Gálvez et al., 2018).

Upon sensing a threat, DC are either on place (resident DC) or actively migrate to the source, employing specialized chemotactic mechanisms. During this migration, they capture antigens using mechanisms such as phagocytosis, receptor-mediated endocytosis, and pinocytosis. This crucial antigen-capture process allows DC to internalize pathogens, cellular debris, and other immunologically relevant molecules. The significance of antigen capture lies in its critical link between innate and adaptive immune responses. After capturing antigens, DC process and present them to T cells. This presentation is essential for instructing T cells to mount specific immune responses against the recognized antigens (Cabeza-Cabrerizo et al., 2021; Mbongue et al., 2017; Solano-Gálvez et al., 2018).

II. Maturation (Activation) of DC: DC maturation is a crucial process in the immune system, representing a remarkable transformation that enables these cells to play their pivotal role in orchestrating immune responses. During the core of DC maturation, their transition from an immature state, primarily focused on antigen capture and immune surveillance, to a mature state that activates and instructs T cells, initiating adaptive immune responses. This transformation is triggered by specific signals that DC receive upon encountering pathogens or tissue damage (Cabeza-Cabrerizo et al., 2021; Liu et al., 2021; Mbongue et al., 2017; Novak et al., 2010; Solano-Gálvez et al., 2018).

One of the hallmark changes during maturation is the upregulation of MHC II molecules on the cell surface, which allows DC to present processed antigens to T cells, a fundamental process in adaptive immunity. DC also increase the expression of co-stimulatory molecules like CD80 and CD86. These molecules serve as activation signals for T cells, ensuring the initiation of an immune response. Cytokines also play a significant role during maturation. DC secrete various cytokines, including a series of interleukins and TNF-α, which influence the differentiation and function of T cells and other immune cells. This secretion helps tailor the immune response to the specific antigen encountered. Mature DC are highly dynamic and migratory. With elevated expression of chemokine receptors such as CCR7, they journey from peripheral tissues to draining lymphoid organs. Maturated DC are pivotal in presenting antigens to T cells in these lymph nodes, effectively triggering the adaptive immune response (Cabeza-Cabrerizo et al., 2021; Liu et al., 2021; Mbongue et al., 2017; Novak et al., 2010; Solano-Gálvez et al., 2018).

III. Cytokine production and induction of the differentiation of naïve T cells: DC are central CD4+ Th cell differentiation regulators, influencing various Th cell subsets, including Th1, Th2, Th17 and Tregs.

Th1 cell differentiation: DC' ability to produce high levels of IL-12 is a pivotal cytokine driving Th1 differentiation(Jasani et al., 2009). The TLR expressed by DC induce them with the capacity to sense pathogens, initiating a cascade of events culminating in Th1 polarization. Furthermore, the strength and duration of T cell receptor (TCR) activation determinant DC-mediated Th1 differentiation. The cooperative involvement of distinct APC subsets, including cDC and moDC, contributes to Th1 responses under specific contexts. DC-derived chemokine, like CXCL10, retains developing Th1 cells and facilitates prolonged interactions between DC and T cells in the T cell zone(Reid et al., 2000; Solano-Gálvez et al., 2018; Yin et al., 2021).

Th2 cell differentiation: Th2 immune responses induced by DC play a crucial role in addressing diverse challenges, including helminth infections and allergic phenomena. DC mediate Th2 differentiation through various mechanisms. This includes DC conditioning by the local inflammatory environment such as epithelial-derived TSLP as a key driver for Th2 response as well as by the TCR interactions and the pivotal roles of IL-4 and IL-2, which induce the expression of GATA3, the primary regulator of Th2 transcriptional programming. IL-4 plays crucial role in type 2 immune responses that initiates Th2

differentiation. The DC are indispensable in Th2 differentiation, demonstrated by numerous studies of food allergy, allergic airway inflammation, and chronic helminth infections. Deletion of DC significantly inhibits Th2 cell generation and diminishes type 2 immune responses(Cabeza-Cabrerizo et al., 2021; Mbongue et al., 2017; Yin et al., 2021).

Th17 cell differentiation: DC subsets play a central role in Th17 cell induction, activating latent TGF-β and producing crucial cytokines, including IL-6, IL-23, and IL-1β, essential for differentiating Th17 cells. Additionally, robust stimulation of the TCR on DC also promotes Th17 differentiation. On the other hand, DC contribute to the polarization of T-cell subsets by creating specific cytokine milieus. IL-12 and IL-4, produced by DC, have been shown to prevent Th17 differentiation, indicating a degree of cross-regulation between different T-cell subsets. DC subsets, including LC (details in 1.1.2.3), cDC, and moDC, showed that they play intricate roles in shaping the differentiation and regulation of Th17 cells in specified tissues and models, influencing both immune defense and potential pathogenicity in autoimmune conditions(Cabeza-Cabrerizo et al., 2021; Mbongue et al., 2017; Terhune et al., 2013; Yin et al., 2021).

T regulatory cell (Treg) differentiation: The dual role of DC and Tregs is crucial for immune homeostasis, preventing detrimental autoimmune responses. Specifically, tolerogenic DC possess a unique capacity to secrete anti-inflammatory cytokines such as TGF-β and IL-10, along with mediators like retinoic acid and IDO. These components inhibit pro-inflammatory cytokines produced by T lymphocytes, including IL-2 and IFN-γ, then impact on series immune response. DC finely tunes the delicate balance between pro-inflammatory T cells and immunosuppressive Tregs. Furthermore, tolerogenic DC, induced by surface receptor costimulatory molecules such as CD86, CD80, CD83, and CD40, actively contribute to the induction of Tregs(Kashem et al., 2017; Kushwah and Hu, 2011; Mbongue et al., 2017; Yin et al., 2021).

1.1.2 Langerhans cells

LC are a specialized type of DC that primarily resides in the epidermis, the outermost layer of the skin. Under normal conditions, they constitute 3-5% of epidermal cells. They are named after the German physician Paul Langerhans, who first described their presence in the skin in 1868. LC are essential components of the skin's immune system and play a pivotal role in immune surveillance, antigen presentation, maintaining immune tolerance,

and against bacterial infections in the skin(Deckers et al., 2018; Merad et al., 2008; Romani et al., 2012).

1.1.2.1. Origins and distribution of LC

LC have a unique ontogeny, distinguishing them from other immune cells. LC precursors initially originate from the primitive hematopoiesis in the yolk sac, subsequently migrating to the skin or fetal liver, where they differentiate into fetal monocytes. During embryonic development, these precursor cells lack the typical dendritic LC morphology and the absence of LC markers like MHC II, Langerin, and CD11c. The entire LC network and phenotype are established during the first one or two weeks after birth(Merad et al., 2008; Romani et al., 2012). Under normal, steady-state conditions, LC self-maintain locally through low-level proliferation without a significant contribution from bone marrow. However, during inflammation or when LC are depleted, bone marrow-derived monocytes are recruited to the epidermis via hair follicles and subsequently differentiate into LC. This recruitment and resupply mechanism is part of the complex process that allows LC to adapt to changing conditions and maintain their presence in the epidermis(Atmatzidis et al., 2017; Merad et al., 2008; Romani et al., 2012; Said and Weindl, 2015).

1.1.2.2. Characteristics of LC

LC are characterized by their unique dendritic morphology, featuring extended branching dendrites, enabling efficient antigen capture, recognition, and immune surveillance. They are identified by distinctive Birbeck granules, an intracellular structure unique to LC. LC express specific surface markers like CD1a, CD11c, CD45, FcεR1, MHC II, and CD207 (Langerin), differentiating them from other immune cells and supporting their involvement in antigen presentation and immune responses(Atmatzidis et al., 2017; Merad et al., 2008; Romani et al., 2012). Humans have high CD1a expression, essential for presenting microbial lipid antigens to T cells(Merad et al., 2008). Human LC also express molecules E-cadherin, enhancing adhesion to neighboring keratinocytes, and epithelial cell adhesion molecule (EpCAM), influencing migration by reducing adhesion to keratinocytes(Doebel et al., 2017; Merad et al., 2008). Some markers are shared between murine and human LC, like CD45, MHC II, and langerin (CD207), while Birbeck granules are the unique feature of epidermal LC (Atmatzidis et al., 2017; Merad et al., 2008; Romani et al., 2012).

LC manifests variable performance depending on whether the skin is in a steady state or an inflamed state.

In the steady state: During the steady state, LC maintain their presence in the epidermis through a combination of mechanisms. About 2-3% of LC are actively proliferating in both the mouse and the human epidermis, which aids in preserving their numbers. Cycling LC contribute to maintain LC populations in the epidermal immune network. Additionally, specialized local precursor cells, possibly residing in the bulge region of hair follicles within the dermis, might play a role in replenishing LC. When skin injuries specifically affect the epidermis, such as UV radiation exposure, LC can be repopulated from these hair follicles(Doebel et al., 2017; Kashem et al., 2017; Merad et al., 2008).

In the inflamed state: In inflamed conditions, like skin injury or inflammation, the homeostasis of LC follows a distinct pattern. In contrast to steady-state conditions, inflamed skin exhibits a specific dynamic where LC are reduced, and potential precursor cells are recruited for epidermal repopulation. When LC are depleted due to skin inflammation, circulating monocytes are recruited from the bloodstream to facilitate this restoration. Key players in this mechanism include M-CSFR signaling and chemokine receptors CCR2 and CCR6 expressed by circulating monocytes. These monocytes respond to chemokines released in the skin's blood vessels around and differentiate into LC under the influence of signals from epidermal-dermal junction keratinocytes(Doebel et al., 2017; Merad et al., 2008).

1.1.2.3. Function of LC

LC have a crucial function in antigen presentation, immune responses, and immune tolerance within the skin or the mucosal surfaces, and their unique characteristics and migratory capabilities place them in a critical position to modulate the local immune response(Atmatzidis et al., 2017; Deckers et al., 2018; Doebel et al., 2017; Merad et al., 2008; Romani et al., 2012).

I. LC surveillance to micro-environment of skin:

LC, the sentinel DC, employ their dendritic morphology for continuous surveillance of the environment beyond tight junctions in the epithelial layer. They utilize dynamic behaviors termed "dendritic surveillance extension and retraction cycling habitude" to sample the microenvironment without compromising the barrier's function[28,29]. Upon detecting microbial agents and antigens that breach the skin's outer layer, LC initiate and induce subsequent immune responses with significant consequences. Their ability and specified

pattern to regulate immune responses depends on barrier integrity and pathogen nature(Doebel et al., 2017; West and Bennett, 2018).

II. LC's function as the professional APC

Antigen uptake: When disturbances in the skin's integrity occur or when they encounter antigens that have breached the skin's barriers, LC extend their dendrites through epidermal tight junctions, enabling them to actively engage in the endocytosis of foreign antigens. This process allows LC to acquire antigens *in situ*(Doebel et al., 2017; Merad et al., 2008; West and Bennett, 2018).

Antigen presentation: After capturing antigens, LC present them to other immune cells, particularly T cells, to initiate immune responses. LC are equipped with the machinery to process antigens. LC upregulate MHC II and co-stimulatory molecules CD40, CD80, and CD86 on their cell surface, migrating from the epidermis to the skin-draining lymph nodes. This upregulation and redistribution of these molecules are essential for optimal antigen presentation. During this process, LC disengage from neighboring keratinocytes by downregulating E-cadherin, making antigen presentation more effective. These activated LC reach the T cell areas of the lymph nodes, where they present antigens to activate immune responses(Atmatzidis et al., 2017; Kashem et al., 2017; Merad et al., 2008; Romani et al., 2012).

Migratory capacity: LC exhibit a remarkable migratory capacity that sets them apart from many other immune cells. While stationed in the epidermal layer of the skin, LC can leave this location and travel to the draining lymph nodes. This migration is essential for transporting antigens and their immune information to sites where they can initiate immune responses. During their migration, LC undergo substantial phenotypic changes, such as the reduction of CD1a, increased of MHCII. They *de novo* express CCR7 in order to respond to its ligand CCL19, guiding them to the draining lymph nodes, positioning themselves strategically within the T cell areas(Doebel et al., 2017; Merad et al., 2008; Romani et al., 2012; Vulcano et al., 2001).

III. LC regulate T cell differentiation

Induction of Treg cells (Foxp3+ CD4+ regulatory T cells): LC play a pivotal role in driving the differentiation and function of Tregs through the secretion of IL-10, retinoic acid, and TGF-β. This local interaction is indispensable for Treg proliferation and the initiation

of tolerance(Doebel et al., 2017). LC are implicated in diverse Treg-dependent immune suppression models in the skin, underscoring their tissue-specific regulatory role. Human epidermal LC actively contribute to skin immune homeostasis by selectively activating and fostering the proliferation of skin-resident Treg cells(Seneschal et al., 2012). In the presence of foreign pathogens, LC shift function to activate effector memory T cells while concurrently restraining Treg activation. Furthermore, during infectious challenges, LC sustain tolerance in normal skin and activate protective skin-resident memory T cells. These findings highlight the dual properties of LC in skin immunity.

Induction of Th17 differentiation: Th17 cell differentiation relies on specific cytokines TGF-β, IL-1β, IL-6, and IL-23(Korn et al., 2009), and is crucial for immune responses against pathogens, like *C. albicans*, in both human and mouse immune systems(Kashem et al., 2017). LC appear to have a significant role in this context. When exposed to *Candida albicans* through skin infection, LC migrate to lymph nodes and express cytokines required for Th17 cell differentiation. Depletion of LC leads to impaired Th17 cell differentiation, highlighting their role in this process(Igyártó et al., 2011). Additionally, in a *S.a.* dysbiosis mice model, LC were found to be necessary for the generation of IL-17-producing CD4+ T cells in the skin(Kobayashi et al., 2015). Moreover, in humans, LC-derived IL-6 and IL-15 prove critical for Th17 cell differentiation(Mathers et al., 2009).

IV. Induction of tolerance and maintain immune homeostasis

The role of LC in inducing tolerance to antigens in the steady state is crucial and continues to be unveiled. LC are pivotal in immune tolerance induction and maintenance, particularly within the skin. Their functions contribute to balanced immune responses, preventing aberrant reactions(Doebel et al., 2017; Kashem et al., 2017). LC-mediated immune tolerance encompasses various mechanisms, including control of self-antigens by promptly clearing apoptotic cells, preventing the accumulation of dead cells, and ensuring local immune tolerance to self-antigens. LC have been demonstrated to uptake self-antigens from sources like hair follicles, potentially preventing autoimmunity. E-cadherin-mediated adhesion(Jiang et al., 2007) and associated NF-κB signaling(Baratin et al., 2015) are involved in the maturation and migration of LC, contributing to immune tolerance(Kashem et al., 2017). LC exhibit a distinctive TLR expression profile compared to dermal DC, with impaired expression of certain bacterial recognition TLR (TLR1/2, TLR2/6, TLR4, and TLR5), potentially contributing to tolerance to bacterial commensals

colonizing the skin(van der Aar et al., 2007). LC contribute significantly to the induction and maintenance of Tregs, playing a role in controlling immune reactions and preserving tolerance (details in III. Regulation of T Cell Function). Upon inflammation, LC undergo maturation, increase migration, and become immune-stimulatory. However, under specific inflammatory conditions, LC also demonstrate an immunosuppressive role. Depletion or targeting of LC in certain inflammatory models resulted in CD8+ T cell hyporesponsiveness or deletion and affected Treg cell levels(Agüero et al., 2012; Kashem et al., 2017).

V. Antimicrobial immunity

LC are central to the skin's immune response to infections. Alongside other skin-resident dendritic cell subsets, LC actively initiate innate and adaptive immune responses within the skin and can induce diverse antigen-specific responses during various skin infections(Deckers et al., 2018; Merad et al., 2008). One feature of LC is their adaptability to different pathogens(Merad et al., 2008). LC in the lymph nodes exhibit a limitation in priming antigen-specific CD8+ T cells after skin infection with HSV. This limitation aligns with the behavior observed in cytolytic viruses like vaccinia viruses. These viruses induce apoptosis in DC, thereby enabling infected DC to prime T cells effectively (Merad et al., 2008). This process also contributes to the differentiation of Th17 cells, which are known for their effectiveness in combatting fungal and bacterial infections(Atmatzidis et al., 2017; Said and Weindl, 2015). LC are necessary and sufficient for antigen-specific Th17 cell responses(Igyártó et al., 2011; Kashem et al., 2017). In epidermal infection models involving pathogens like *Candida albicans* and *S. a.*, LC induce protective Th17 cell responses through maturation and antigen presentation and induce T helper cytokines, high IL1β, IL-6, and IL-23 in response to skin infection(Aliahmadi et al., 2009; Igyártó et al., 2011; Kashem et al., 2017; Kobayashi et al., 2015).

1.2 The TLR2-NF-κB signaling pathway

1.2.1 The Toll Like Receptor 2

Toll-like receptors (TLR) are crucial components of the innate immune system, acting as membrane receptors that recognize and respond to pathogenic threats. They are widely expressed on immune cells like DC and macrophages, as well as non-immune cells such as fibroblasts and epithelial cells. TLR are divided into cell surface structures (e.g., TLR1, TLR2, TLR4), predominantly identifying microbial membrane components like lipids, lipoproteins, and proteins, and intracellular structures (e.g., TLR3, TLR7), mainly recognizing microbial nucleic acids, such as double-stranded RNA and DNA. The recognized molecules belong to the PAMPs from various pathogens, including viruses, bacteria, fungi, and parasites. Upon recognizing PAMPs, TLR initiate signaling pathways involving specific adaptor molecules like MyD88, TIRAP (Mal), TRIF, and TRAM, activating transcription factors, like NF-κB and AP-1, and subsequent immune responses. The diversity in TLR responses arises from their ability to engage distinct adaptor proteins, tailoring immune responses based on detected pathogens. TLR serve as a critical interface between innate and adaptive immunity, contributing to initiating immune responses necessary for infections(Barton and Medzhitov, 2003; Hennessy et al., 2010; Jin and Lee, 2008; Liew et al., 2005; O'Neill, 2008).

TLR2 is an essential member of the TLR family. A distinctive feature of TLR2 is its capability to form heterodimers with fellow receptors TLR1 or TLR6, that TLR2/1 and TLR2/6 heterodimers exhibit the capacity to distinguish and bind different ligands, thereby broadening the signaling capabilities of TLR2. TLR2/1 heterodimers are adept at sensing Gram-negative bacteria or Mycoplasma, while TLR2/6 heterodimers recognize LTA from Gram-positive bacteria and Mycoplasma. TLR2 ligands for both in vitro and in vivo studies include Pam2CSK4(Pam2Cys), Pam3CSK4(Pam3Cys), and FSL-1. TLR2 is expressed on various cell types, including immune, endothelial, and epithelial cells, underscoring its significance as a frontline receptor during bacterial infections. Recognizing PAMPs, TLR2 contributes to the pathogenesis of inflammation and related diseases. During bacterial infections, TLR2 activation, often in collaboration with TLR1 or TLR6, initiates signaling cascades leading to NF-κB activation, inflammasome assembly, and the production of key inflammatory cytokines. This early immune response shapes downstream immune responses, influencing disease course and host outcomes. On the other hand, excessive TLR2 signaling can also lead to tissue damage and disease progression(Colleselli et al.,

2023; Hennessy et al., 2010; Hu and Spaink, 2022; Jin and Lee, 2008; Simpson and Petri, 2020).

1.2.2 The TLR2-NF-κB signaling pathway

Activation of the TLR2-NF-κB signaling pathway: The TLR2-MyD88-NF-κB signaling pathway is a critical component of the innate immune response. TLR2 recognition of specific patterns activates MyD88, initiating downstream signaling pathways that activate NF-κB. This activation results in the transcription of genes vital for the immune response, inflammation, and cell survival. TLR2 engages with TLR1 or TLR6 upon ligand binding, leading to downstream adaptor proteins MAL (TIRAP) and MyD88 recruitment. MyD88 initiates a signaling cascade by activating members of the IRAK family, including IRAK1, IRAK2, and IRAK4. The activated IRAK complex engages TRAF6, an E3 ubiquitin ligase, leading to the ubiquitination of proteins within the signaling cascade. TRAF6 activation ultimately leads to the stimulation of the TAK1 complex. Activated TAK1, in turn, phosphorylates the IKK (IκB kinase) complex, composed of IKKα, IKKβ, and NEMO, ultimately leading to the activation of NF-κB. The phosphorylation of IκB by the IKK complex results in its degradation, freeing NF-κB from inhibition. The released NF-κB translocates to the nucleus, initiating the transcription of a series of genes(Barton and Medzhitov, 2003; Colleselli et al., 2023; Hu and Spaink, 2022; Li and Wu, 2021; O'Neill, 2008).

Negative regulation of the TLR2-NF-κB signaling pathway: The TLR2 serves as the primary sensor of microbial products and initiates signaling pathways that lead to the expression of immune and pro-inflammatory genes. However, maintaining a delicate balance between activation and inhibition is essential for the immune system to prevent harmful and inappropriate inflammatory responses, requiring tight regulation of TLR2 signaling. The identification of numerous negative regulators prompts many mechanisms to control TLR2 signaling. Loss of individual negative regulators results in hyper-activation of TLR2 signaling, emphasizing the nonredundant role played by each regulator. A combination of synergistic effects among negative regulators is necessary for suppression(Hu and Spaink, 2022; Kawasaki and Kawai, 2014; Kondo et al., 2012; Liew et al., 2005).

The negative regulation of TLR2 signaling, in particular, involves various mechanisms, including extracellular, the prevention of receptor–ligand binding, and three major

intracellular mechanisms: (i) dissociation of adaptor complexes, (ii) degradation of signal proteins, and (iii) transcriptional regulation. Soluble TLR2, a smaller isoform, competes with TLR2 on cell membranes by binding ligands, inhibiting signaling. Negative regulators, such as a short form of MyD88 (sMyD88) and SOCS1, contribute to the dissociation of adaptor complexes and the degradation of signal proteins, respectively. TOLLIP inhibits TLR2 signaling by targeting IRAK1, suppressing phosphorylation, or directly interacting with TLR2. Proteins binding to TRAF6, such as A20, NLRX1, and CYLD, act as negative regulators of TLR2 signaling. Additionally, negative transcription regulators, such as ATF3 and Bcl-3, play a role in suppressing the transcription of genes(Hu and Spaink, 2022; Kondo et al., 2012; Liew et al., 2005; Liu et al., 2019).

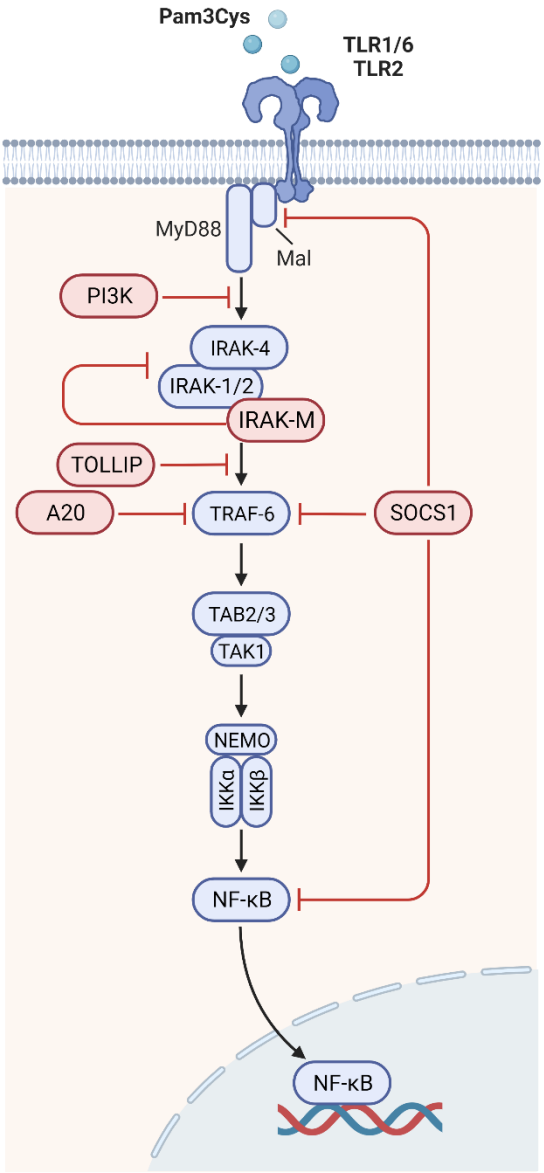

Figure. 1: Adaptor molecules and intracellular inhibitor of the TLR2-NF-κB signaling pathway. TLR2 ligands engage TLR2 to initiate signaling adaptor proteins. MAL and MyD88 recruit and interact with the IRAK family (IRAK1/2 and IRAK4), leading to interaction with TRAF6. TRAF6 activation stimulates the TAK1 complex (TAB2/3 and TAK1), phosphorylating the IKK complex (IKKα, IKKβ, and NEMO). Its degradation enables the translocation of NF-κB to the nucleus and the subsequent initiation of gene transcription. TLR signaling pathways are tightly regulated by endogenous regulators at multiple levels. Inhibitory proteins SOCS1, IRAKM, TOLLIP, PI3K, and A20 selectively suppress IRAK function by targeting various stages of the TLR signaling pathways. The figure was adapted from (Liew et al., 2005)

1.2.3 The role of TLR2 in LC

TLR2 expression on LC has been identified, indicating its capacity to induce a cascade of immune responses upon ligand engagement(Colleselli et al., 2023; Iwasaki and Medzhitov, 2004; Kawasaki and Kawai, 2014; Renn et al., 2006; Simpson and Petri, 2020).

Initiation of maturation: Activation of TLR2 on LC induces the upregulation of the mature marker CD83 and the costimulatory molecules CD80 and CD86, along with MHC II molecules. This maturation process is indispensable for eliciting both innate and adaptive immune responses(Deckers et al., 2018; Kashem et al., 2017; Merad et al., 2008; Said and Weindl, 2015).

Cytokine production: Stimulation of TLR2 in LC leads to elevated secretion of inflammatory but also of anti-inflammatory cytokines as well as cytokines involved in the T cell differentiation, including TNFα, TGF-β, IL-6, IL-8, IL-10, IL-12, and IL-23 (Atmatzidis et al., 2017; Peiser et al., 2008). These cytokines play a pivotal role in recruiting other immune cells, facilitating pathogen clearance, and influencing the differentiation of Th17 cells (details in 1.1.2.2 LC: Function, 5. Antimicrobial Immunity) (Aliahmadi et al., 2009; Atmatzidis et al., 2017; Merad et al., 2008; Peiser et al., 2008; Ratzinger et al., 2004).

Migration: TLR2 activates LC to undergo chemotaxis primarily through the detection of CCR7, guiding their migration to regional lymph nodes. This migratory process is crucial for presenting antigens to T cells and initiating adaptive immune responses(Deckers et al., 2018; Kashem et al., 2017; Liu et al., 2021; Ohl et al., 2004; Otsuka et al., 2018; Romani et al., 2012).

1.3 Atopic Dermatitis

1.3.1 Introduction of AD

Atopic dermatits (AD) is the most common chronic and inflammatory skin condition, which is clinically characterized by recurrent skin lesions, intense itching, and dry skin (Xerosis). AD affects a substantial portion of the population (10-15% of children and 3-8% of adults) significantly impacting patients' quality of life. Although AD often starts in early childhood, it has unexpected courses with either spontaneous remission or persistence into adulthood.

AD skin lesions are characterized as red patches, papules, plaques, and vesicles, along with a variable course of itching and/or burning sensation. Skin barrier dysfunction is one

of the major characteristics of AD. It explains its highy susceptibilty to irritation and environmental factors. In individuals, the clinical severity and presentation of AD can exhibit substantial variability(Weidinger et al., 2018). AD is considered as the port of entry for numerous sensitizations to food and environmental allergens. Thus, usually AD does not exist in isolation but is often the first disorder which is then by followed by other atopic diseases, including asthma, allergic rhinitis, and food allergies. This scenario is referred to as "the atopic march"(Weidinger et al., 2018).

The pathophysiology of AD is complex and influenced by various factors, including genetics, immune system dysregulation, and environmental elements(Weidinger et al., 2018; Weidinger and Novak, 2016).

Given the multifaceted nature of AD's pathophysiology, a comprehensive approach is imperative for its treatment. Current therapeutic options encompass a spectrum of interventions, ranging from topical treatments like corticosteroids and calcineurin inhibitors to phototherapy and systemic immunosuppressants. Recent advancements in research have led to the development of new therapies, including JAK inhibitors and the more targeted therapies with cytokine/receptors-specific biological agents. These latest treatments promise more precise and effective management of AD, tailored to individual characteristics and subtypes(Bieber, 2022; Weidinger et al., 2018).

1.3. [TB1]Pathogenesis of AD

The pathogenesis of AD is characterized by a complex interplay of various factors, including genetic predisposition, environmental influences, and immune dysregulation. This intricate cascade of events results in complex pathophysiological changes underlying mirrored by a complex phenotype and course of AD.

One pivotal element is epidermal barrier dysfunction, a process influenced by the interplay of host genetics, inflammation and environmental factors. This intricate interaction results in the genetically driven disruption of the epidermal barrier which is aggravated by immune dysregulation and inflammation. In AD individuals, the outermost layers of the epidermis exhibit a compromised protein and lipid barrier. This impairment primarily stems from reduced expression of critical proteins involved in epidermal differentiation, notably filaggrin, and essential components of tight junctions, which serve to prevent transepidermal water loss. Furthermore, there is a reduction in the concentration of fatty acids and ceramides. This compromised barrier renders the skin more susceptible to

external assailants, including microbes, proinflammatory allergens, toxins, and irritants. The skin microbiome also assumes a vital role in the pathogenesis of AD. Dysbiosis of the skin microbiota contributes to the disease by disrupting the balance of microorganisms on the skin. This imbalance, in turn, fosters inflammation and T-cell infiltration and further exacerbates barrier dysfunction (Bieber et al., 2022; Hülpüsch et al., 2021; Ständer, 2021; Weidinger et al., 2018; Weidinger and Novak, 2016; Werfel et al., 2016).

A predominant skewing towards the Th2 immune response typifies the immune dysregulation observed in AD. The immune system's response to immunogenic antigens primarily revolves around the interaction between CD4+ T cells and keratinocytes. These intricate interactions culminate in an immune response predominantly characterized by Th2 cells, which leads to heightened local production of signature Th2 cytokines, including IL-IL-13. IL-5 and IL-31. IL-4 and IL-13 contribute to the polarization of Th2 cells, IgE class-switching, eosinophil recruitment, and further deterioration of the epidermal barrier by inhibiting epidermal differentiation, lipid production, and antimicrobial peptide expression. While Th2 skewing represents a common feature among individuals with AD, there exists variability in the activation of other Th cell-driven pathways, such as Th1 in adults and Th17 in children and Asians. These variances may be associated with factors like age and race (Bieber et al., 2022; Hülpüsch et al., 2021; Ständer, 2021; Weidinger et al., 2018; Weidinger and Novak, 2016; Werfel et al., 2016).

Moreover, a multitude of external factors (e.g., allergens, irritants, pathogens) and internal factors (e.g., cytokines, neuropeptides, lipids) serve as pruritogens, directly stimulating or modulating the sensation of itch by activating receptors on sensory neurons in the dorsal root ganglion. The activation of cytokine receptors (e.g., IL-4, IL-13, IL-31, IL-33, TSLP), G-protein-coupled receptors, and transient receptor potential channels culminates in generating action potentials. These mediators play a dual role by transmitting sensory information to the central nervous system while encouraging the local production of inflammatory mediators, such as calcitonin gene-related peptide and substance P. This intricate web of interactions collectively contributes to the complex pathogenesis of AD (Bieber et al., 2022; Hülpüsch et al., 2021; Ständer, 2021; Weidinger et al., 2018; Weidinger and Novak, 2016; Werfel et al., 2016).

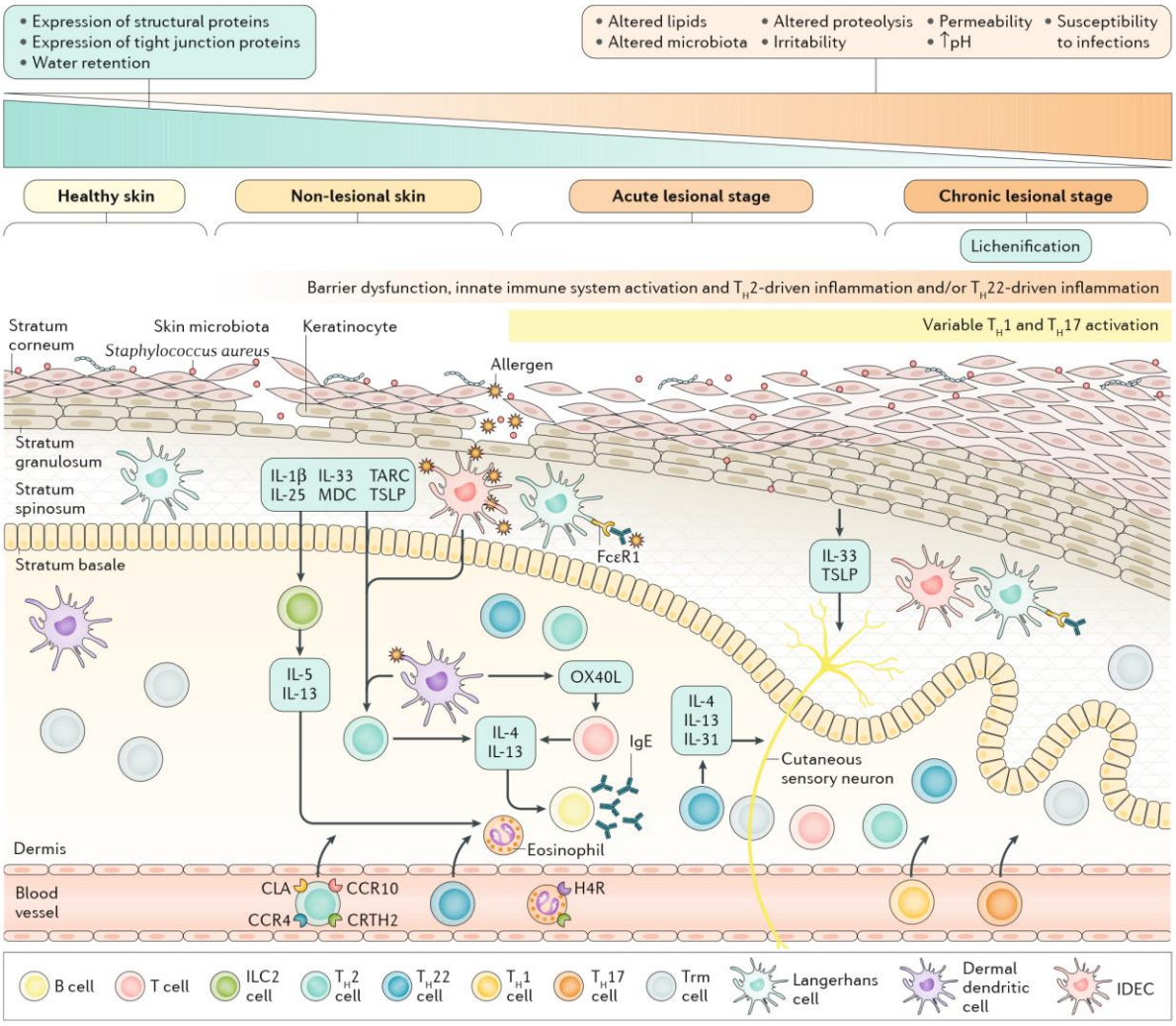

Figure. 2: Stage-based pathogenesis and main mechanisms of AD. Epidermal barrier disruption induces keratinocytes to express chemokines (e.g., TARC, CCL17, CCL22) and innate immune cytokines (alarmins, IL-1β, IL-33, TSLP). These signals activate skin-resident ILC2s and Th2 cell-mediated immune responses. Activated APC present antigens to naive T cells, triggering immune responses, releasing Th2 cytokines IL-4 and IL-13, and promoting IgE class switching in AD skin. DC subtypes increased in AD, including LC, expressing FcεR1. IgE-bound DC by FcεR1 facilitate allergen uptake, initiating T cell-mediated hypersensitivity reactions. IL-33, TSLP, and downstream Th2 cytokines directly communicate with cutaneous sensory neurons, exacerbating pruritus. In chronic stages, a mixed T cell infiltrate and potential autoimmune mechanisms sustain inflammation, promoting cutaneous remodeling and neuroinflammation. The figure was adapted from(Weidinger et al., 2018)

1.3.1.2. Therapy of AD

AD requires multiple approaches to its management, focusing on relieving symptoms, controlling the disease, and enhancing the quality of life for individuals living with this chronic skin condition. The choice of therapeutic strategies in AD is influenced by various

factors, including the patient's age, disease severity, comorbidities, and individual treatment goals(Bieber, 2022; Bieber et al., 2022; Langan et al., 2020; Weidinger et al., 2018).

One fundamental aspect of AD management is basic skin care and avoidance of triggering factors. Regular use of emollients and moisturizers helps restore the impaired skin barrier, maintain hydration, and reduce dryness and itchiness. Identifying and avoiding irritants and allergens, such as harsh soaps and fragrances, can also help minimize flare-ups(Bieber, 2022; Bieber et al., 2022; Langan et al., 2020; Weidinger et al., 2018).

In mild to moderate AD cases, topical therapies are often the initial approach. TCS is often the first line of treatment, especially for mild to moderate cases. They effectively reduce inflammation and alleviate symptoms. In cases where TCS are unsuitable, especially on the face or in areas requiring long-term treatment, TCIs such as tacrolimus and pimecrolimus are viable alternatives. Additionally, the introduction of PDE4 inhibitors, such as crisaborole, offers an alternative for mild to moderate AD. Phototherapy with ultraviolet light can provide relief from AD symptoms. However, the long-term use of UV phototherapy increases the risk of skin cancer(Bieber, 2022; Bieber et al., 2022; Langan et al., 2020; Weidinger et al., 2018).

For moderate to severe cases of AD, systemic therapies are considered. Options include cyclosporin A, an immunosuppressant approved for severe AD that can effectively control symptoms but may come with safety concerns with long-term use. *Methotrexate* is an antimetabolite that helps manage symptoms but requires careful monitoring for potential side effects. Other systemic immunosuppressants, such as azathioprine and mycophenolate mofetil, may be considered in cases where the patient is unresponsive to other treatments(Bieber, 2022; Bieber et al., 2022; Langan et al., 2020; Weidinger et al., 2018) but are not approved for this indication.

In recent years, there have been new developments in biological treatments for AD. Monoclonal antibodies targeting Th2 cytokines or their receptors have shown promise in AD management. JAK inhibitors, both topical and systemic, represent a novel approach to target immune dysregulation, although the safety profiles require further evaluation. Additionally, targeted immune interventions encompass a range of strategies that provide treatment alternatives such as active substances addressing AhR, the blockade of H4R, and the promotion of anti-inflammatory cytokines through PDE4 inhibitors. Each of these

approaches addresses various aspects of the inflammatory response(Bieber, 2022; Bieber et al., 2022; Hülpüsch et al., 2021; Langan et al., 2020; Weidinger et al., 2018).

Microbiome manipulation is an emerging strategy in AD management, focusing on reducing the overgrowth of *S. a.* and promoting beneficial bacteria like *Staphylococcus hominis* (Bieber, 2022; Bieber et al., 2022; Hülpüsch et al., 2021; Langan et al., 2020; Weidinger et al., 2018).

Furthermore, managing pruritus/itch is critical in enhancing patients' quality of life. Comprehensive patient and caregiver education programs are fundamental to optimize AD management and foster self-management skills. The multifaceted nature of AD demands a holistic approach, combining essential skincare, pharmacological interventions, and patient education to meet the dual goals of effectively treating acute flares and maintaining long-term disease control (Bieber, 2022; Bieber et al., 2022; Hülpüsch et al., 2021; Langan et al., 2020; Weidinger et al., 2018).

JAK inhibitors in AD: The JAK/STAT signaling pathway is pivotal in many cellular processes, which involves over 50 cytokines, its influence extends to critical physiological processes such as hematopoiesis, immune fitness, tissue repair, inflammation, apoptosis, and adipogenesis. Dysregulation of this pathway has been implicated in the pathogenesis of various cancers and immune diseases(Damsky and King, 2017; Hu et al., 2021; McLornan et al., 2021; Schwartz et al., 2017). The JAK plays a pivotal role in the pathogenesis of AD. The influence of JAK extends to immune responses, particularly affecting Th2 cell-mediated immune reactions, skin barrier integrity, pruritus, and the broader inflammatory conditions associated with AD (Chovatiya and Paller, 2021; Guttman-Yassky et al., 2023).

Over the past decades, the pivotal treatment for AD has predominantly involved topical steroids, with therapeutic options gradually expanding to encompass phototherapy and oral steroids. However, recent breakthroughs in translational research have unveiled a deeper understanding of AD's pathophysiology, contributing to novel treatment options. JAK inhibitors have emerged as a promising avenue, showcasing their efficacy in topical and oral formulations in AD(Bieber, 2022; Bieber et al., 2022; Chovatiya and Paller, 2021). Topical JAK inhibitors, such as ruxolitinib (JAK1/2) and delgocitinib (JAK1/2/3 and TYK2), have shown significant efficacy in treating mild-to-moderate AD, with rapid symptom relief and minimal adverse events. Delgocitinib in 2019 approved in Japan for pediatric and adult AD highlights their efficacy and safety, making them a promising

treatment(Chovatiya and Paller, 2021; He and Guttman-Yassky, 2019). Oral JAK inhibitors, including baricitinib (JAK1/2), abrocitinib (JAK1), and upadacitinib (JAK1), have emerged as robust contenders in moderate-to-severe AD. Clinical trials demonstrate their efficacy in achieving clear or almost precise AD scores, positioning them as valuable therapeutic options. Notably, these oral inhibitors exhibit a rapid and profound improvement in pruritus, addressing a critical aspect of AD symptomatology. The safety profile of oral JAK inhibitors remains favorable, with mild to moderate treatment-emergent adverse events(Chovatiya and Paller, 2021; He and Guttman-Yassky, 2019). While clinical trials provide foundational evidence, the need for real-world data is underscored to comprehensively understand the long-term safety, durability, and treatment success of JAK inhibitors in routine clinical practice.

1.3.2 The role of LC in AD

Antigen capture: Epidermal tight junctions serve as protective barriers that prevent the penetration of external substances into deeper layers of the skin. LC, however, possess a distinctive capability to extend their dendrites through these tight junctions(Deckers et al., 2018), especially in the dysfunctional skin barrier, effectively breaching this protective boundary(Yoshida et al., 2014). The behavior of LC at tight junctions distinguishes them from IDEC which lack LC-specific marker Langerin(Yoshida et al., 2014). These distinctive features contribute significantly to understanding AD's underlying pathophysiology.

The high-affinity receptor for IgE (FcεRI) expression on the LC: The expression of FcεRI on the surface of LC is a significant aspect of allergen-specific IgE interaction in AD(Deckers et al., 2018). Individuals with AD who become sensitized to allergens produce allergen-specific IgE antibodies that can bind to FcεRI on the surface of LC(Bruynzeel-Koomen et al., 1986; Kwiek et al., 2017). When these IgE antibodies encounter the corresponding allergens, they facilitate the uptake and presentation of the allergen by LC(Novak et al., 2003). AhR may serve as a crucial structure in AD since its activation, particularly induced by factors like UVB irradiation, has the ability to downregulate the expression of FcεRI on LC(Koch et al., 2017a) and other immune cells. This can result in the attenuation of the allergic response seen in AD.

Th17 responses against microbes: In AD, LC are critical in promoting cutaneous Th17 responses against bacterial infections(Deckers et al., 2018). The barrier defect of AD creates an environment conducive to microbial dysbiosis, particularly colonization by *S.*

a., complicating the immunological condition(Kobayashi et al., 2015; Van Dalen et al., 2019). Studies have demonstrated that LC play an essential role in *S. a.*-induced immune responses, with their absence leading to the abrogation of cutaneous Th17 responses(Igyártó et al., 2011). LC are necessary and sufficient for antigen-specific Th17 cell development(Deckers et al., 2018). Understanding the cytokine profile involved in Th17 commitment, including IL-1β, IL-6, TGF-β, and IL-23, provides insights into LC-mediated immune responses(Aliahmadi et al., 2009; Igyártó et al., 2011). Furthermore, TLR2 activation in LC was found to be instrumental in inducing Th17 responses in inflamed skin(Aliahmadi et al., 2009).

1.3.3 The role of TLR2 in AD

TLR2 is assumed to play multiple roles in the pathophysiology of AD.

Genetic polymorphisms and susceptibility: Genetic polymorphisms in TLR2 contribute to altered innate immune responses, rendering the AD skin more vulnerable to bacterial or viral infections. Monocytes from AD patients with TLR2 polymorphisms exhibit heightened cytokine production in response to TLR2 stimulation, potentially explaining the increased susceptibility to skin infections(Niebuhr et al., 2008).

Skin barrier disruption: TLR2 dysfunction is associated with compromised skin barrier function. In healthy skin, TLR2 activation enhances the expression of tight junction proteins and antimicrobial peptides. However, in AD, decreased TLR2 activity correlates with reduced expression of these proteins and peptides, further weakening the skin barrier. The dysbiosis of the skin microbiome and impaired TLR2 function create a vicious cycle in AD pathogenesis(Kuo et al., 2013; Leung, 2013). Increased TLR2 activity is linked to enhanced tight junction function, which is decreased in AD. This suggests that altered TLR2 signaling may be related to abnormal skin barrier function in AD.

Impaired TLR2 function: One of the prominent features of AD is the impaired function of TLR2 in the lesional skin of affected individuals. TLR2 is essential for recognizing components of *S. a.*. In AD, compromised TLR2 function disrupts the normal immune response to *S. a.,* leading to increased colonization in the lesional skin(Sun et al., 2019). Our previous studies showed that LC isolated from AD lesions are tolerized toward TLR2 activation, indicating impaired TLR2-mediated sensing of *S.aureus*-derived signals(Iwamoto et al., 2018). This is also manifested by reduced TLR2 levels in macrophages and PBMCs isolated from AD patients(Niebuhr et al., 2009, 2008).

Cytokine dysregulation and skewed AD inflammation: Stimulation of TLR2 ligands in AD patients induces a distinct cytokine profile in macrophages and PBMC. There is a notable decrease in the production of Th1/Th17 cytokines (IFNγ, IL-12, IL-17F) and an increase in the Th2 cytokine IL-5(Yu et al., 2015). This shift towards a Th2-dominant immune phenotype is characteristic of allergic diseases, including AD. TLR2 in AD also appears to evolve during different phases of the condition. While impaired TLR2 signaling during the acute phase favors Th2 responses, aberrant activation of TLR2 may contribute to chronic inflammation, potentially through Th1 pathways. TSLP, a cytokine crucial in linking innate and adaptive immune responses, is implicated in this transition(Vu et al., 2010).

1.4 Objectives of this work

Previous findings from our lab revealed that LC isolated from AD lesions exhibit tolerization to TLR2 activation, indicating impaired TLR2-mediated sensing of *S. a.*-derived signals in AD skin(Iwamoto et al., 2018). Our study hypothesis is that the tolerization of LC develops from constant TLR2 stimulation in AD lesions, attributed to increased *S. a.* colonization. Through this hypothesis, the objective is to establish an in vitro model that mimics these tolerized LC observed in AD, providing a comprehensive understanding of the molecular and functional characteristics of tolerized LC in AD pathogenesis. By investigating the mechanisms underlying the emergence of these tolerized LC, the model also allows the exploration of potential strategies that can restore the LC response to TLR2-induced activation.

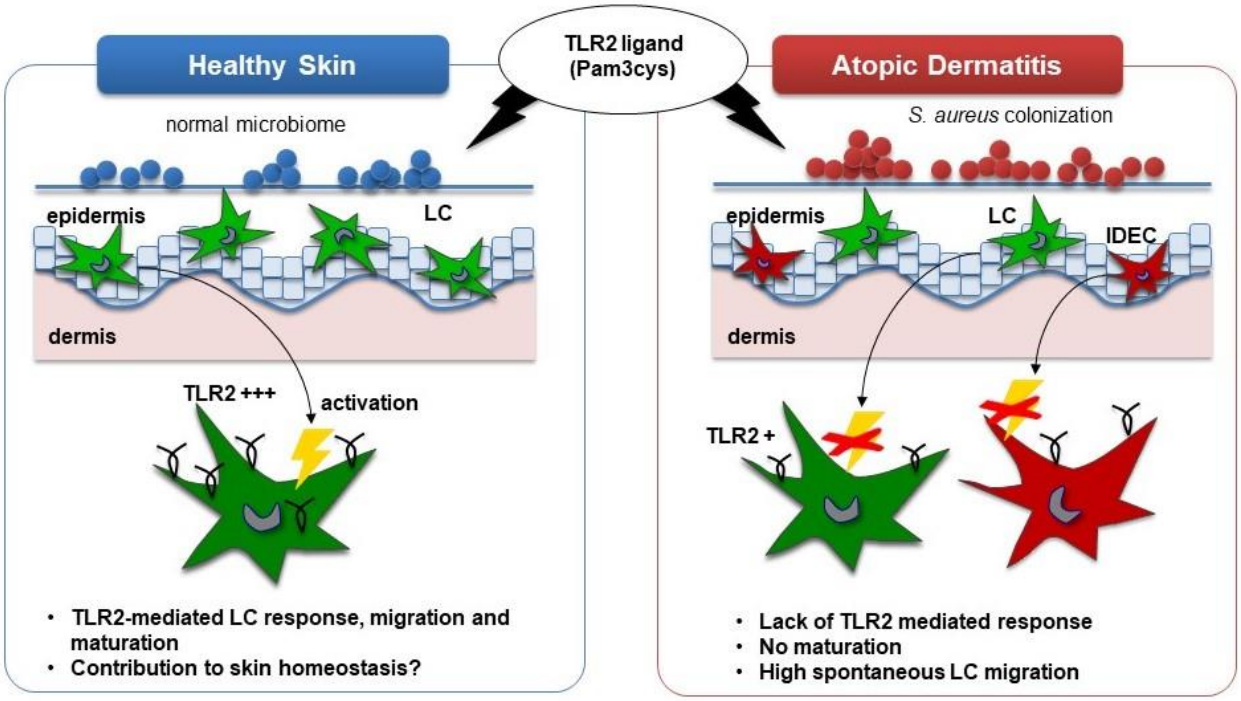

Figure. 3: LC in AD skin express less TLR2 compared to healthy skin. LC in AD skin demonstrate reduced TLR2 expression compared to those in healthy skin. While stimulation of LC from normal skin with a TLR2 ligand induces their maturation and enhances their migratory activity, LC in AD skin fail to respond to TLR2 activation. The figure was adapted form(Iwamoto et al., 2018).

Using a model of human CD34+-derived LC the following aims were addressed:

1. Characterize the behavior of these tolerized LC, including cell phenotype and function upon exposure to TLR2 engagement.
2. Analyze the TLR2 downstream signaling pathway in the tolerized LC.
3. Identify critical factors in potential mechanisms involved in the TLR2-NF-κB signaling pathway of tolerized LC.
4. Based on the identified mechanisms, attempt to identify putative methods or approaches to reverse LC tolerization or inhibit the tolerization process.

2. Material and methods

2.1 Material

2.1.1 Chemicals

Table 1 Chemicals

Chemical	Manufacturer
2-Mercaptoethanol	Sigma-Aldrich Chemie GmbH; Taufkirchen, Germany
7-AAD	Sigma-Aldrich Chemie GmbH; Taufkirchen, Germany
Agarose	Sigma-Aldrich Chemie GmbH; Taufkirchen, Germany
Antibiotic-antimycotic (100x)	Gibco®; Karlsruhe, Germany
BMS-911543	InvivoChem, Vernon Hills, IL, USA
BSA	Sigma-Aldrich Chemie GmbH; Taufkirchen, Germany
CCL19 / MIP-3 beta	ImmunoTools, Friesoythe, Germany
Chloroform	AppliChem GmbH; Darmstadt, Germany
Decernotinib (VX-509)	InvivoChem, Vernon Hills, IL, USA
Dextran	Sigma-Aldrich Chemie GmbH; Taufkirchen, Germany
DMSO	Sigma-Aldrich Chemie GmbH; Taufkirchen, Germany
dNTP	Life Technologies GmbH; Darmstadt, Germany
DTT	Carl Roth GmbH & Co. KG; Essen, Germany
EDTA	Merck KGaA, Darmstadt, Germany
Ethanol	AppliChem GmbH; Darmstadt, Germany
Ethidium bromid solution	Sigma-Aldrich Chemie GmbH; Taufkirchen, Germany
Fetal calf serum (Gibco®)	Life Technologies GmbH; Darmstadt, Germany
Filgotinib	InvivoChem, Vernon Hills, IL, USA
FLT3L (rhFlt3/Flk2 ligand)	R&D Systems Inc.; Minneapolis, USA
Gel Loading Dye Blue, (6x)	New England Biolabs; Frankfurt am Main, Germany
Glycin	AppliChem GmbH; Darmstadt, Germany
GM-CSF	Bayer AG; Leverkusen, Germany
Human IgG, Myeloma	Calbiochem® by Merck Chemicals GmbH; Darmstadt, Germany
Hydrocortison	Sigma-Aldrich Chemie GmbH; Taufkirchen, Germany
Isopropanol	AppliChem GmbH; Darmstadt, Germany

LB Broth (Lennox)	Carl Roth GmbH + Co. KG; Karlsruhe, Germany
Lymphoprep™	Progen Biotechnik GmbH; Heidelberg, Germany
Normal mouse serum	Jackson ImmunoResearch Labaratories, Inc; West Grove, USA
Opti-MEM® I Reduced Serum Medium (Gibco™)	Life Technologies GmbH; Darmstadt, Germany
Pam3Cys-Ser-(Lys)4 trihydrochloride	EMC microcollections GmbH; Tübingen, Germany
RPMI Medium 1640 (1x) + GlutaMAX™ -I (Gibco®)	Life Technologies GmbH; Darmstadt, Germany
Ruxolitinib	InvivoChem, Vernon Hills, IL, USA
SCF	R&D Systems Inc.; Minneapolis, USA
SYBR® Green Supermix with ROX™	Bio-Rad Laboratories Inc.; Hercules, USA
Tacrolimus monohydrate	Adooq Bioscience, Irvine, CA
TGF-ß	R&D Systems Inc.; Minneapolis, USA
TNF-α	R&D Systems Inc.; Minneapolis, USA
TRIzol®	Life Technologies GmbH; Darmstadt, Germany
Vitamin D_3, 1α, 25-Dihydroxy, 1.25$(OH)_2$-D_3	Sigma-Aldrich Chemie GmbH; Taufkirchen, Germany

2.1.2 Buffers

Table 2 Composition of buffers

Buffers (1x)	Composition
FACS buffer	137 mM NaCl; 75 mM Na2HPO4; 32.5 mM NaH2PO4; 10 % (v/v) FCS; 155 mM NaN3
MACS buffer	137 mM NaCl; 2.7 mM KCl; 8.5 mM Na2HPO4; 1.47 mM KH2PO4; 0.5 % (w/v) BSA; 1 % (v/v) 0.5 M EDTA
PBS	137 mM NaCl; 2.7 mM KCl; 8.5 mM Na2HPO4; 1.47 mM KH2PO4
TAE buffer	40 mM Tris/acetic acid, pH 7.8; 10 mM NaAc; 1 mM EDTA, pH 8.0

2.1.3 Cell culture media

Table 3 Composition of cell culture medium

Name	Composition
CD34 medium	RPMI Medium 1640 (1x) + GlutaMAX™ -I; 10 % (v/v) FCS; 1 % (v/v) AB/AM; 50 µM 2-mercaptoethanol
freezing medium	FCS; 10 % DMSO

2.1.4 Kits

Table 4 Kits

Kit	Manufacturer
BD Cytofix/Cytoperm™	Beckton Dickinson GmbH; Heidelberg, Germany
CD1a MicroBeads, human	Miltenyi Biotec GmbH; Bergisch Gladbach, Germany
DNA-free™ DNA Removal Kit (Ambion®)	Life Technologies GmbH; Darmstadt, Germany
Human Inflammation Panel 1 Standard	LEGENDplex™, BioLegend, San Diego, USA.
TaqMan® MicroRNA Assays: • hsa-miR-155-5p (ID 002623) • hsa-miR-146a-5p (ID 000468) • RNU48 (ID 001006)	Life Technologies GmbH; Darmstadt, Germany

2.1.5 Antibodies

Table 5 Antibodies and control used for flow cytometry analysis

Antibody / conjugation	Immunogen / specificity	Clone	Species	Isotype	Manufacturer
CCR6	human CD196/CCR6	11A9	mouse	IgG1	R&D Systems Minneapolis, USA
CCR7	human CCR7	150503	mouse	IgG1	R&D Systems Minneapolis, USA
CD14-APC	human CD14	TÜK4	mouse	IgG2a	Miltenyi Biotec GmbH; Bergisch Gladbach, Germany
CD1a-RD1 (T6-RD1)	human CD1a	SFCI19 Thy1A8	mouse	IgG1	Beckman Coulter Inc.; Krefeld, Germany
CD34-PE	human CD34	581	mouse	IgG1, κ	Beckton Dickinson GmbH; Heidelberg, Germany
CD80	human CD80	L307.4	mouse	IgG1	BD Pharmingen, Heidelberg, German
CD83	human CD83	HB15a	mouse	IgG2b	Santa Cruz Biotechnology
CD86	human CD86	IT2.2	mouse	IgG1	BD Pharmingen, Heidelberg, German
FcεRIα	human FcεRIα	AER-37(CRA 1)	mouse	IgG2b, κ	eBioscience; San Diego, USA
Goat anti-mouse IgG, Fcγ -FITC	mouse IgG Fcγ	polyclon al	goat	IgG	Jackson ImmunoResearch Europe Ltd.; Suffolk, UK
Langerin (CD207)	CD34-derived dendritic cells	DCGM4	mouse	IgG1	Beckman Coulter Inc.; Krefeld, Germany
MHC II		L243			provided*
TLR2	human TLR2	1030A5. 138	mouse	IgG1	Immgenex; San Diego, USA
IgG1, κ	isotype	MOPC -21	mouse		Sigma-Aldrich Chemie GmbH; Taufkirchen, Germany
IgG1-PE	isotype	X40	mouse		Beckton Dickinson GmbH; Heidelberg, Germany
IgG1-RD1	isotype	2T8-2F5	human		Beckman Coulter Inc.; Krefeld, Germany

IgG2a-APC	isotype	S43.10	mouse	Miltenyi Biotec GmbH; Bergisch Gladbach, Germany
IgG2b, κ	isotype	MOPC -141	mouse	Sigma-Aldrich Chemie GmbH; Taufkirchen, Germany

2.1.6 Oligonucleotides

Table 6 Amplicons, Oligonucleotides and cDNA clone used for qPCR. Matching sequences for oligonucleotides in amplicons are underlined. Amplicons and oligonucleotides were manufactured by Life Technologies GmbH; Darmstadt, Germany.

Name	Forward sequence (5' → 3')	Reverse sequence (5' → 3')
Amplicon	Amplicon sequence (5' → 3')	
hACTB	AGCGCGGCTACAGCTTCA	TCCTTAATGTCACGCACGATTT
Amplicon hACTB	TCCTCACCGAGCGCGGCTACAGCTTCACCACCACGGCCGAGCGGGAAATCGTGCGTGACATTAAGGAGAAGCTGT	
TLR1	TGTGCTGCCAATTGCTCATT	TTTTCCCCATAAGTCTCTCCTAAGAC
Amplicon TLR1	CACTTAGAAAAATCTAGTGTGCTGCCAATTGCTCATTTGAATATCAGCAAGGTCTTGCTGGTCTTAGGAGAGACTTATGGGGAAAAAGAAGACCCT	
TLR2	CCAAGGAAGAATCCTCCAATCA	GCTGCCCTTGCAGATACCA
Amplicon TLR2	ATCAGCCTCTCCAAGGAAGAATCCTCCAATCAGGCTTCTCTGTCTTGTGACCGCAATGGTATCTGCAAGGGCAGCTCAGGATCTT	
MYD88	TCACTGTCTGCGACTACACCAA	GGCAAGGCGAGTCCAGAAC
Amplicon MYD88	CCTGAGGTTCATCACTGTCTGCGACTACACCAACCCCTGCACCAAATCTTGGTTCTGGACTCGCCTTGCCAAGGCCTTGT	
CCR6	CCATTCTGGGCAGTGAGTCA	GCACGTGGCATTGCTGAA
Amplicon CCR6	TCTTACTCTCCCATTCTGGGCAGTGAGTCATGCCACCGGTGCGTGGGTTTTCAGCAATGCCACGTGCAAGTTGCTAA	
CCR7	GCTGCGTCAACCCTTTCTTG	AAGAGATCGTTGCGGAACTTG
Amplicon CCR7	TGCGTCCGCTGCTGCGTCAACCCTTTCTTGTACGCCTTCATCGGCGTCAAGTTCCGCAACGATCTCTTCAAGCTCTTC	
IRAK1	GCCCCTTTCCGTTTTGCT	ATCTTGAGCTCCTCCGAGAAGTT
Amplicon IRAK1	CAGGGAGCCCGCCCCTTTCCGTTTTGCTGGCCCCTCTGTGAGATTTCCCGGGGCACCCACAACTTCTCGGAGGAGCTCAAGATCGGGGAGGGT	
IRAK2	GGAAACAGACGACGTTGACAATT	AGGGTGCCACACTCATGGA
Amplicon IRAK2	CAACACCCCAGAGGAAACAGACGACGTTGACAATTCCAGCCTTGATGCCTCCTCCTCCATGAGTGTGGCACCCTGGGCAGGGGC	
IRAK4	CAGACTCTCTTGCTTGGATGGT	GCTGCACCCTGAGCAATCTT
Amplicon IRAK4	CATTGCTAGACAGACTCTCTTGCTTGGATGGTACTCCACCACTTTCTTGGCACATGAGATGCAAGATTGCTCAGGGTGCAGCTAATGGCATC	
TRAF6	CACCCCTGGAAAGCAAGTATG	ACTGCTTCTCGTAATGCCATCA
Amplicon TRAF6	GAGTTTGACCCACCCCTGGAAAGCAAGTATGAATGCCCCATCTGCTTGATGGCATTACGAGAAGCAGTGCAAACGCCA	
SOCS1	GCTGGCCCCTTCTGTAGGAT	CTGCTGTGGAGACTGCATTGTC

Amplicon SOCS1	CACCCCTCCGGCTGGCCCCTTCTGTAGGATGGTAGCACACAACCAGGTGGCAGCCGACAATGCAGTCTCCACAGCAGCAGAGCCCCG	
A20	CCATCCATGGACTGTGATTCTG	GAGCAGCTTGTTTTTCTGTCAATG
Amplicon A20	AAATGCAGAACCATCCATGGACTGTGATTCTGAGGCTGCTGAGACTGAACATGTTCACATTGACAGAAAAACAAGCTGCTCTTTATAATAT	
TOLLIP	CCTGATGCCAACAGTGTACCA	GCGGGCATCCCTGTGA
Amplicon TOLLIP	AGCCCGTGGTCCTGATGCCAACAGTGTACCAGCAGGGCGTTGGCTATGTGCCCATCACAGGGATGCCCGCTGTCTGTAGC	
PI3K	TCTTAGGTCAGAAGTGCACATTCC	CCCCGGCAGTATGCTTCA
Amplicon PI3K	TATTTTGGCATCTTAGGTCAGAAGTGCACATTCCTGCTGTCTCAGTACAATTTGGTGTCATCCTTGAAGCATACTGCCGGGGAAGTGTGGGG	
IRAKM	GCCTGGATTCATGTCTCTCATTT	AACAGAAGAGCTTGGCAGAGAAAT
Amplicon IRAKM	GAGAAGAGAGGCCTGGATTCATGTCTCTCATTTCTAGATAAGAAAGTGCCTCCCTGCCCTCGGAATTTCTCTGCCAAGCTCTTCTGTTTGGCAGGCCG	
C-FOS	GGCGTTGTGAAGACCATGAC	TAACTGTTCCACCTTGCCCC
Amplicon C-FOS	CTCCAGGGCTGGCGTTGTGAAGACCATGACAGGAGGCCGAGCGCAGAGCATTGGCAGGAGGGGCAAGGTGGAACAGTTATCTCCAGAAGA	

2.1.7 Devices and consumables

Table 7 Devices and consumables

Name	Manufacturer
15 mL / 50 mL CELLSTAR® Polypropylene Tube	Greiner Bio-One GmbH; Frickenhausen, Germany
CELLSTAR® Serological Pipet, 10 mL, sterile	Greiner Bio-One GmbH; Frickenhausen, Germany
Costar® 24 Well Clear TC-Treated Multiple Well Plates, Individually Wrapped, sterile	Corning GmbH HQ; Wiesbaden, Germany
Costar® Stripette® Serological Pipets, Polystyrene, 5 mL / 10 mL, sterile	Corning GmbH HQ; Wiesbaden, Germany
Falcon® 14 mL Round Bottom High Clarity PP Test Tube, Graduated, with Snap Cap, Sterile,	Corning GmbH HQ; Wiesbaden, Germany
MicroAmp® Fast Optical 96-Well Reaction Plate with Barcode, 0.1 mL	Applied Biosystems® by Life Technologies GmbH; Darmstadt, Germany
Mr. Frosty™ Freezing Container	Thermo Fisher Scientific Inc.; Waltham, USA
Nunc™ Biobanking and Cell Culture Cryogenic Tubes, 1.8 mL	Thermo Fisher Scientific Inc.; Waltham, USA
Opti-Seal Optical Disposable Adhesive	BIOplastics; Landgraaf, Netherlands
Pipettors	Gilson Inc.; Middleton, USA Eppendorf AG; Hamburg, Germany
Polycarbonate Membrane Transwell® Inserts, 24-well, 5.0 µm	Corning, NY, USA
Polypropylene Tubes - Two-Position Vent Stopper Tube, 5 mL	Greiner Bio-One GmbH; Frickenhausen, Germany
Pre-Separation Filters (30 µm)	Miltenyi Biotec GmbH; Bergisch Gladbach, Germany
Safe-Lock Tubes, 0.5 mL / 1.5 mL, PCR clean	Eppendorf AG; Hamburg, Germany
Whatman® Puradisc 30 syringe filters, pore size 0.2 µm	GE Healthcare; Chalfont St. Giles, Great Britain

2.1.8 Instruments

Table 8 Instruments

Name	Manufacturer
Autoclave Varioclav 500 H+P	Labortechnik AG; Oberschleißheim, Germany
AutoMACS Pro® Separator	Miltenyi Biotec GmbH; Bergisch Gladbach, Germany
Centrifuge 5417R	Eppendorf AG; Hamburg, Germany
Centrifuge Allegra® X-15R	Beckman Coulter Inc.; Brea, USA
Centrifuge Rotixa 120 RS	Hettich GmbH & Co.KG; Tuttlingen, Germany
Flow Cytometer FACSCanto™	Beckton Dickinson GmbH; Heidelberg, Germany
Horizontal Electrophoresis System Wide Mini-Sub Cell GT Cell	Bio-Rad Laboratories GmbH; München; Germany
ImageQuant™ LAS 4000	GE Healthcare; Chalfont St. Giles, UK
Incubator Heracell™ 150 and 150i	Thermo Fisher Scientific Inc.; Waltham, USA
Laboclav 135 MSLV	SHP Steriltechnik AG; Detzel Schloss, Germany
Mastercycler nexus gradient	Eppendorf AG; Hamburg, Germany
Microscope Leica DM IRB	Leica Camera AG; Bensheim, Germany
Microscope Nikon Eclipse TS100	Nikon GmbH; Düsseldorf, Germany
Milli-Q® Reference Water Purification System	Merck KGaA, Darmstadt, Germany
Neubauer improved hemocytometer	Brand GmbH & Co. KG; Wertheim, Germany
Power supply PowerPac™ 3000	Bio-Rad Laboratories GmbH; München; Germany
qPCR machine StepOne™ plus	Applied Biosystems® by Life Technologies GmbH; Darmstadt, Germany
Synergy™ HT Multi-Mode Microplate Reader	BioTek Germany; Bad Friedrichshall, Germany
Thermomixer 5436	Eppendorf AG; Hamburg, Germany

2.1.9 Software

Table 9 Software

Software	Manufacturer
BD FACS Diva Software	Beckton Dickinson GmbH; Heidelberg, Germany
Microsoft Office 2016	Microsoft Corporation; Redmond, USA
IBM SPSS Statistics 22	IBM Deutschland GmbH; Ehningen, Germany
NCBI/ Primer-BLAST	www.ncbi.nlm.nih.gov/tools/primer-blast/
Legendplex	https://legendplex.qognit.com/workflow
Biorender	www.biorender.com/
GraphPad Prism v10	Dotmatics, GraphPad Software; Boston, USA
StepOne™ Software v2.2.2	Applied Biosystems® by Life Technologies GmbH; Darmstadt, Germany
FlowJo 10.8.1	FlowJo, LLC Data Analysis Software; Ashland, USA
Primer Express 3.0.1	Applied Biosystems® by Life Technologies GmbH; Darmstadt, Germany

2.2 Methods

2.2.1 Cell biological methods

CD34 hematopoietic stem cells sorted from cord blood and buffy coat samples were differentiated into CD34LC according to an established protocol in the lab (ref. Allam et al, JID 2004). Subsequently, Toll-like receptor ligands and other chemical stimuli were applied to the CD34LC, followed by the assessment of LC surface molecules, migration capacity, cytokine production, and sorting of CD1a cells. These analyses were conducted using flow cytometry, transwell migration assays, magnetic-activated cell sorting (MACS®), and cytokine bead assays, respectively.

2.2.1.1. Isolation of peripheral blood mononuclear cells (PBMC) from human cord blood and buffy coat

Human cord blood samples generously provided by Johanniter-Hospital Bonn and St. Marien-Hospital Bonn, Germany, and buffy coats sourced from voluntary blood donors at the University Hospital Bonn were obtained with ethical approval from the local ethics committee of the University of Bonn, following the principles of the Declaration of Helsinki. Cord blood or buffy coat specimens were collected in 50 mL tubes containing 250 µL of Heparin and stored at 4°C until further processing. The isolation of PBMCs involved the use of Lymphoprep™ density gradient medium. Diluted at a 1:2 ratio with PBS, carefully layered onto the Lymphoprep™ gradient, and subjected to centrifugation (800 x g, 20°C, 28 min, without brake). The resulting interphase, enriched with PBMCs, was meticulously collected. Following isolation, the collected PBMCs underwent subsequent processing for magnetic-activated cell sorting (MACS®) to isolate CD34 hematopoietic stem cells. Details information in Section 2.2.1.9. This method ensures a high-quality isolation of PBMCs and allows for the targeted extraction of CD34 hematopoietic stem cells for further experimental analyses.

2.2.1.2. Utilization of magnetic-activated cell sorting (MACS®)

In this investigation, the MACS® technology employed by Miltenyi Biotec GmbH in Bergisch Gladbach, Germany. This methodology allowed us to augment specific cell populations within a heterogeneous single-cell solution accurately. Leveraging magnetic particles for labeling cell surface molecules, the AutoMACS Pro® Separator, also provided

by Miltenyi Biotec GmbH, generated a magnetic field, facilitating the efficient separation of these cells.

The preparation of PBMCs (see Section 2.1.1) commenced with an initial washing step involving 15 mL of PBS (centrifugation at 400 x g, 20°C, for 10 min). A subsequent wash followed suit, employing 25 mL of 4°C MACS buffer (centrifugation at 230 x g, 4°C, for 10 min). Following these preparatory steps, the cells were resuspended in 1 mL of 4°C MACS buffer and labeled with magnetic beads, adhering to the guidelines stipulated in the CD34 MicroBead Kit (Miltenyi Biotec GmbH). These meticulous efforts culminated in the successful isolation of CD34+ hematopoietic stem cells, poised for cryopreservation in liquid nitrogen (see Section 2.1.3) or for differentiation into CD34+ hematopoietic stem cell-derived Langerhans cells (CD34LC) (see Section 2.1.4).

Isolate CD1a+ cells from the CD34LC population, adhered to the manufacturer's protocol for the CD1a MicroBeads kit, also provided by Miltenyi Biotec GmbH in Bergisch Gladbach, Germany. The CD1a enriched cells were then resuspended in 1 mL of TRIzol® reagent (see Section 2.2.2) to enable subsequent RNA isolation.

To ensure the integrity and purity of our enriched cell fractions, a comprehensive validation was conducted through flow cytometry analysis (see Section 2.2.6).

2.2.1.3. Cryopreservation of CD34 hematopoietic stem cells

Freshly isolated CD34 stem cells were preserved in liquid nitrogen, ensuring their viability and usability in subsequent experiments conducted at later time points.

I. Freezing of CD34 hematopoietic stem cells

CD34 hematopoietic stem cells underwent an enumeration process utilizing a Neubauer-improved hemocytometer, followed by centrifugation (300 x g, 4°C, 5 min). Subsequently, the cells were suspended in 1 mL of freezing medium and cautiously transferred into a 1.8 mL cryogenic tube. Employing a controlled slow freezing method within an isopropanol freezing container, the cells experienced gradual cooling at a rate of 1°C/min. To initiate the stabilization process, the cells were initially stored at -70°C for one day, paving the way for their subsequent seamless transfer into liquid nitrogen for extended-term preservation.

II. Thawing of CD34 hematopoietic stem cells

The process of thawing CD34 hematopoietic stem cells from liquid nitrogen is followed by controlled thawing in a 37°C water bath. Subsequent to thawing, the cells underwent

washing in 37°C RPMI Medium 1640 supplemented with GlutaMAX™-I (Gibco®), facilitated by centrifugation (300 x g, 20°C, 10 min). The cell concentration was then precisely adjusted to a range of 0.6 to 0.8 x 10^6 cells/mL in CD34 medium, preparing them for the subsequent steps (see Section 2.1.4), dedicated to the generation of in vitro-derived CD34LC.

2.2.1.4. *In vitro* generation of CD34 hematopoietic stem cell-derived LC (CD34LC)

Freshly isolated or thawed CD34 hematopoietic stem cells were adjusted to achieve a concentration within the range of 0.6 to 0.8 x 10^6 cells/mL in CD34 medium. Following this preparation, the cells were cultured in a 24-well plate under optimal conditions, maintaining the culture at 37°C with 5% CO2 for a duration spanning 8 to 10 days (details culture conditions in Table 10). Harvesting of the cells was performed within the timeframe of days 8 to 10. Subsequently, flow cytometry analysis was conducted to assess the LC phenotype (see Section 2.1.9). The generated CD34LC was utilized for further experiments, showcasing the systematic progression of the experimental workflow.

Table 10: Culture conditions for CD34 hematopoietic stem cell-derived LC. The table below outlines the final concentrations of culture components.

Reagent	Day 0	Day 2	Day 4	Day 6	Day 10
GM-CSF	300 U/mL		200 U/mL		300 U/mL
mIgE	10^3 ng/mL	10^3 ng/mL	10^3 ng/mL	10^3 ng/mL	10^3 ng/mL
FLT3L	10 ng/mL				
SCF	10 ng/mL				
TGF-ß	0.5 ng/mL		0.5 ng/mL		0.5 ng/mL
TNF-α	20 U/mL				
Culture volume / well	0.50 mL	0.50 mL	0.75 mL	0.75 mL	1.00 mL

2.2.1.5. Toll-like receptor-ligands priming and stimulate on CD34LC

During the culture period, the initiation of the priming treatment was scheduled for day 6 or 7 of the experiment. CD34LC were comprising exposure to 10 ng/mL Pam3Cys or 1.0 ng/mL LPS, while untreated cells served as controls. Each treatment regimen was administered every 24 h, repeated a total of three times throughout this priming phase.

After the completion of the third priming treatment 24 h, CD34LC were ready to stimulation. Cells were adjusted to a concentration of 10^6 cells/mL and uniformly distributed into 24-well plates, with each well containing 1 mL of the cell suspension. Then cells were stimulated with 1.0 µg/mL Pam3Cys or 100 ng/mL LPS(Details information in Table 11) for 6 or 24 h or indicated time, while unstimulated cells served as controls, incubation at 37°C with 5% CO^2. The ensuing effects of stimulation were comprehensively assessed through flow cytometry analysis performed on all CD34LC (see Section 2.1.7).

Furthermore, the CD1a enriched cell fractions (see Section 2.1.8) underwent detail examination through quantitative polymerase chain reaction (qPCR) analysis (see Section 2.2.4) and TaqMan® MicroRNA Assays (see Section 2.2.5).

Table 11: Ligands for TLR-mediated stimulation of CD34LC

Stimulant / treatment	Derived from	Final concentration	Used as ligand for	Achieved from
Pam3Cys	Synthetic triacylated lipopeptide	1.0 µg/mL	TLR1 / TLR2	EMC microcollections GmbH; Tuebingen, Germany
LPS	E. coli 0111:B4	0.1 µg/mL	TLR4	InvivoGen; San Diego, USA
FSL-1	Synthetic diacylated lipoprotein derived from Mycoplasma salivarium	16.6 x 10^{-3} µg/mL	TLR2 / TLR6	EMC microcollections GmbH; Tübingen, Germany

2.2.1.6. Exposure of CD34LC to pharmacological compounds

On day 8 for cord blood CD34LC or day 14 for buffy coat CD34LC, after the completion of the third priming treatment, a subsequent phase involving the application of specific pharmacological agents was initiated. This phase was characterized by the introduction of various compounds targeting different pathways and cellular mechanisms. The selected compounds included, Vitamin D analogues 1.25$(OH)_2$-D_3 (10 nM), hydrocortisone (2.7 µM), tacrolimus (10 µM), JAK inhibitors including JAK1/2 inhibitor ruxolitinib (10 µM), JAK1 inhibitor filgotinib (10 µM), JAK2 inhibitor BMS-911543 (10 µM), and JAK3 inhibitor VX-509 (10 µM) (details information in table 1). Cells were exposed to these pharmacological agents for a duration of 12 h, and DMSO was used as a negative control at an equal concentration. Subsequent to this treatment phase, cells were adjusted to a standardized concentration of 10^6 cells/mL, setting the stage for the subsequent. During this phase,

cells were stimulated with 1.0 µg/mL Pam3Cys, following a similar protocol as mentioned previously, extending the stimulation for 24 h or a specified duration.

2.2.1.7. Flow cytometry Analysis

Surface immunofluorescence staining methods were employed to assess various aspects, including CD34+ hematopoietic stem cell enrichment, CD1a cell identification, characterization of the CD34LC phenotype, and the evaluation of treatment effects. The specific antibodies utilized for staining in this study are details in Table 5. The first antibody stained with 5 x 10^4 cells in a total volume of 100 µL FACS buffer at 4°C for 25 min. Subsequently, washing was performed in 1 mL FACS buffer (400 x g, 4°C, 3 min). Viability assessment of the cells was conducted through 7-AAD stained with the same cell number and buffer volume for 25 min, then washing as above. Goat anti-mouse IgG added and incubated for 10 min for blocking, then the second (mix) antibody stained for 25 min and washed as the above.

The stained cells were measured and analyzed using a FACSCanto™ flow cytometer from Beckton Dickinson GmbH (Heidelberg, Germany) and analyzed with FACSDiva™ software. Alternatively, data analysis was performed using FlowJo 7.6.1 software from FlowJo, LLC Data Analysis Software (Ashland, USA).

2.2.1.8. The relative fluorescence index (rFI) calculation

The relative fluorescence index (rFI), which quantitatively measures the fluorescence intensity observed during the flow, was calculated for statistical analysis and calculated as follows:

$$\mathrm{rFI} = \frac{\mathrm{MFI\ target} - \mathrm{MFI\ isotype\ control}}{\mathrm{MFI\ isotype\ control}}$$

(MFI = mean fluorescence intensity)

2.2.1.9. Purity assessment of CD34 hematopoietic stem and CD1a+ cell enrichment

To evaluate the purity of CD34+ enriched cells (see Section 2.1.2), staining conducted with either 0.15 µg/mL PE-conjugated anti-CD34 monoclonal antibody (mAb) or 2.5 µg/mL PE-conjugated anti-IgG1 as an isotype control. This staining process was carried out for 15 min at room temperature. Regarding CD1a enriched cells (see Section 2.1.8), the mix antibody consisting of IgG2a-APC, IgG1-RD1, and 7-AAD, or CD14-APC, CD1a-RD1, and

7-AAD, respectively. The final concentrations of the respective antibodies employed for staining CD1a enriched cells can be found in Table 5.

2.2.1.10. Phenotypic characterization of CD34LC

The expression of specific surface molecules, staining using unconjugated mouse monoclonal antibodies targeting Langerin (CD207), FcεRI, TLR2, CD80, CD83, CD86, and MHC II. As an isotype control antibody, unspecific mouse IgG2b was utilized. Subsequently, FITC-conjugated goat-anti-mouse IgG polyclonal antibodies were employed as secondary antibodies. To prevent nonspecific binding, free antigen-binding sites were blocked using 2.5 mg/mL of mouse serum for 15 min at 4°C. Finally, an antibody mix comprising IgG2a-APC, IgG1-RD1, and 7-AAD, or CD14-APC, CD1a-RD1, and 7-AAD, as appropriate, was introduced. Details regarding the concentrations of antibodies utilized for surface staining are provided in Table 12 below.

Table 12 Antibody concentrations used for surface staining

Antibody		Stock concentration (mg/mL)	Working concentration (µg/mL)	Volume per test (µL)	Final concentration (µg/mL)
1st	IgG2b, κ	1.0	50	5	2.5
	Langerin (CD207)	0.2	50	5	2.5
	FcεRIα	1.0	50	5	2.5
	TLR2	0.2	50	5	2.5
	CD83	0.2	50	5	2.5
	CD80	0.2	50	5	2.5
	CD86	0.2	50	5	2.5
	MHC II				
	CCR6	0.2	50	5	2.5
	IgG2a, κ	1.0	50	5	2.5
	CCR7	0.2	50	5	2.5
Blocking	Goat anti-mouse IgG, Fcγ	1.0	50	5	2.5

Mix(2nd)	IgG2a-APC	0.011	2.75	5	0.14
	CD14-APC	0.011	2.75	5	0.14
	IgG1-RD1	1.0	50	3	1.5
	CD1a-RD1	0.25	25	3	0.75
	7-AAD	1.0	50	2	1.0

2.2.1.11. Gating strategy for CD1a in *in vitro* generated CD34LC (details in results 3.1).

2.2.1.12. Migration transwell

Cell migration was evaluated utilizing a 24-well transwell chamber (5.0 µm, Corning, NY, USA) in a transwell migration assay. Cells were either left unstimulated (-) or stimulated (+) with Pam3Cys (1 µg/mL) for 24 h. Following 24 h of stimulation, harvested 1×10^6 cells of each condition, were centrifuged at 400×g, for 5 min, and resuspended at 100 µL. This cell suspension was transferred into the upper compartment of each transwell chamber. 300 µL complete medium with 1 µg/mL of chemokine CC19L warmed at 37 °C then carefully added to the lower compartment. Subsequently, the transwell chambers were incubated at 37°C in a 5% CO2 environment for 6 h. Following the incubation period, the cells that successfully migrated into the lower compartment were collected and analyzed. Migrated cells were counted into the average number and analyzed for CD1a expression by flow cytometry.

2.2.1.13. Flow cytometry-based cytokine analysis

Cytokines were analyzed using flow cytometry, employing BioLegend's LEGENDplex™ assays, which operate on the principles of bead-based immunoassays similar to sandwich immunoassays. Beads, distinguished by size and internal fluorescence, were conjugated with specific antibodies and acted as capture beads for individual analytes. When mixed with a sample containing target analytes, each analyte is bound to its corresponding capture bead. Following washing, a biotinylated detection antibody cocktail formed capture bead-analyte-detection antibody sandwiches. Subsequent addition of streptavidin labeled with PE produced fluorescent signals proportional to bound analytes. Flow cytometry allowed for the differentiation of analyte-specific populations, with PE signals

quantified. The concentration of each cytokine was calculated using LEGENDplex™ 7.0 data analysis software, with two sets of beads differentiated by size and further resolved based on internal APC intensities. This method, employing six populations for smaller beads (A) and seven populations for larger beads (B), associated each analyte with a specific bead set.

The Human Inflammation Panel 1(IL-1β, IFN-α2, IFN-γ, TNF-α (TNFSF2), CCL2 (MCP-1), IL-6, CXCL8 (IL-8), IL-10, IL-12p70, IL-17A, IL-18, IL-23, IL-33) was used to analyze the supernatants from CD34LC cultures (see Section 2.1.4), which were collected after stimulation 24 h and stored at ≤ -80°C. The V-bottom Plate was utilized for the assay, following the manufacturer's instructions. Thawing aliquots of supernatant and preparing antibody-immobilized beads, wash buffer, and standard were performed as the manufacturer's instructions. The standard involved serial 1:4 dilutions from C7 to C1, supplemented with an assay buffer for the 0 pg/mL standard (C0). All reagents were acclimated to room temperature (20 - 25°C) before use. Throughout the process, the plate remained upright and covered with aluminum foil during incubation steps. Standards and samples were duplicated in a specified order on the plate. The prescribed sequence involved adding assay buffer, matrix, standards, samples, and mixed beads, followed by incubation on a shaking plate at 500 rpm for 1 to 2 h at room temperature. Post-incubation, centrifugation at 800 × g for 5 min using a swinging bucket rotor (G.H 3.8) with a microplate adaptor was conducted, and the supernatant or wash buffer was removed. The washing step entailed adding 200 µL of wash buffer into each well, incubating for one minute, and then centrifuging at 800 × g for 5 min. Following this, SA-PE was added with 30 min incubation before repeating the washing step. The beads in each well were finally resuspended with 150 µL of wash Buffer. Subsequently, samples were read on the flow cytometer, following the manual's instructions for proper setup. The assay FCS files are analyzed by BioLegend's LEGENDplex™ data analysis online (https://legendplex.qognit.com/workflow).

2.2.2 Molecular biological methods

Magnetic-activated cell sorting (MACS®) to isolate CD1a+ cells from the CD34LC population. Subsequently, RNA isolation was performed to capture LC molecules, cytokines, microRNAs, molecules associated with the TLR2 pathway, and negative regulators. Following reverse transcription into mRNA, these samples were subjected to quantitative real-time PCR (qPCR) analysis to evaluate gene expression levels.

2.2.2.1. Quantification and assessment of nucleic acid concentration and purity

The concentrations and purity of nucleic acids were determined utilizing the Synergy™ HT Multi-Mode Microplate Reader manufactured by BioTek Germany in Bad Friedrichshall, Germany. Measurements were conducted by assessing RNA and DNA at a wavelength of λ = 260 nm. Purity evaluation was carried out by examining the λ 260/280 ratio. Data analysis and calculations were performed using the Gen5™ software from BioTek Germany in Bad Friedrichshall, Germany. Each nucleic acid and reference sample underwent measurement using 2 µL, accompanied by nuclease-free water for RNA reference or 5 mM Tris/HCL buffer for DNA reference.

2.2.2.2. RNA isolation

For CD1a enriched cells (see Section 2.1.9), RNA extraction was performed using the phenol/chloroform method with TRIzol® reagent, following the recommended protocol provided by the manufacturer. The resulting RNA was subsequently resuspended in 25 µL of nuclease-free water. To eliminate any DNA contamination, the DNA-free™ DNA Removal Kit (Ambion®, Life Technologies GmbH; Darmstadt, Germany) was utilized in accordance with the manufacturer's instructions. Subsequent assessments involved evaluating RNA concentration and purity (see Section 2.2.2). The isolated RNA underwent additional processing, including reverse transcription to cDNA for gene expression experiments (see Section 2.2.3), utilization in TaqMan® MicroRNA Assays (see Section 2.2.5), or storage at -70°C for future use.

2.2.2.3. Reverse transcription for gene expression experiments

In the process of preparing complementary DNA (cDNA), RNA underwent reverse transcription. Specifically, 1 µg of RNA dissolved in 15.5 µL of nuclease-free water was initially denatured at 65 °C for 3 min and subsequently transferred directly onto ice.

Following this, 34.5 µL of a reverse transcription reaction mix (details information in Table 12) was added to the RNA, and the resulting mixture was incubated at 37 °C for 1 hour. The reaction was halted by heating to 95 °C for 3 min. The volume of the cDNA was adjusted to 100 µL using nuclease-free water. The resultant cDNAs were either immediately utilized in quantitative PCR (qPCR) or stored at -20 °C for future applications.

Table 13: Components of the reverse transcription reaction Mix

Reagent	Final concentration
5x reverse transcription buffer	1x
dNTP	4 µM (each)
DTT	100 µM
Final volume	34.5 µL
Random primer	2.4 ng/µL
RNAsin	1 U/µL
SuperScript™ Reverse Transcriptase	4 U/µL

2.2.2.4. Quantitative real-time PCR (qPCR) for gene expression analysis

The process commences with the reverse transcription of mRNA into cDNA. Subsequently, the amplification of this cDNA is tracked in "real-time" utilizing a fluorescence dye such as SYBR® Green, binding to double-stranded DNA sequences, or through fluorescence-labeled specific oligonucleotide probes, as observed in TaqMan® MicroRNA Assays (see Section 2.2.5). The accumulation of amplification products leads to an upsurge in fluorescence intensity. The cycle threshold (Ct) is reached when the amplification-based signals surpass the background fluorescence. The Ct value indicates the number of cycles necessary to exceed this threshold.

In this study, the iTag™ SYBR® Green Supermix with ROX™ was utilized. This compound comprises SYBR® Green I, a DNA dye with an absorption maximum at λ = 497 nm and an emission maximum at λ = 520 nm. Additionally, it incorporates ROX™, a passive reference dye employed to normalize fluorescence variations unrelated to PCR processes. The qPCR experimentation and subsequent data analysis were conducted using StepOnePlus™ qPCR devices alongside StepOne™ Software v2.2.2

(manufactured by Applied Biosystems® and provided by Life Technologies GmbH; Darmstadt, Germany). For the generation of amplicons, synthetic DNA molecules mimicking the gene sequences specific to particular primer pairs were utilized. The design of these amplicons and primers (details to Table 6) was executed utilizing Primer Express 3.0.1 software, also from Applied Biosystems® under Life Technologies GmbH in Darmstadt, Germany. Primer specificity for target genes was validated using NCBI/Primer-BLAST (www.ncbi.nlm.nih.gov/tools/primer-blast/).

Absolute quantification of gene expression transcripts was achieved by employing standard curves with a defined number of amplicon molecules, calculated based on their nanomolar quantity as indicated by the manufacturer as follows:

$$\text{Molecules} = x \text{ mole} * 6.022 * 10^{23}$$

The amplicon stock solutions were adjusted to a concentration of 3 x 10^13 molecules/µL in nuclease-free water and stored at 4°C. To establish standard curves, a series of six dilutions were prepared, covering concentrations ranging from 3 x 10^8 molecules/µL to 3 x 10^3 molecules/µL. Six standard curves corresponding to a specific primer pair. Mean Ct values were plotted against these concentrations (see Figure 2). Utilizing the linear function derived from the regression line, quantities of molecules were determined. The outcomes were then normalized to 10^3 molecules of actin. Importantly, the primer efficiency exceeded 80%.

The qPCR master mix (details in Table 14) was prepared, reaching a total volume of 9µL and dispensed into 96-well plates. Following this, 1 µL of target cDNA (see Section 2.2.3), standard dilution series, or nuclease-free water for the non-template control was added to the respective qPCR master mix wells. All samples and controls were processed in triplicates to ensure robustness and reliability.

The cycling conditions are succinctly summarized in Table 15, were employed for the amplification process. Additionally, a melting curve analysis was conducted to identify any presence of primer dimers or PCR byproducts, ensuring the specificity and reliability of the results obtained.

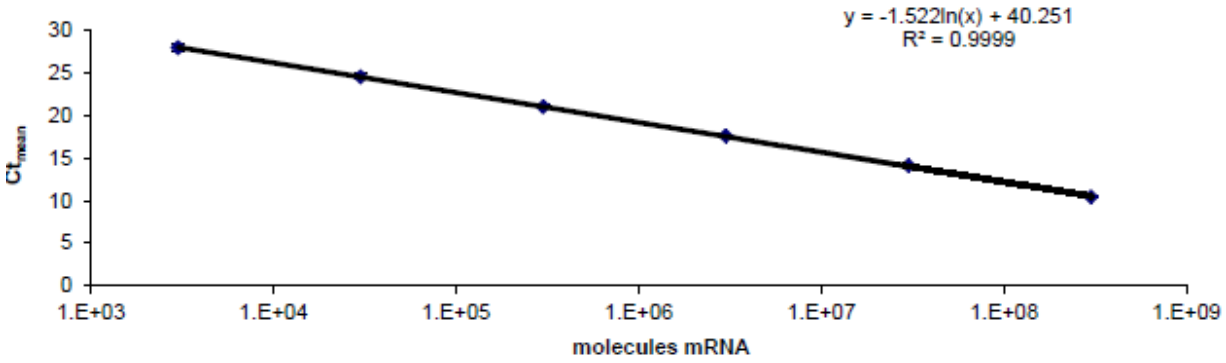

Figure. 4: Standard curve for actin gene expression

A dilution series of the actin amplicon was prepared as details in the text. The regression line was generated using the mean Ct values obtained from n= 6 experiments.

cDNA samples:

$$y = -1.522 * \ln(X) + 40.251$$

$$x = EXP((y-40.251)/(-1.522))$$

Table 14 Components of qPCR reaction mix for gene expression experiments. Forward and reverse primers were mixed together (1:1).

Reagent	Volume	Final concentration
iTaq™ SYBR® Green Supermix with ROX™ (2x)	5.0 µL	1x
Primer mix (5 µM)	0.4 µL	0.2 µM
cDNA / standard dilution / nuclease-free water	1.0 µL	10%
Nuclease-free water	3.6 µL	-
Final volume	10.0 µL	

Table 15 Thermal cycling conditions for qPCR for gene expression experiments (40 cycles)

Step	Duration	Temperature
Initial denaturation	10 min	95 °C
Denaturation	15 s	95 °C

Annealing and elongation	1 min	60 °C
Melting curve	15 s	+0.3 °C (until 95 °C)

2.2.2.5. MicroRNA assays

TaqMan® MicroRNA Assays (Life Technologies GmbH; Darmstadt, Germany) were employed for the detection and quantification of mature miRNA molecules. The short length of mature miRNA molecules, approximately 22 nucleotides, presents challenges for conventional reverse transcription reactions using random hexamer or oligo-desoxythymidine primers. The kit offers specialized small miRNA-specific stem-loop primers designed exclusively for reverse transcription of mature miRNA. These stem-loop primers form a complex with the miRNA, enabling a 3' extension of the synthesized cDNA, thereby facilitating subsequent hybridization with the reverse qPCR primer. The forward primer used in this assay is complementary to the miRNA sequence.

During the qPCR process, cDNA amplification is monitored using specific TaqMan® MGB probes. These probes incorporate a reporter dye (FAM™ dye) and a nonfluorescent quencher, which serves to suppress the reporter fluorescence signal. The probes are designed to anneal specifically to complementary amplified DNA sequences positioned between the forward and reverse primer sites. In the subsequent polymerization step, the hybridized probes are cleaved by a hot-start DNA polymerase, leading to the separation of the reporter dye from the probe. Once released, the fluorescence of the isolated reporter dye is no longer suppressed by the quencher molecule and becomes detectable by the qPCR device.

TaqMan® MicroRNA Assays targeting miRNA-155-5p, miRNA-146a-5p, and RNU48 (an endogenous control) were conducted in accordance with the manufacturer's guidelines. The reverse transcription PCR was conducted utilizing 10 ng of total RNA isolated from TRIzol® samples (see Section 2.2.2) in a 15 µL reaction volume, employing the Mastercycler nexus gradient from Eppendorf. The thermal cycling conditions for this process were as follows: 30 min at 16°C, 30 min at 42°C, 5 min at 85°C, and then holding indefinitely at 4°C. The resulting products were subsequently diluted 1:1 (v/v) with nuclease-free water and were either employed in TaqMan® qPCR reactions or stored at -20°C for a duration of up to one week.

QPCR procedures were carried out in triplicates, with 1 µL of cDNA per 9 µL reaction mix (details in Table 16). The processing and analysis of TaqMan® MicroRNA Assays were executed utilizing the StepOne™ plus machine and StepOne™ Software v2.2.2 (both products of Applied Biosystems® under Life Technologies GmbH in Darmstadt, Germany). The thermal cycling conditions for qPCR in Table 17

Table 16 Composition of qPCR reaction mix for TaqMan® MicroRNA Assays

Component	Volume per reaction	Final concentration
TaqMan® small RNA Assays (20x)	0.5 µL	1x
TaqMan® Universal PCR MasterMix II (2x), no UNG	5.0 µL	1x
Nuclease-free water	3.5 µL	3.5%
cDNA	1.0 µL	1.0%
Final volume	10.0 µL	

Table 17 Thermal cycling conditions for qPCR for TaqMan® MicroRNA Assays (40 cycles)

Step	Duration	Temperature
Initial denaturation	10 min	95°C
Denaturation	15 s	95°C
Annealing and elongation	1 min	60°C

3. Results

In this study, CD34LC were investigated as the LC model *in vitro.*

3.1 LC from CD34 hematopoietic stem cells show the phenotype of LC.

CD34LC cultured *in vitro* (as outlined in Section 3.1.4) needed validation as a suitable cellular model. Following the generation of CD34 hematopoietic stem cells for a duration of 6 to 8 days, the phenotypic and maturation status of CD34LC were assessed via flow cytometry analysis. Cellular gating was performed based on morphological characteristics, viability assessed through 7-AAD staining, and CD1a expression, the gating strategy showed in Figure 5. Subsequently, these CD1a+ cells were further studied for Langerin expression as well as other maturation-associated markers of LC(Merad et al., 2008).

Upon 6 to 8 days of *in vitro* generation, CD34LC exhibit a population containing approximately 30 to 70% CD1a+ cells, of which 65.11% (± 10.94%) express Langerin (Figure 6 and Table 18). The maturation-associated markers CD80, CD83, CD86, and MHC II were assessed on CD34LC (Figure 6 and Table 18). The relatively low or absent surface expression of CD83 indicates the immature phenotype of CD34LC.

In conclusion, the *in vitro* culture of CD34LC for 6 to 8 days resulted in developing LC-like phenotypes with an immature status, rendering them appropriate for subsequent study.

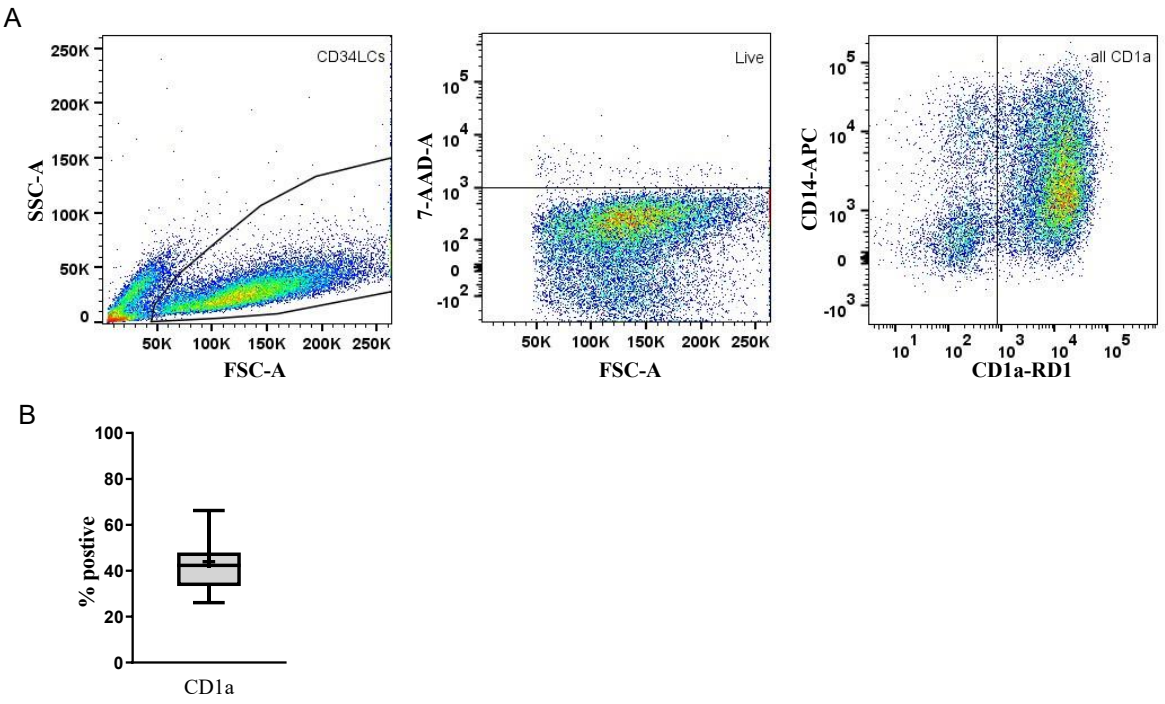

Figure. 5: Gating strategy for CD1a cell populations in *in vitro* generated CD34LC. Isolation of PBMCs from cord blood was achieved through density gradient medium separation, followed by CD34 hematopoietic stem cell enrichment utilizing MACS®. CD34LC were generated through a cultivation process of CD34 hematopoietic stem cells for 6 to 8 days, as described in the methods section. Subsequent analysis was conducted using flow cytometry. (A) The CD34LC population was gated using CD1a-RD1 and CD14-APC, with exclusion of dead cells using 7-AAD staining. (B) The percentage of CD1a-positive cells within the entire cell population is represented in the boxplots (n = 12), with the mean indicated by "+".

Table 18 *In vitro* generated CD34LC show LC phenotype.

Cell surface molecule	Positive expression of CD1a (mean±SD)
Langerin	65.11 ± 10.94
CD80	86.61 ± 6.39
CD83	4.75 ± 6.66
CD86	59.81 ± 16.21
MHC II	62.63 ± 27.37

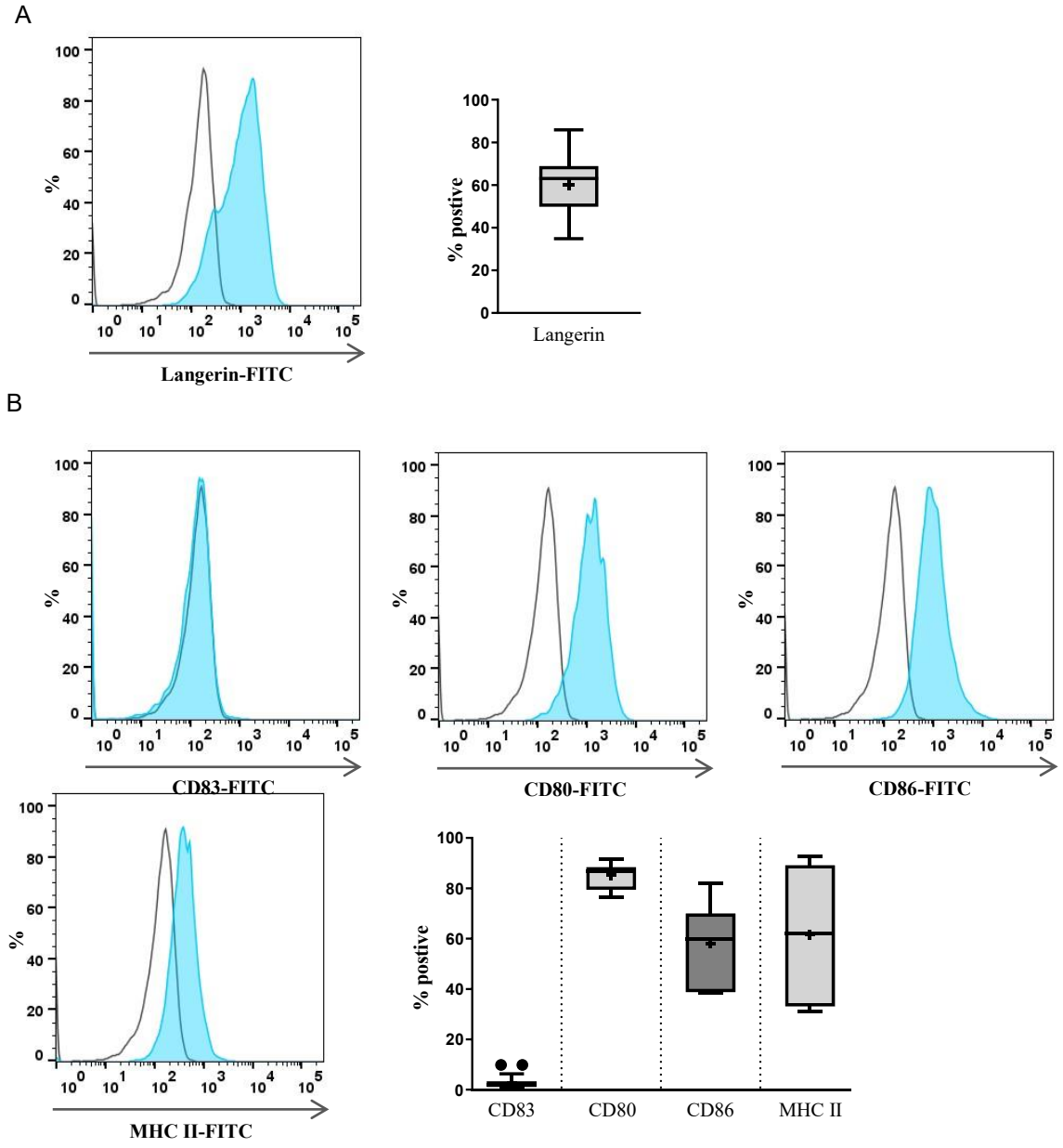

Figure. 6: Immature LC phenotype of *in vitro* generated CD34LC. CD34LC were generated in vitro as previously described. (A and B)Cells were stained with antibodies against Langerin, CD80, CD83, CD86, and MHCII (blue), while IgG2b (grey) served as an isotype, were counterstained with FITC-labeled goat anti-mouse IgG antibody. Subsequent analysis was conducted using flow cytometry. A representative histogram depicts the proportion of Langerin-positive cells within the CD34LC population. The percentage of indicated positive-cell populations is represented in the boxplots (n = 6-12), with the mean indicated by "+".

3.2 Low-dose ligand priming treatment establishes LC with low response to TLR2- and TLR4-driven activation.

The initial approach aimed to mimic the previous observations of tolerized LC in AD skin exhibiting impaired TLR2-driven activation and maturation(Iwamoto et al., 2018). Therefore CD34LC were generated *in vitro* and subjected to repeated exposure of low doses of the TLR2 ligand Pam3Cys.

CD34LC were divided into two main groups: the primed group and the unprimed control group. The primed group was subjected to a priming treatment using Pam3Cys or LPS at a low concentration (0.01 µg/mL and 1ng/ml respectively) for three consecutive days (Figure 7). As a control, the unprimed group was exposed to the culture medium without any treatment. Following the priming phase, both primed and unprimed CD34LC were exposed to high stimulation-concentrations of Pam3Cys (1 µg/mL) or LPS (100 ng/mL) (Figure 7). The maturation phenotype of CD34LC was assessed using flow cytometry analysis, aiming to elucidate the impact of the priming treatment on TLR2 or TLR4-driven activation and maturation.

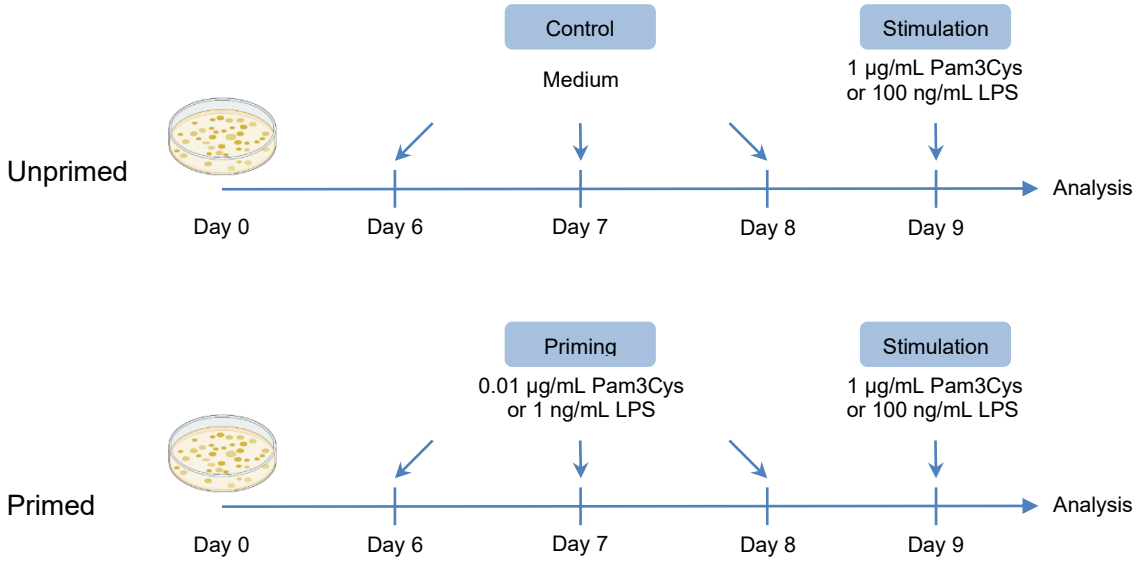

Figure. 7: Schematic flow chart of the priming treatment. CD34LC were cultured *in vitro for* 6 days, the primed group underwent a treatment by low dose Pam3Cys (0.01 µg/mL) or LPS (1 ng/mL) for three consecutive days or only the culture medium as a control. Following the priming phase, high stimulation concentrations of Pam3Cys (1 µg/mL) or LPS (100 ng/mL) were exposed to both primed and unprimed CD34LC.

3.2.1 Low-dose ligand priming treatment induces the tolerized LC in TLR2 and TLR4 homologous activation.

After the three-day priming treatment, there was no significant difference in the percentage of CD1a+ cells between the primed and unprimed groups (Figure 8A). The priming treatment led to a slight increase in the expression of CD83 and CD86 on CD34LC, while the expression of CD80 and MHC II mainly remained unchanged (Figure 8B). These primed cells did not exhibit activation, as indicated by the lack of notable changes in the overlap graph (Figure 8B left). These findings suggest that the priming treatment with low concentrations of TLR2 ligands mildly influenced CD34LC maturation but did not induce their activation.

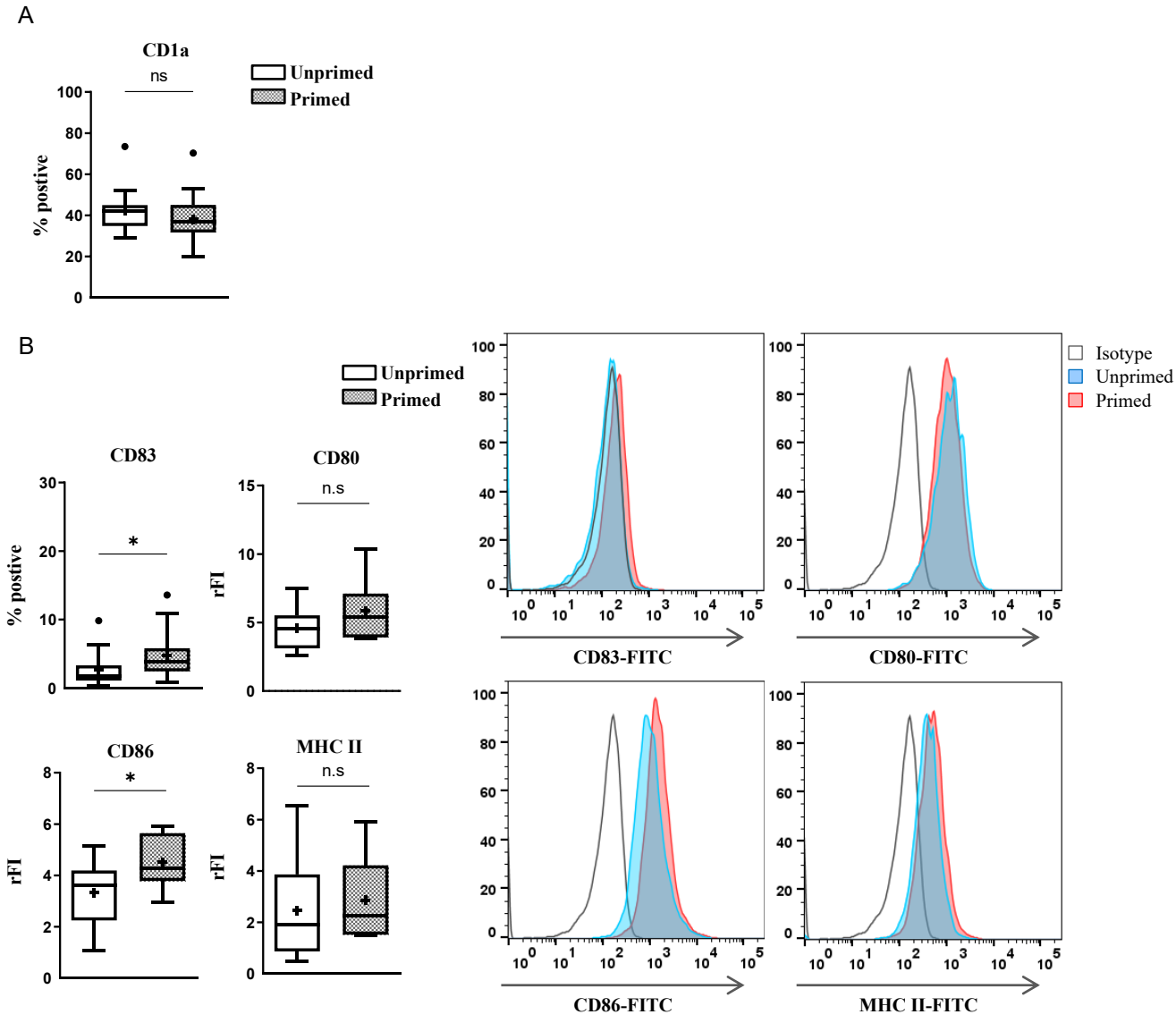

Figure. 8: Impact of priming treatment on CD34LC. CD34LC were cultured *in vitro for* 6 days, either in the absence (Unprimed) or presence (Primed) of Pam3Cys (0.01 µg/mL),

administered three times every 24 h. Cells were analyzed using Flow cytometry. (B) CD1a positive cells were identified by gating through CD1a-RD1 and CD14-APC.The percentage of CD1a positive cells within the total cell population is depicted through boxplots(n = 12), with the mean marked as "+". (C) Cells were stained with antibodies against CD80, CD83, CD86, and MHC II, or isotype control (empty). CD14 and CD1a gates were used, and dead cells were excluded using 7-AAD staining. Representative histograms illustrate unprimed (blue) and stimulated (red) cells, with results presented in boxplots (n = 6 -12), the mean is marked as "+", and outliers are represented as "●". Statistical significance was assessed using the Wilcoxon Signed Ranks Test in SPSS. *p < .05; **p < .01; ns indicates non-significant (p > .05). rFI, the relative fluorescence index.

Unprimed cells displayed a considerable increase in the expression of the maturation marker CD83 upon Pam3Cys stimulation following in both 6 h and 24 h. In contrast, the primed cells exhibited significant inhibition of CD83 upregulation, evidenced by the notably lower CD83 expression in primed cells following Pam3Cys exposure compared to unprimed cells. The priming treatment alone group did lead to a slight increase in CD83 expression, while its significantly lower expression than activated CD34LC (Figure 9A), indicated that only the priming treatment was insufficient to trigger CD34LC activation. This inhibitory effect induced by priming persisted at 6 h, 24 h, and even up to 96 h after Pam3Cys exposure (Figure 9B).

The effects of the priming treatment using the TLR4 ligand LPS were also investigated. Similar results were observed in CD34LC primed with LPS, where the priming treatment significantly suppressed the upregulation of CD83 in response to LPS exposure in unprimed cells (Figure 9C).

In summary, the application of a priming treatment involving low concentrations of TLR2-ligand Pam3Cys or TLR4-ligand LPS effectively rendered CD34LC hyporesponsive to TLR2-driven or TLR4-driven maturation in an *in vitro* setting, mirroring the behavior of tolerized LC isolated from AD skin.

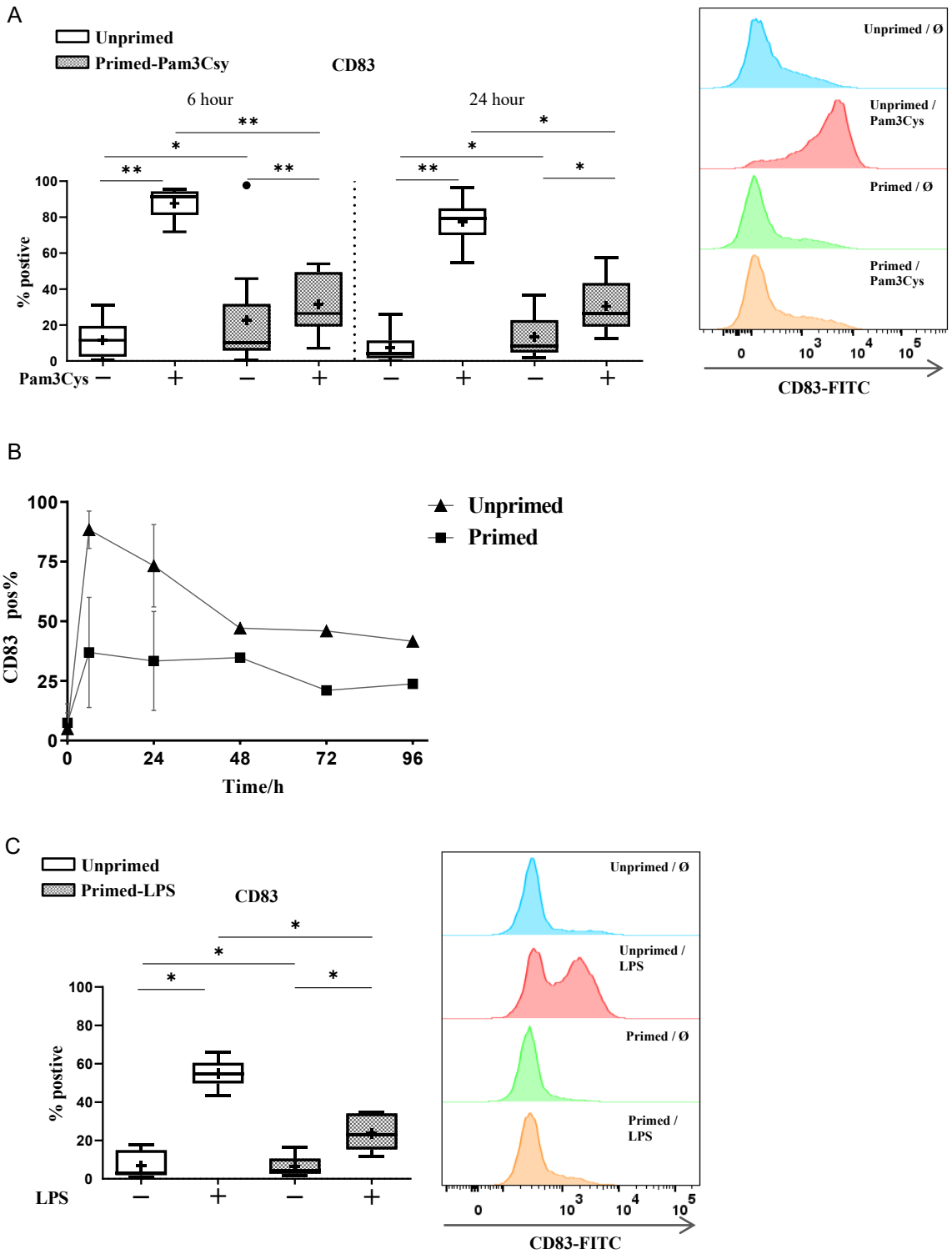

Figure. 9: Inhibition of maturation marker CD83 on primed CD34LC in TLR2 or TLR4-mediated activation. CD34LC were cultured in vitro for 6 days and subjected to either unprimed or primed conditions using the TLR2 ligand Pam3Cys (0.01 µg/mL) or the TLR4 ligand LPS (1 ng/mL), administered three times every 24 h. On day 9, cells were either left unstimulated (-) or stimulated (+). Primed-Pam3Cys cells and Primed-LPS cells were exposed to Pam3Cys (1 µg/mL) for indicated time (A and B) or LPS (100 ng/mL) for 24 h, respectively(C). Cells were labeled with antibodies targeting CD83(A n = 6-12, C n = 6) or an isotype control. Gating was performed using CD14 and CD1a markers, and dead cells

were excluded using 7-AAD staining. Flow cytometry was employed for analysis. CD83 results are presented as the percentage of positive cells within the population (Positive %). (B) Post priming or unprimed conditions, cells were either left unstimulated (-) or stimulated (+) with Pam3Cys (1 µg/mL) for 6, 24, 48, 72, and 96 h. The percentage of CD83 positive cells (CD83 %) was computed for each time point. Values are presented as mean ± SEM, originating from two independent experiments. The histogram represents one representative experiment depicting unprimed cells (blue), primed-Pam3Cys cells (red) and primed-LPS (orange) after Pam3Cys or LPS stimulation or medium control (empty). Results are presented as boxplots, with the mean indicated by "+", and outliers shown as "•". Statistical significance was assessed using SPSS, applying the paired Wilcoxon Ranks Test. P-values are shown the above graph.

3.2.2 Low-dose ligand priming treatment induces hyposensitive LC in heterologous activation between TLR2 and TLR4.

Tshe maturation phenotype of CD34LC was then analyzed using heterologous activation approaches. In this context, CD34LC were first primed with either Pam3Cys (TLR2 ligand), or LPS (TLR4 ligand). Subsequently, these primed cells were stimulated with the other TLR ligand (heterologous activation or cross-stimulation).

Primed-Pam3Cys cells exhibited notably diminished CD83 expression levels upon subsequent LPS exposure (Figure 10), while Primed-LPS cells similarly displayed reduced CD83 expression following Pam3Cys stimulation (Figure 10).

Additionally, the discrimination of ligand activation between the TLR2 and TLR4 exhibited CD34LC distinct responses to TLR2 and TLR4-driven stimulations, evidenced by the LPS-induced CD83 was significantly lower than Pam3Cys-induced in unprimed cells.

Thus, these findings showed that the priming-induced hyposensitivity of LC not only in TLR2 or TLR4-driven homologous activation but also extends to heterologous TLR2 and TLR4. Moreover, TLR2-activation discriminates between homologous and heterologous priming while TLR4-activation is less selective on the priming agent.

In conclusion, the priming strategy employed on CD34LC involving repeated exposure to low levels of TLR2 or TLR4 ligands effectively induced a hyposensitive state resembling the behavior of LC during TLR2-driven or TLR4-driven maturation, as observed *in vitro*. Moreover, extended investigations revealed that the tolerized CD34LC exhibited a similar hypo-responsive pattern not only upon homologous activation but also upon heterologous activation involving both TLR2 and TLR4 pathways. This indicates a broader impact of the priming treatment on the cellular responsiveness to various immune triggers.

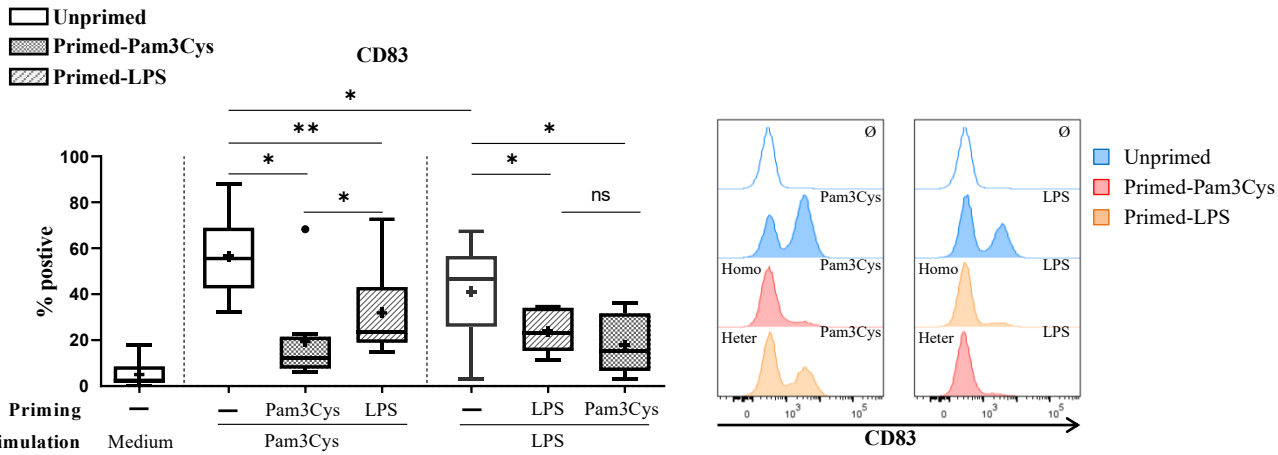

Figure. 10: Inhibition of maturation marker CD83 on primed CD34LC in TLR2 and TLR4 heterologous-mediated activation. CD34LC were cultured *in vitro* for 6 days, either in the absence (Unprimed) or presence (Primed) of Pam3Cys (0.01 µg/mL) or the TLR4 ligand LPS (1 ng/mL), administered three times every 24 h. On the 9th day, cells underwent either no stimulation (-) or were subjected to a 24-hour stimulation (+). Specifically, Primed-Pam3Cys cells were stimulated with LPS (100 ng/mL), while Primed-LPS cells were treated with Pam3Cys (1 µg/mL). Flow cytometry was employed for analysis. Cells were stained with CD83 antibodies or an isotype control. CD14 and CD1a gates were used, and dead cells were excluded using 7-AAD staining. Flow cytometry was employed for analysis. Representative histograms are indicated, and results are displayed as boxplots (n = 6-8), with the mean represented by "+", and outliers indicated as "●". Statistical significance was assessed using the Wilcoxon Signed Ranks Test in SPSS. *p < .05; **p < .01; ns indicates non-significant (p > .05).

3.3 Priming treatment-induced tolerization LC show impaired activation towards TLR2-driven stimuli.

Next, the effect of the priming on the maturation of LC was explored.

3.3.1 Priming treatment impaires CD34LC maturation upon TLR2 and TLR4-driven activation.

Flow cytometry and qPCR analyses were employed to investigate the phenotypic maturation of primed CD34LC.

Robust TLR2-driven maturation of CD34LC was witnessed by the upregulation of co-stimulatory markers, CD80 and CD86, as well as MHC II, upon exposure to Pam3Cys stimulation (Figure 11A). In contrast, primed CD34LC exhibited a significant downregulation in the expression of all the molecules mentioned above upon Pam3Cys stimulation (Figure 11A). Importantly, no significant differences in CD80, CD86, and MHC II expression levels were observed between the primed and unprimed without stimulus (Figure 11A).

MicroRNA-155 has been established as a crucial player in DC maturation and function, and its upregulation is known to be triggered by TLR ligands. Aligning with prior findings, a substantial increase in *MicroRNA-155A* levels in unprimed CD34LC following Pam3Cys stimulation was found (Figure 11B). In contrast, the expression of MicroRNA-155 was notably reduced in primed cells after Pam3Cys (Figure 11B).

Additionally, primed-LPS cells displayed marked inhibition in their response to LPS stimulation, as evidenced by a significant decrease in the expression of CD80, CD86, and MHC II (Figure 12).

An additional investigation was conducted to determine whether the impaired maturation observed with TLR2 ligand also applied to TLR4 ligand heterologous activation. CD34LC were initially primed with either Pam3Cys (a TLR2 ligand) or LPS (a TLR4 ligand). Following this priming, these cells were then stimulated with the alternate TLR ligand (heterologous activation or cross-stimulation). In primed-Pam3Cys cells, the expression levels of CD80, CD86, and MHC II were significantly dampened upon subsequent LPS stimulation, in contrast to the robust response observed in unprimed cells, where these molecules were notably upregulated (Figure 13). This compromised maturation pattern in tolerized CD34LC was consistently observed, as evidenced by the downregulation of CD80, CD86, and MHC II expression, which was also evident in Primed-LPS cells following Pam3Cys exposure (Figure 13).

These findings indicate that the priming treatment impaired the maturation of CD34LC in response to both TLR2- or TLR4-driven activation, as well as for the TLR2 and TLR4 heterologous stimulation.

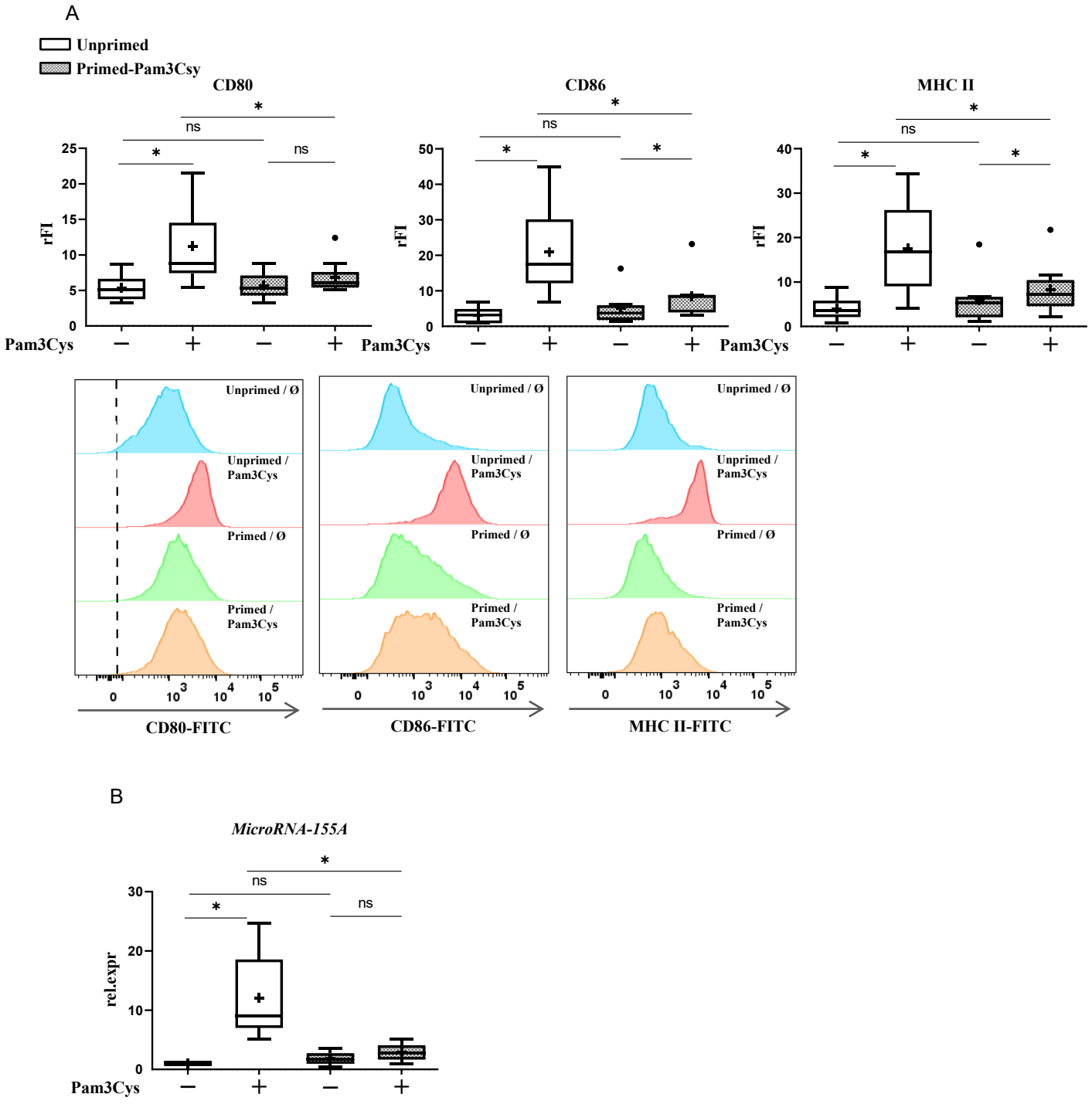

Figure. 11: Impaired maturation of primed CD34LC upon TLR2-mediated activation. CD34LC were generated in vitro as described above. Cells exposure to either the priming treatment (Primed) or were left untreated (Unprimed). Subsequently, cells were subjected to either no stimulation (−) or stimulation (+) with Pam3Cys (1 µg/mL) for 24 h for FACS (A) or 6 h for MicroRNA assay (B). (A) Cells exposure to either the priming treatment or were left untreated (Unprimed). Cells were stained with antibodies against CD80, CD86, MHC II, or an isotype control. CD14 and CD1a gates were utilized for selection, and dead cells were excluded using 7-AAD staining. Flow cytometry was employed to perform the analysis. (B) MicroRNA assay was conducted by sorting CD1a-positive cells through

magnetic separation, and *microRNA-155* levels were quantified and fold change presentation. Representative histograms are indicated, and results are displayed as boxplots (n = 6-12), with the mean represented by "+", and outliers indicated as "●". Statistical significance was determined using the Wilcoxon Signed Ranks Test in SPSS. *p < .05; **p < .01; ns indicates non-significant (p > .05).

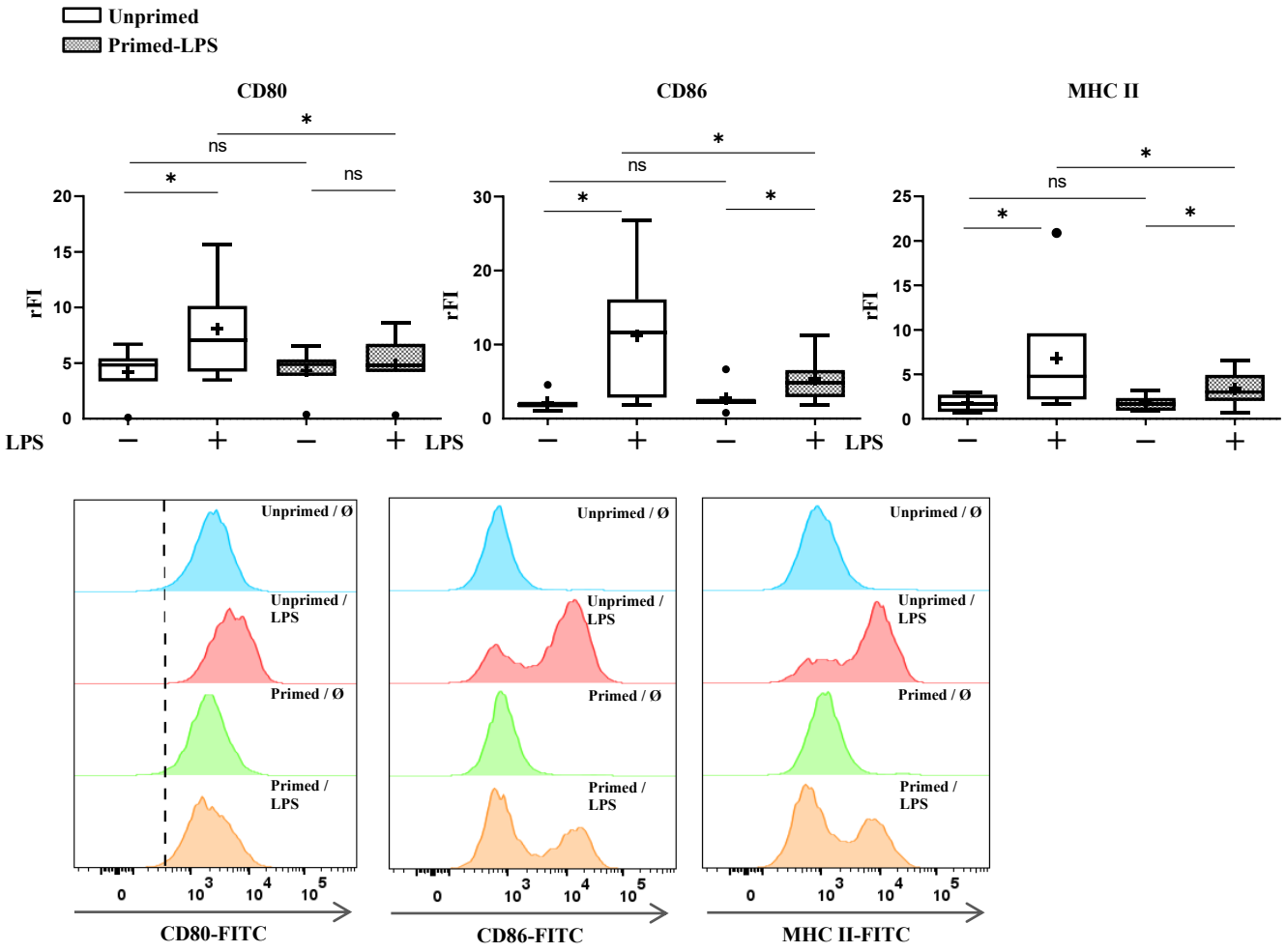

Figure. 12: Impaired maturation of primed CD34LC upon TLR4-mediated activation. CD34LC were cultured *in vitro* for 6 days, either in the absence (Unprimed) or presence (Primed) of the TLR4 ligand LPS (1 ng/mL), administered three times every 24 h. Cells were then either unstimulated (-) or stimulated (+) with the TLR4 ligand LPS (100 ng/mL) for 24 h. Flow cytometry was employed for analysis.Cells were stained with antibodies against CD80, CD86, MHC II, or an isotype control. CD14 and CD1a gates were utilized for selection, and dead cells were excluded using 7-AAD staining. Representative histograms are indicated, and results are displayed as boxplots (n = 6), with the mean represented by "+", and outliers indicated as "●". Statistical significance was determined using the Wilcoxon Signed Ranks Test in SPSS. *p < .05; **p < .01; ns indicates non-significant (p > .05).

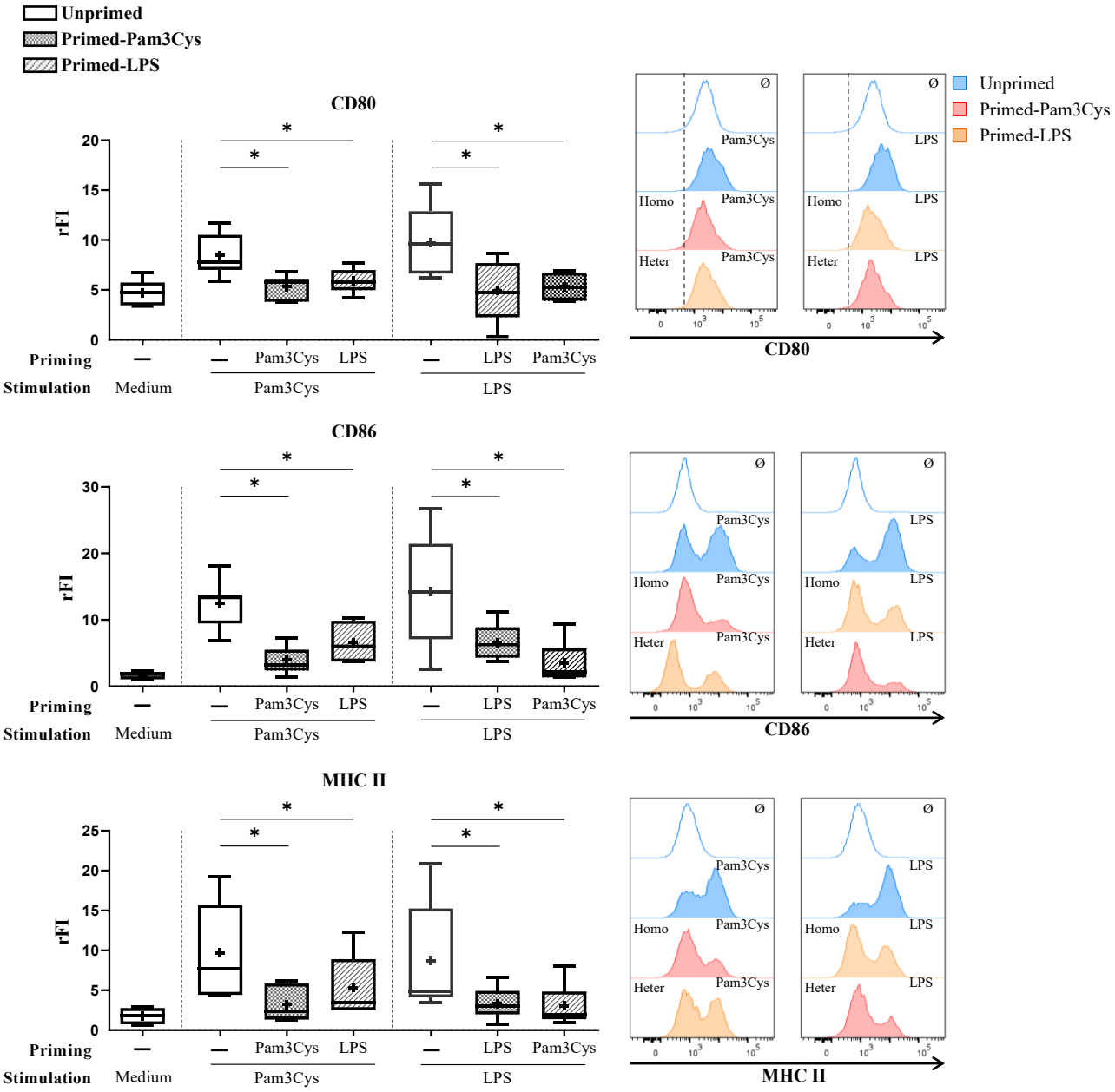

Figure. 13: Impaired maturation of primed CD34LC upon TLR2 or TLR4-mediated activation. CD34LC were cultured *in vitro* for 6 days, either in the absence (Unprimed) or presence (Primed) of Pam3Cys (0.01 µg/mL) or the TLR4 ligand LPS (1 ng/mL), administered three times every 24 h. On the 9th day, cells underwent either no stimulation (-) or were subjected to a 24-hour stimulation (+). Specifically, Primed-Pam3Cys cells were stimulated with LPS (100 ng/mL), while Primed-LPS cells were treated with Pam3Cys (1 µg/mL). Cells were stained with antibodies against CD80, CD86, MHC II, or an isotype control. CD14 and CD1a gates were utilized for selection, and dead cells were excluded using 7-AAD staining. Flow cytometry was employed to perform the analysis. Representative histograms are indicated, and results are displayed as boxplots(n = 6-12), with the mean represented by "+", and outliers indicated as "●".Statistical significance was determined using the Wilcoxon Signed Ranks Test in SPSS. *p < .05; **p < .01; ns indicates non-significant (p > .05).

3.3.2 Priming treatment impairs the TLR2-driven migratory competence of CD34LC.

In previous skin studies(Iwamoto et al., 2018), a reduced migratory activity of LC was observed, as well as migratory-associated molecules impaired in AD patients. Therefore, we explored whether the priming treatment influences the migratory activity of CD34LC in *the in vitro* setting. CCR6, a distinctive marker found on immature LC, is pivotal in maintaining LC within the tissue architecture(Doebel et al., 2017; Merad et al., 2008). Conversely, CCR7, typically expressed on activated cells, facilitates the migratory process towards lymph nodes(Doebel et al., 2017; Liu et al., 2021; Merad et al., 2008). The examination of CCR6 and CCR7 expression levels were investigated using flow cytometry analysis and qPCR.

Upon Pam3Cys stimulation, unprimed CD34LC exhibited a notable reduction in CCR6 expression coupled with an elevation in CCR7 expression, indicative of an alteration in their migratory behaviour (Figure 14A). Intriguingly, primed CD34LC demonstrated a significant CCR6 reduction and this downregulation persisted despite subsequent Pam3Cys stimulation (Figure 14A). In contrary, the priming treatment did not induce any noticeable alteration in CCR7 expression, and subsequent Pam3Cys stimulation also failed to induce significant changes (Figure 14A). Parallel results were observed at the mRNA level (Figure 14A). These findinsgs suggest a modulation of crucial migration-associated molecules in CD34LC.

To further unravel the migratory potential of CD34LC, a transwell assay employing CCL19(Doebel et al., 2017; Liu et al., 2021), the ligand for CCR7, was established. This assay enabled the quantification of migrated cells, thereby providing insight into the maturation migratory capacity of CD34LC. In the transwell assay, using CCL19, unprimed CD34LC exhibited a notable increase migration (Figure 14B), indicating the propensity of TLR2-driven activation to induce spontaneous migratory behavior in CD34LC. Conversely, in primed cells, the count of migrated cells witnessed only a marginal rise following subsequent Pam3Cys stimulation and notably fewer than the unprimed condition (Figure 14B).

Thus, these outcomes suggest an alteration in the migratory capability of tolerized CD34LC, as evidenced by the expression of migratory molecules and their migration activity.

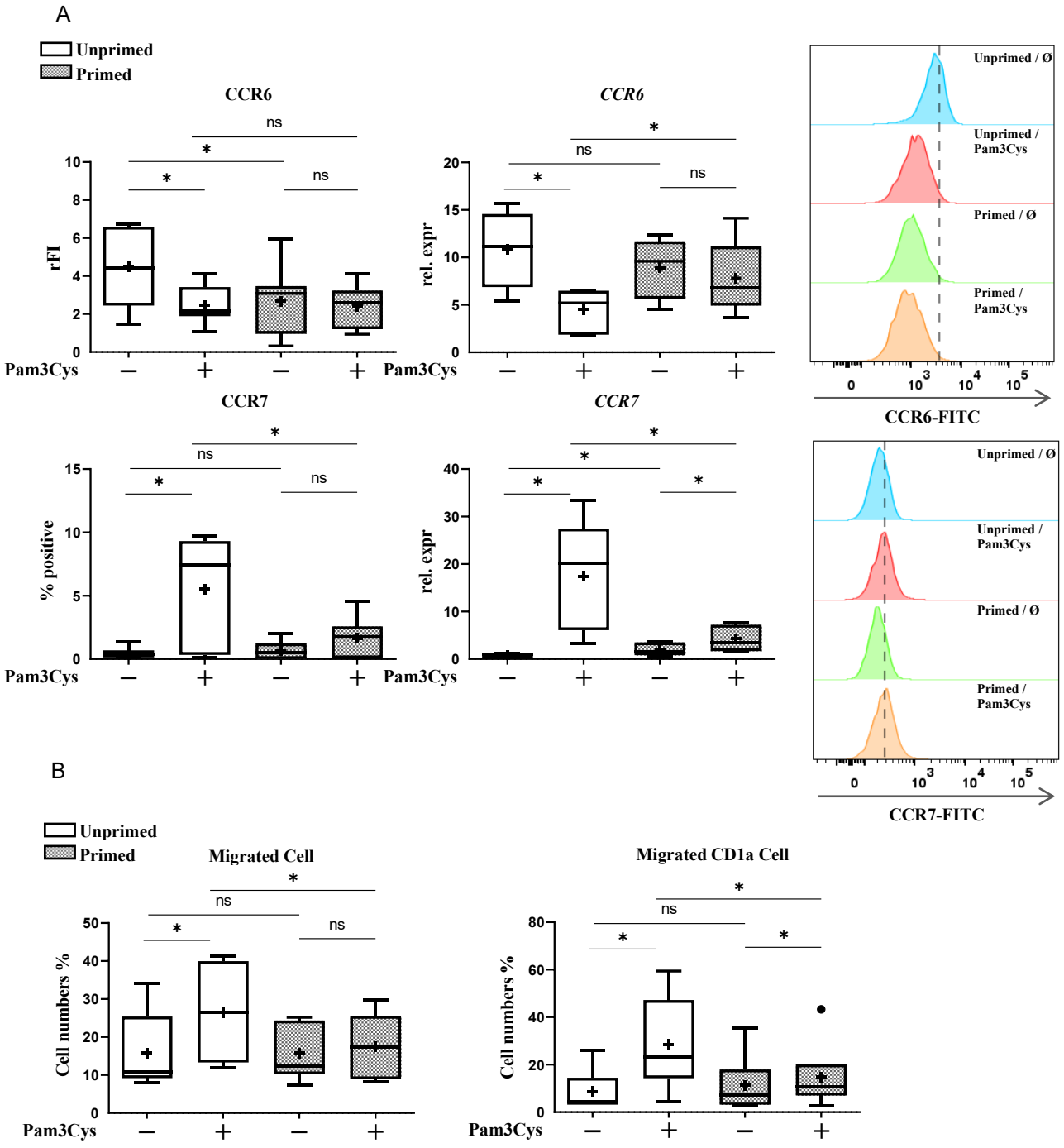

Figure. 14: Impaired migration capacity of primed CD34LC upon TLR2-driven activation. CD34LC were generated *in vitro* as described above and the priming treatment as the above. Cells were subjected to either no stimulation (−) or stimulation (+) with Pam3Cys (1 µg/mL) for 6 h for qPCR or 24 h for FACS. (A) Cells were stained with antibodies against CCR6, CCR7 or an isotype control. CD14 and CD1a gates were utilized for selection, and dead cells were excluded using 7-AAD staining. Flow cytometry was employed to perform the analysis. The qPCR was conducted by sorting CD1a-positive cell sorting via magnetic separation, followed by mRNA quantification, normalization to a housekeeping gene, and fold change presentation. Representative histograms are indicated, and results are displayed as boxplots (n = 6-8), with the mean represented by "+", and outliers indicated as "•". (B)The number of cells that migrated across the transwell

membrane was quantified by averaging four random fields per well under a microscope. The number of CD1a-positive cells among the migrated cells was calculated before and after the transwell assay, and analysis by Flow cytometry (n = 6). Statistical significance was determined using the Wilcoxon Signed Ranks Test in SPSS. *p < .05; **p < .01; ns indicates non-significant (p > .05).

3.3.3 Priming treatment alters the cytokine production of CD34LC.

Next, the effect of the priming was investigated on the cytokine profile. The cytokine production of both unprimed and primed CD34LC was analyzed in their supernatants following a 24-hour Pam3Cys stimulation, utilizing a bead-based assay for a comprehensive analysis.

In line with previous research, activation of TLR2 resulted in the secretion of pro-inflammatory cytokines, including IL-6, IL-8, IL-23, and TNF-α, alongside the immunomodulatory cytokine IL-10 in LC(Aliahmadi et al., 2009; Deckers et al., 2018; Kashem et al., 2017). This phenomenon was evidenced by the notable increase in IL-6, IL-8, IL-23, IL-10, and TNF-α levels in unprimed CD34LC following Pam3Cys stimulation in unprimed cells (Figure 15A in unprimed). In contrast, unstimulated primed CD34LC displayed a diminished production of these cytokines. Furthermore, there was only a marginal increase in the levels of these cytokines following Pam3Cys stimulation in the primed cells (Figure 15A in primed). Notably, the pro-inflammatory cytokine TNF-α appeared largely unaffected by the priming treatment. This observation is supported by the induction of TNF-α production from primed cells upon Pam3Cys stimulation (Figure 15B). Unexpectedly, upon subsequent Pam3Cys stimulation, primed CD34LC displayed a noteworthy upregulation of IL-1β and IL-18 (Figure 15C) which are considered as pivotal components in the primary immune responses of AD, (Bernard et al., 2017; Clausen et al., 2020; Honda and Kabashima, 2020; Kou et al., 2012; Murphy et al., 2000; Weidinger et al., 2018). This response contrasted sharply with the minimal induction observed in unprimed cells (Figure 15C). Additionally, even priming alone resulted in a slight (but significant) increase in IL-1β production.

In summary, the cytokine profile of tolerized CD34LC in response to TLR2-driven activation revealed distinct patterns which highlighting the intricate interplay between priming treatment and cytokine regulation.

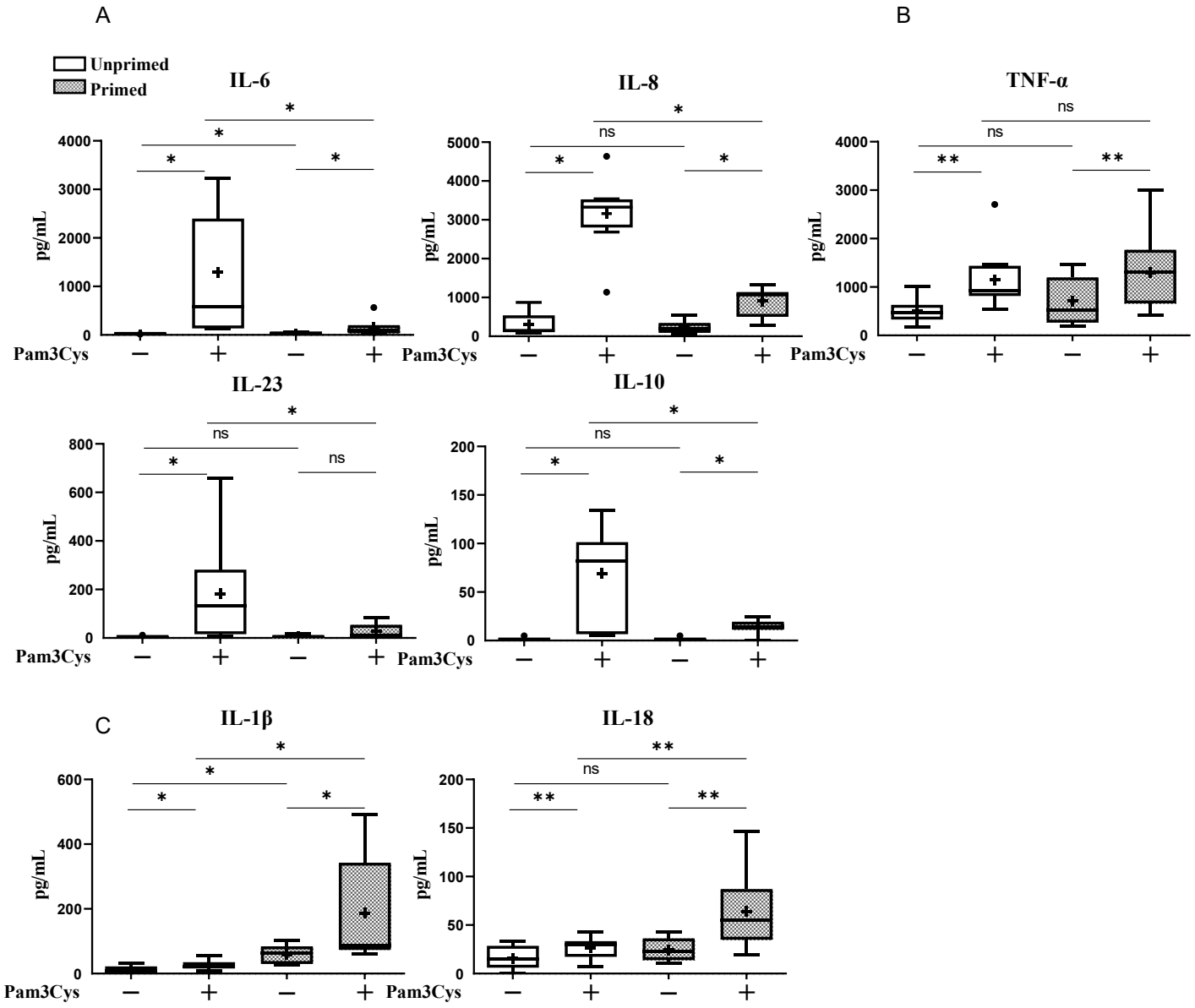

Figure. 15: Altered cytokines production of primed CD34LC upon TLR2-driven activation: CD34LC were generated *in vitro* as described above and the priming treatment as the above. Cells were subjected to either no stimulation (−) or stimulation (+) with Pam3Cys (1 µg/mL) for 24 h, collecting the culture supernatant. Cytokine levels in the culture supernatant were assessed using the LEGENDplex Cytometric Bead Assay (BioLegend™), with triplicate analyses. Results are displayed as boxplots(n = 7-10), with the mean represented by "+", and outliers indicated as "●". Statistical significance was determined using the Wilcoxon Signed Ranks Test in SPSS. *p < .05; **p < .01; ns indicates non-significant (p > .05).

3.4 Role of the TLR2-NF-κB signaling pathway in the mechanisms leading to tolerization.

The TLR2-NF-κB signaling pathway plays a pivotal role in LC' maturation and subsequent immune responses(Barton and Medzhitov, 2003; de Oliviera Nascimento et al., 2012). Therefore a series of experiments were performed to unravel the its putative role in the mechanisms underlying the tolerization phenomenon.

The analysis centered on assessing the expression of TLR1/2 receptors and quantifying the mRNA levels of key signaling molecules. These molecules encompassed MyD88, IRAK1, IRAK2, IRAK4, and TRAF6, all of which have been extensively implicated in the activation of NF-κB transcription downstream of TLR2 engagement(Barton and Medzhitov, 2003; Jin and Lee, 2008; O'Neill, 2008; O'Neill and Bowie, 2007).

3.4.1 Signaling molecules of TLR2-NF-κB signaling pathway show hypo-response in tolerized LC.

In unprimed cells, the involvement of the TLR2 signaling pathway is shown by the upregulation of TLR2 surface expression and the mRNA levels of *TLR1, TLR2,* and *MyD88* upon Pam3Cys stimulation (Figure 16A and B in unprimed). However, in contrast, primed cells no discernible changes were seen in TLR2 receptor expression or the mRNA levels of *TLR1, TLR2,* and *MyD88* following Pam3Cys stimulation (Figure 16A and B in primed). Regarding further downstream signaling molecules, unprimed cells exhibited a slight reduction in the expression of *IRAK1* and *IRAK4*, coupled with upregulation of *IRAK2* upon Pam3Cys stimulation, although these changes did not reach statistical significance. In contrast, in primed cells no differences were observed in *IRAK1, IRAK2, IRAK4,* and *TRAF6* expression levels (Figure 16C).

These findings indicate that the TLR2-NF-κB signaling pathway components exhibited a distinctive response in primed CD34LC, but a potential pivotal role cannot be concluded from these experiments.

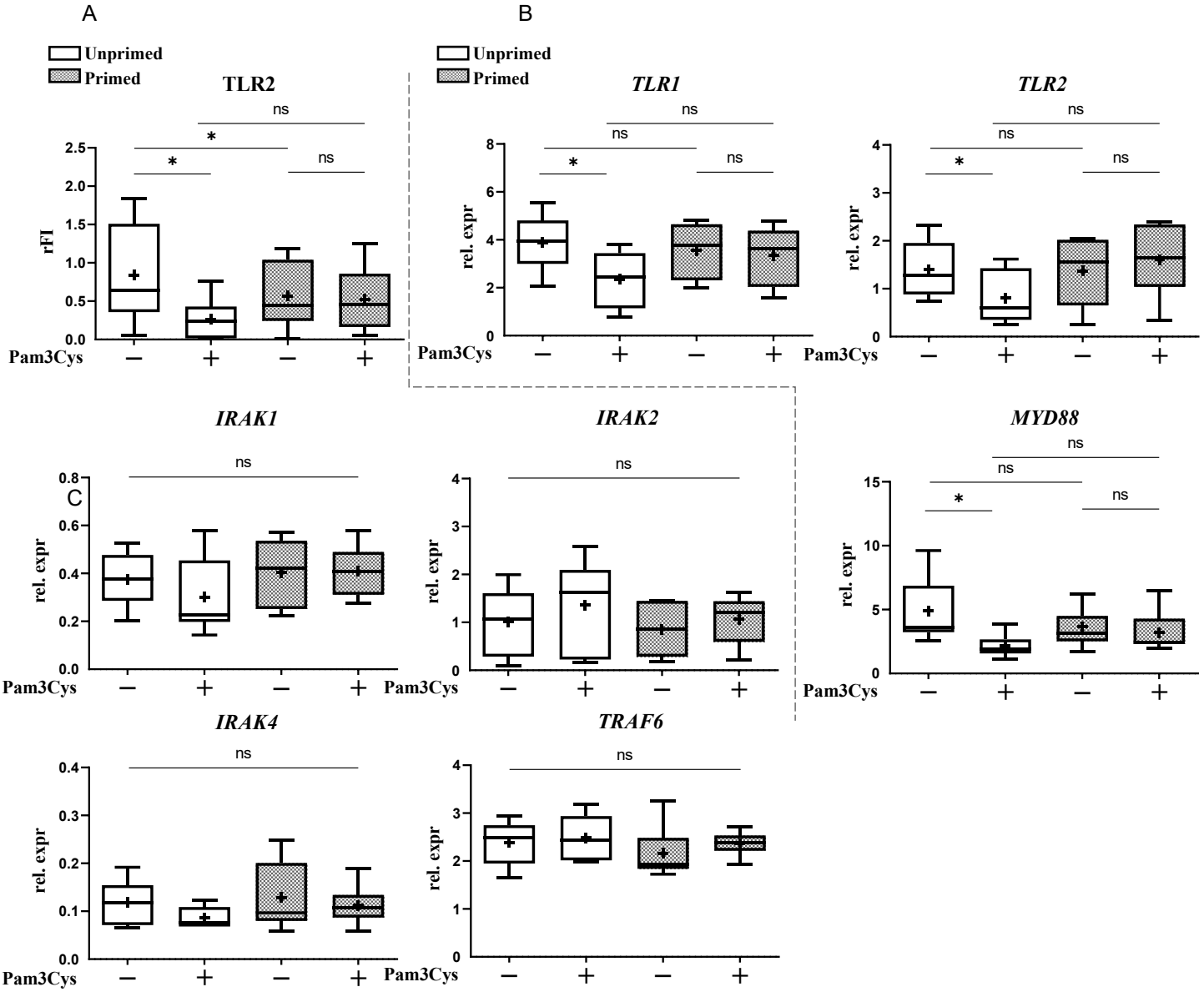

Figure. 16: TLR2 receptor and signaling molecules of TLR2-NF-κB signaling pathway on primed CD34LC upon TLR2-driven activation. CD34LC were generated *in vitro* as described above and the priming treatment as the above. Cells were subjected to either no stimulation (−) or stimulation (+) with Pam3Cys (1 µg/mL) for 6 h for qPCR or 24 h for FACS. (A) Cells were stained with antibodies against TLR2 or an isotype control. CD14 and CD1a gates were utilized for selection, and dead cells were excluded using 7-AAD staining. Flow cytometry was employed to perform the analysis. (B and C) The qPCR was conducted by sorting CD1a-positive cell sorting via magnetic separation, followed by mRNA quantification, normalization to a housekeeping gene, and fold change presentation. Representative histograms are indicated, and results are displayed as boxplots (n = 6-8), with the mean represented by "+", and outliers indicated as "●". Statistical significance was determined using the Wilcoxon Signed Ranks Test in SPSS. *p < .05; **p < .01; ns indicates non-significant (p > .05).

3.4.2 Evidence for an essential role of TLR2-NF-κB signaling pathway-associated negative regulators.

The outcomes of the previous experiments prompted an exploration into the potential involvement of negative feedback mechanisms likely induced by the priming treatment. In this context, several intracellular negative regulators operating within the TLR2 pathway have been identified, including TOLLIP, A20, IRAKM, PI3K, and SOCS1(Kondo et al., 2012; Liew et al., 2005; O'Neill, 2008). To investigate this potential suppressive influence, the mRNA expression of these regulatory genes was assessed in the CD34LC treated as described above.

In unprimed CD34LC, stimulation with Pam3Cys led to an upregulation of *SOCS1* and *A20* and a downregulation of *TOLLIP* and *PI3K* (Figure 17A in unprimed), while the expression of *IRAK-M* remained unchanged (Figure 17B in unprimed). This observation suggests that TLR2-driven activation triggers alterations in the expression of negative regulatory elements within the TLR2-NF-κB pathway at the mRNA level.

Conversely, distinctive expression patterns of these inhibitory molecules emerged in primed cells. The regulators *A20*, *TOLLIP*, and *PI3K* remained unchanged toward Pam3Cys (Figure 17A in primed) while *SOCS1, A20,* and *IRAK-M* expression displayed significant alterations even without Pam3Cys stimulation in the primed cells (Figure 17A and B in primed). Notably, the expression levels of *SOCS1* and *IRAK-M* were further heightened and prominently pronounced in primed cells treated with Pam3Cys (Figure 17A and B in primed).

Hence, the augmented induction of negative regulators, specifically *SOCS1* and *IRAK-M*, in primed cells upon TLR2 stimulation, might play a pivotal role in the phenomenon of tolerization in CD34LC.

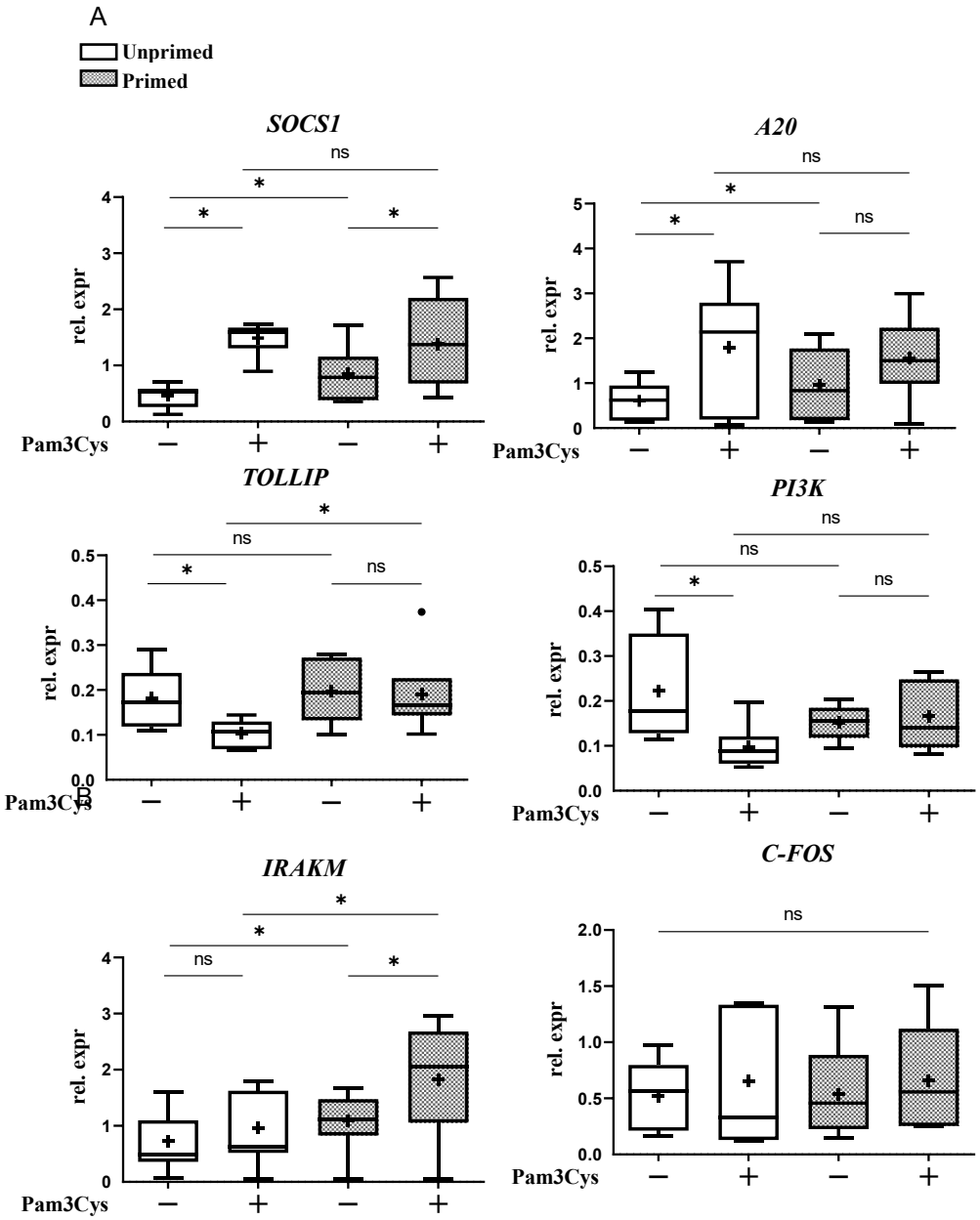

Figure. 17: Negative regulators of TLR2-NF-κB signaling pathway on primed CD34LC upon TLR2-driven activation. CD34LC were generated *in vitro* as described above and the priming treatment as the above. Cells were subjected to either no stimulation (−) or stimulation (+) with Pam3Cys (1 µg/mL) for 6 h for qPCR. (A and B)The qPCR was conducted by sorting CD1a-positive cell sorting via magnetic separation, followed by mRNA quantification, normalization to a housekeeping gene, and fold change presentation. Representative histograms are indicated, and results are displayed as boxplots(n = 6-8), with the mean represented by "+", and outliers indicated as "●". Statistical significance was determined using the Wilcoxon Signed Ranks Test in SPSS. *p < .05; **p < .01; ns indicates non-significant (p > .05).

3.4.3 The induction of SOCS1 and IRAKM by priming treatment is involved in the mechanism of tolerization of LC.

Further investigation into these negative regulators following the priming treatment, preceding exposure to Pam3Cys. The priming procedure induced a slight yet significant upregulation of both *SOCS1* and *IRAK-M* (Figure 18A), even without Pam3Cys stimulation. Conversely, *A20, TOLLIP,* and *PI3K* expression levels remained unaltered (Figure 18B). Interestingly, despite the priming treatment enhancing the expression of *SOCS1* and *IRAK-M*, it failed to activate CD34LC, as indicated by the expression profile of maturation markers in primed cells, as described in result 3.2, Figure 9.

In conclusion, the investigation delves into the intricate mechanisms governing the tolerization of CD34LC, with a specific focus on the TLR2-NF-κB signaling pathway. The findings propose that the priming treatment instigates the upregulation of negative regulators, specifically SOCS1 and IRAKM, which appear pivotal in developing tolerized LC in response to TLR2-driven activation.

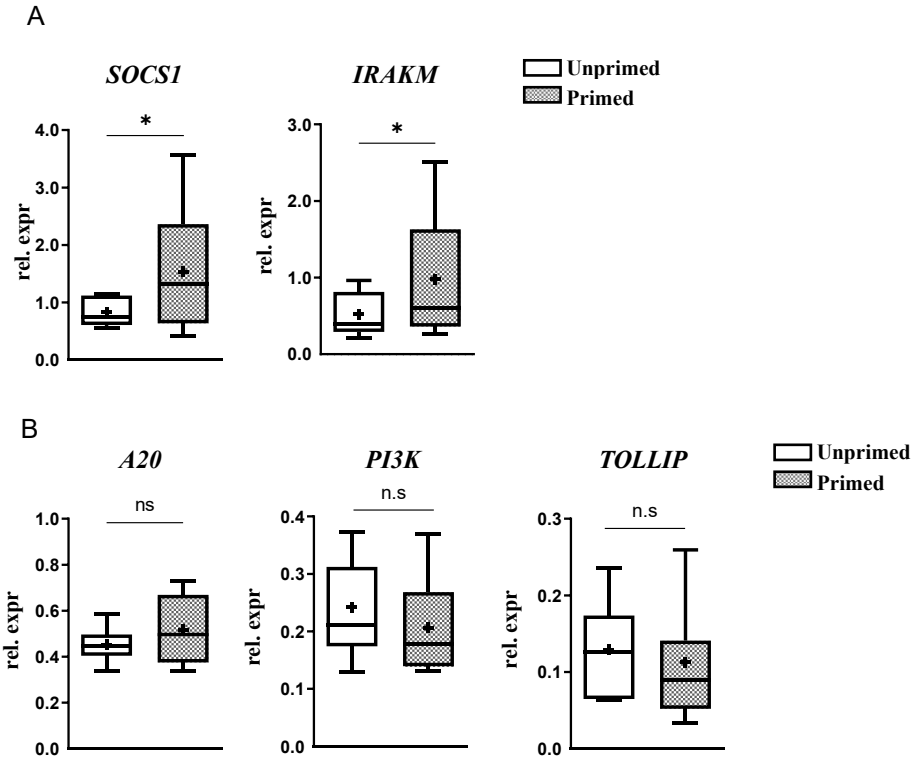

Figure. 18: Negative regulators of TLR2-NF-κB signaling pathway on primed CD34LC absence of TLR2-driven activation. CD34LC were generated *in vitro* as described above. Cells exposure to either the priming treatment (Primed) or were left untreated (Unprimed). (A and B) The qPCR was conducted by sorting CD1a-positive cell sorting via magnetic separation, followed by mRNA quantification, normalization to a

housekeeping gene, and fold change presentation. Representative histograms are indicated, and results are displayed as boxplots (n = 6-8), with the mean represented by "+", and outliers indicated as "●". Statistical significance was determined using the Wilcoxon Signed Ranks Test in SPSS. *p < .05; **p < .01; ns indicates non-significant (p > .05).

3.5 JAK inhibitors affect the priming treatment-induced tolerization of LC.

The impact of the pharmacological compounds of commonly prescribed topical medications for AD on the maturation-associated characteristics of tolerized CD34LC was investigated(Philipp et al., 2024). The unprimed and primed CD34LC were first incubated for 12 hours with a range of agents, including the classical compounds: hydrocortisone (a glucocorticosteroid), tacrolimus (a calcineurin inhibitor), Vitamin D analogs $1,25(OH)_2$-D_3 followed by stimulation with Pam3Cys. In a second round of experiments, the more recent compounds, i.e. JAK inhibitors, including ruxolitinib (JAK1/2 inhibitor), filgotinib (JAK1 inhibitor), BMS-911543 (JAK2 inhibitor) and VX-509 (JAK3 inhibitor) were tested. The phenotype and maturation state of CD34LC were investigated.

3.5.1 Lack of effect of classical compounds on the tolerization of LC.

First, the effects of traditional topical medications for AD on tolerized LC were analysis. Following the treatment with $1,25(OH)_2$-D_3, hydrocortisone, and tacrolimus separately, primed LC displayed reduced CD83 expression upon Pam3Cys induction compared to untreated primed LC in all of them (individual data, Figure 19). These findings suggested that the common topical medications for AD did not improve the maturation of tolerized LC in response to TLR2-driven activation.

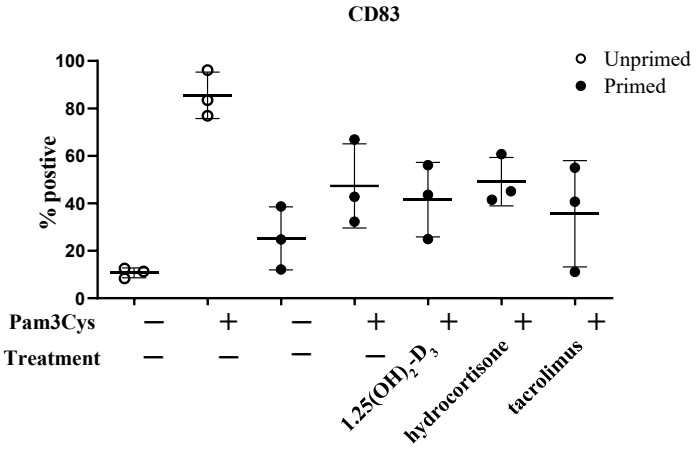

Figure. 19: The effect of AD comment topical medicines on maturation of tolerization LC. CD34LC were generated *in vitro* as described above. Cells exposure to either the priming treatment (Primed) or were left untreated (Unprimed). For primed cells, Vitamin D analogues 1.25$(OH)_2$-D_3 (10 nM), hydrocortisone (2.7 µM), tacrolimus (10 µM) for a duration of 12 h, or left untreated. Subsequently, the cells were either left unstimulated (−) or stimulated (+) with Pam3Cys (1.0 µg/mL) for 24 h. Flow cytometry was employed to perform the analysis. Cells were stained with antibodies against CD83,or an isotype control. CD14 and CD1a gates were utilized for selection, and dead cells were excluded using 7-AAD staining. Results are displayed as scatter plots, show individual data points and Mean ± SD (n = 3).

3.5.2 JAK inhibitors partly restore the maturation of tolerized LC.

JAK inhibitors, which target the JAK-STAT pathways implicated in cytokine signaling, have been recognized for their efficacy in alleviating AD severity and associated symptoms(Bieber, 2022; Chovatiya and Paller, 2021; Langan et al., 2020). In light of this, the impact of JAK inhibitors on the maturation process of tolerized CD34LC was further investigated..

Upon exposure to ruxolitinib (JAK1/2i), a discernible and significant enhancement in CD83 expression was observed in primed LC upon subsequent Pam3Cys stimulation (Figure 20A). Likewise, treatment with BMS-911543 (JAK2i) and VX-509 (JAK3i) led to moderate yet significant increases in CD83 expression, while filgotinib (JAK1i) induced only a slight elevation of CD83 (Figure 20A). Notably, the exposure to JAK inhibitors did not impact the differentiation of CD34LC after 12 h of incubation, as evidenced by the unchanged CD1a% compared to the untreated cells (Figure 20B).

Furthermore, ruxolitinib exhibited an upregulatory effect on the expression of CD86 and MHC II in primed cells following Pam3Cys stimulation (Figure 20C). However, it did not induce a similar response in CD80 expression (Figure 20C).

Thus, these data suggest that JAK inhibitors, especially the JAK1/2 inhibitor ruxolitinib, have the capacity to partially restore the maturation process of tolerized LC in response to TLR2-driven activation.

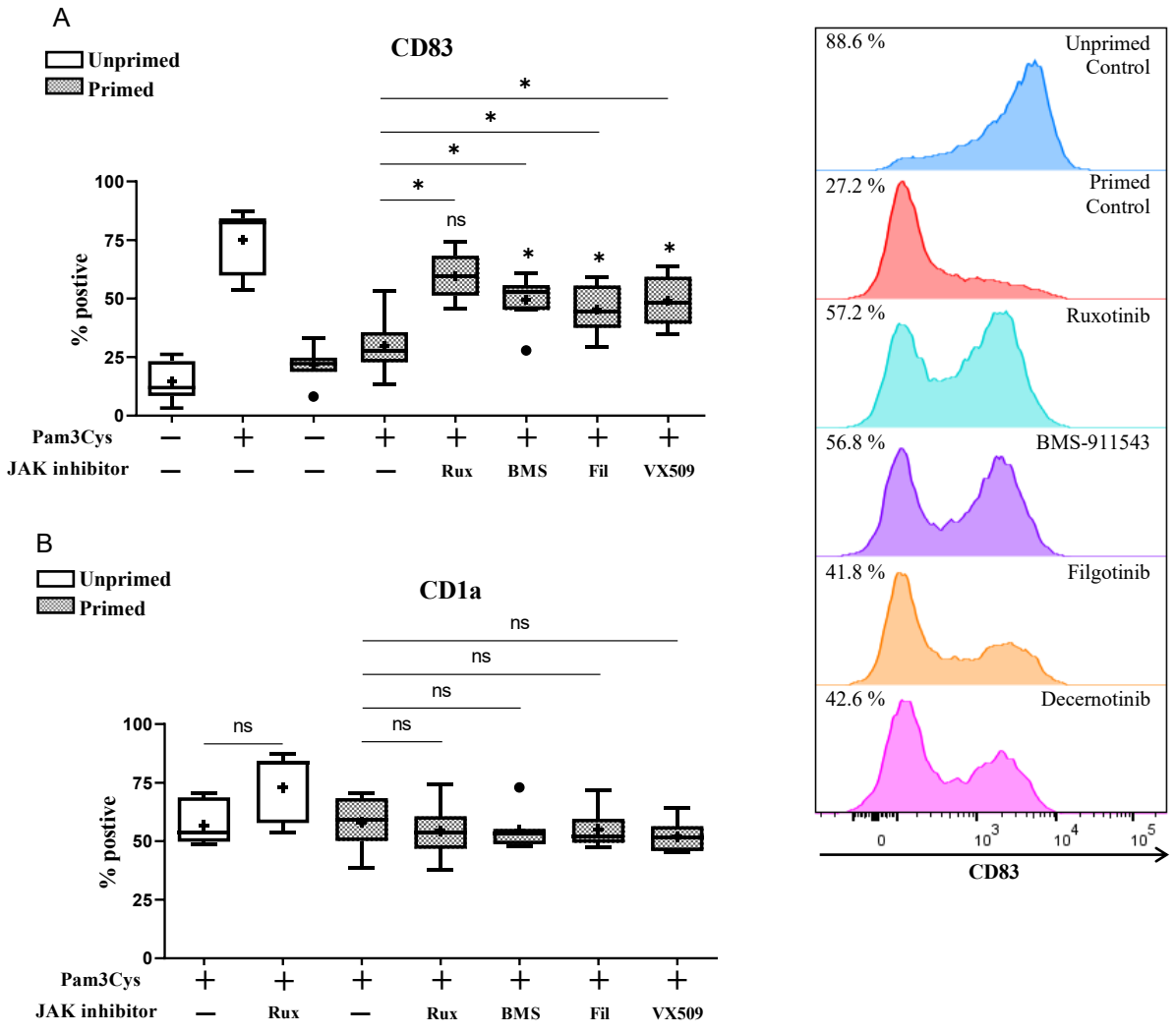

C

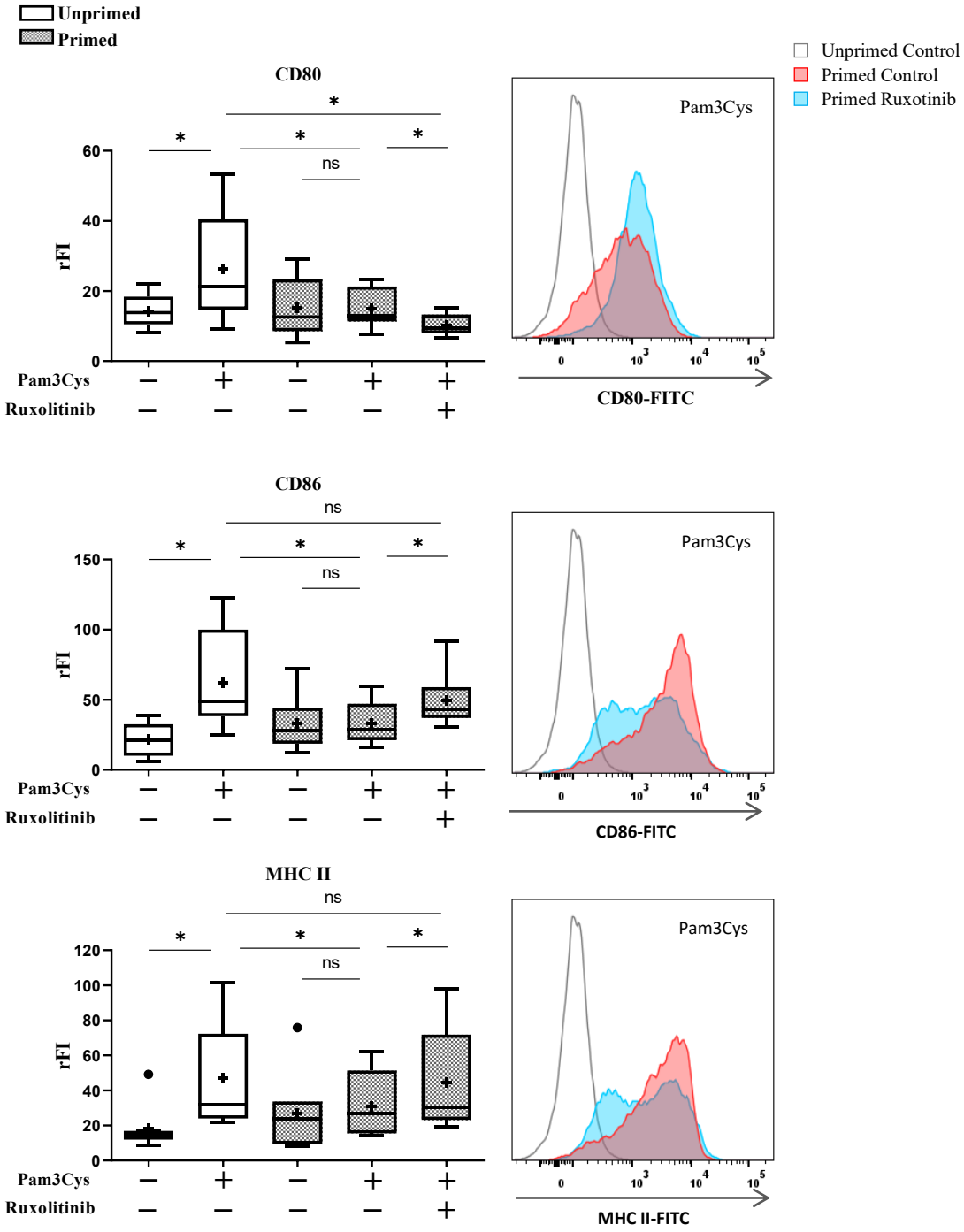

Figure. 20: The effect of JAK inhibitors on maturation of tolerization LC. CD34LC were generated *in vitro* as described above. Cells exposure to either the priming treatment (Primed) or were left untreated (Unprimed). For primed cells, JAK inhibitors including Ruxolitinib, Filgotinib, BMS-911543, and Decernotinib (VX-509) were applied at a concentration of 1 µmol/L (µM) for a duration of 12 h, or left untreated. Subsequently, the cells were either left unstimulated (−) or stimulated (+) with Pam3Cys (1.0 µg/mL) for 24 h. Flow cytometry was employed to perform the analysis. (B) CD1a positive cells gated by CD1a-RD1 and CD14-APC, and dead cells were excluded using 7-AAD stain. Percentage of CD1a positive cells in the whole cells population showed in the boxplots with the mean

indicated by "+"(n = 6 -10). (A and C) Cells were stained with antibodies against CD83, CD80, CD86, MHC II or an isotype control. CD14 and CD1a gates were utilized for selection, and dead cells were excluded using 7-AAD staining. Representative histograms are indicated, and results are displayed as boxplots (n = 6-10), with the mean represented by "+", and outliers indicated as "●". Statistical significance was determined using the Wilcoxon Signed Ranks Test in SPSS. *p < .05; **p < .01; ns indicates non-significant (p > .05).

3.5.3 JAK1/2 inhibitor decrease the cytokines of tolerized LC.

The next series of experiments was aimed to assess whether JAK inhibitors could restore the cytokine production of primed LC upon TLR2 stimulation, similar to the observed effects on maturation phenotype. The cytokine profile of primed LC in response to Pam3Cys was assessed following treatment with the JAK1/2 inhibitor, ruxolitinib.

Following ruxolitinib treatment, primed LC released IL-6, IL-8, IL-10, and IL-23 without a noticeable increase, and levels of IL-6, IL-8, and IL-23 were lower than those in untreated primed LC (Figure 21A). The enhanced production of IL-1β and IL-18 in primed LC decreased following ruxolitinib. Additionally, TNF-α, which exhibited unimpaired release in primed LC, showed a reduction after ruxolitinib treatment (Figure 21B).

These findings suggest that the JAK1/2 inhibitor ruxolitinib failed to restore the cytokine production capacity of primed LC upon TLR2 activation, and even downregulated cytokine release.

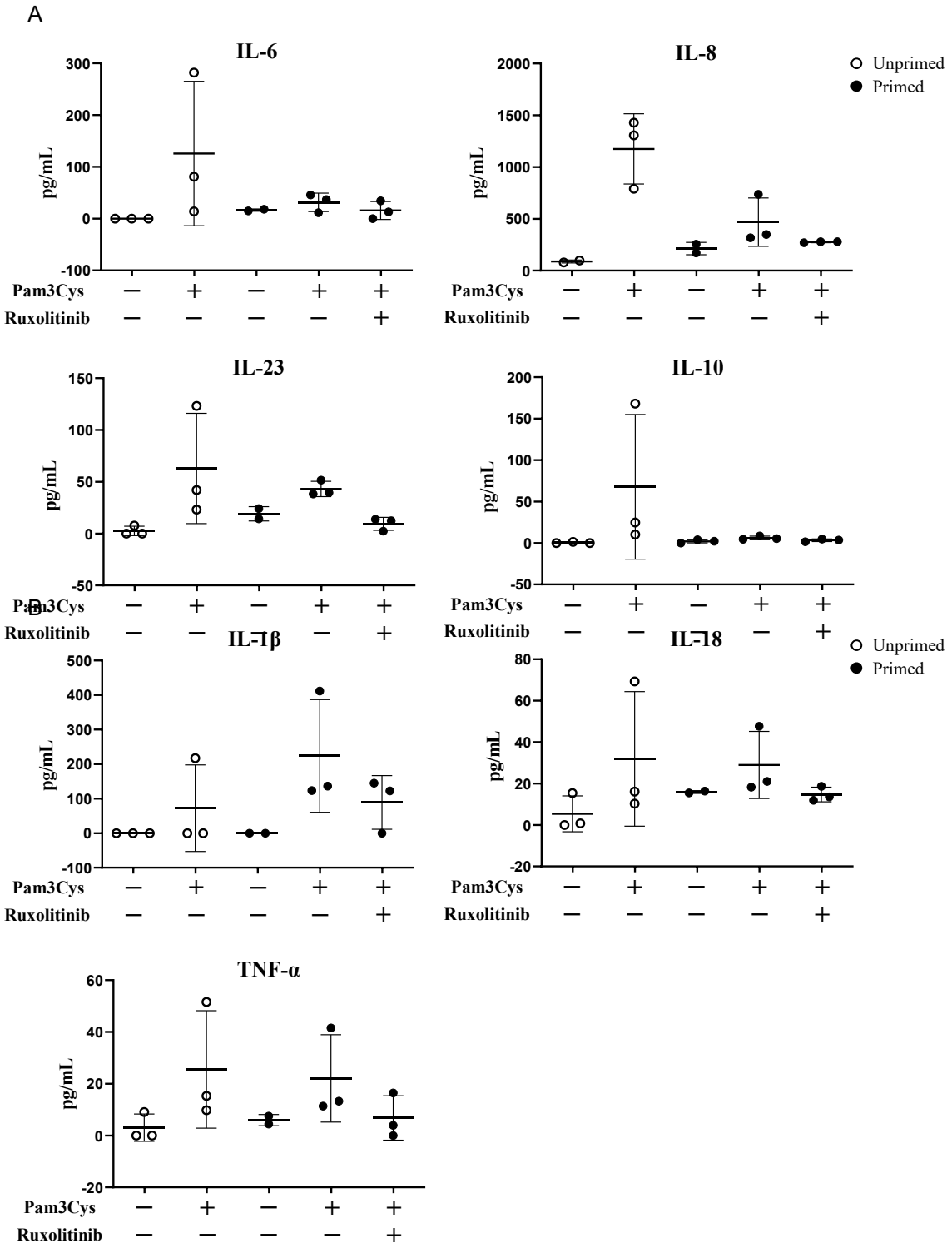

Figure. 21: Cytokines production of primed of LC following JAK1/2 inhibitor upon TLR2-Driven Activation. CD34LC were generated *in vitro* as described above. Cells exposure to either the priming treatment (Primed) or were left untreated (Unprimed). JAK1/2 inhibitor Ruxolitinib (1.0 μM) for a duration of 12 h, or left untreated. Subsequently, cells were subjected to either no stimulation (−) or stimulation (+) with Pam3Cys (1.0 μg/mL) for 24 h, collecting the culture supernatant. Cytokine levels in the culture supernatant were assessed using the LEGENDplex Cytometric Bead Assay

(BioLegend™), with triplicate analyses. Results are displayed as scatter plots, show individual data points and Mean ± SD (n = 3).

3.5.4 JAK1/2 inhibitor downregulate SOCS1 in tolerization LC, not IRAKM.

While the precise mechanisms dictating the impact of JAK inhibitors on LC activation remain partially elusive, existing research suggests that activation of the JAK/STAT pathway could trigger the expression of SOCS1(Baker et al., 2009; Krebs and Hilton, 2001; Morris et al., 2018; Yoshimura et al., 2007). Building on this knowledge, it was hypothesized that the JAK1/2 inhibitor-induced recovery of maturation in tolerized LC might cause a reduction in *SOCS1* expression, given its pronounced presence in primed LC, as show above (Figure 17A and 18A).

To investigate the potential suppressive influence of ruxolitinib on LC, the levels of *SOCS1* and *IRAK-M* were quantified in primed LC treated with ruxolitinib in the absence of subsequent Pam3Cys stimulation. Intriguingly, the observations revealed that, in comparison to unprimed cells, ruxolitinib led to a noteworthy downregulation of *SOCS1* expression after 2 h, with a further reduction to control levels in primed LC after 4 h (Figure 22). In contrast, *IRAK-M* sustained its elevated expression in primed cells, showing no reduction upon treatment with ruxolitinib at both the 2 h and 4 h time points (Figure 22).

In conclusion, the utilization of the JAK1/2 inhibitor demonstrated a partial restoration of tolerized LC maturation in response to TLR2-driven activation. This effect could potentially be attributed to the downregulation of the negative regulatory molecule SOCS1.

In summary, these results suggest that JAK inhibitors, particularly JAK1/2 inhibitors ruxolitinib, have the potential to modulate the maturation process of tolerized LC in response to TLR2-driven activation, shedding light on their role in the complex regulatory mechanisms governing LC in the context of AD.

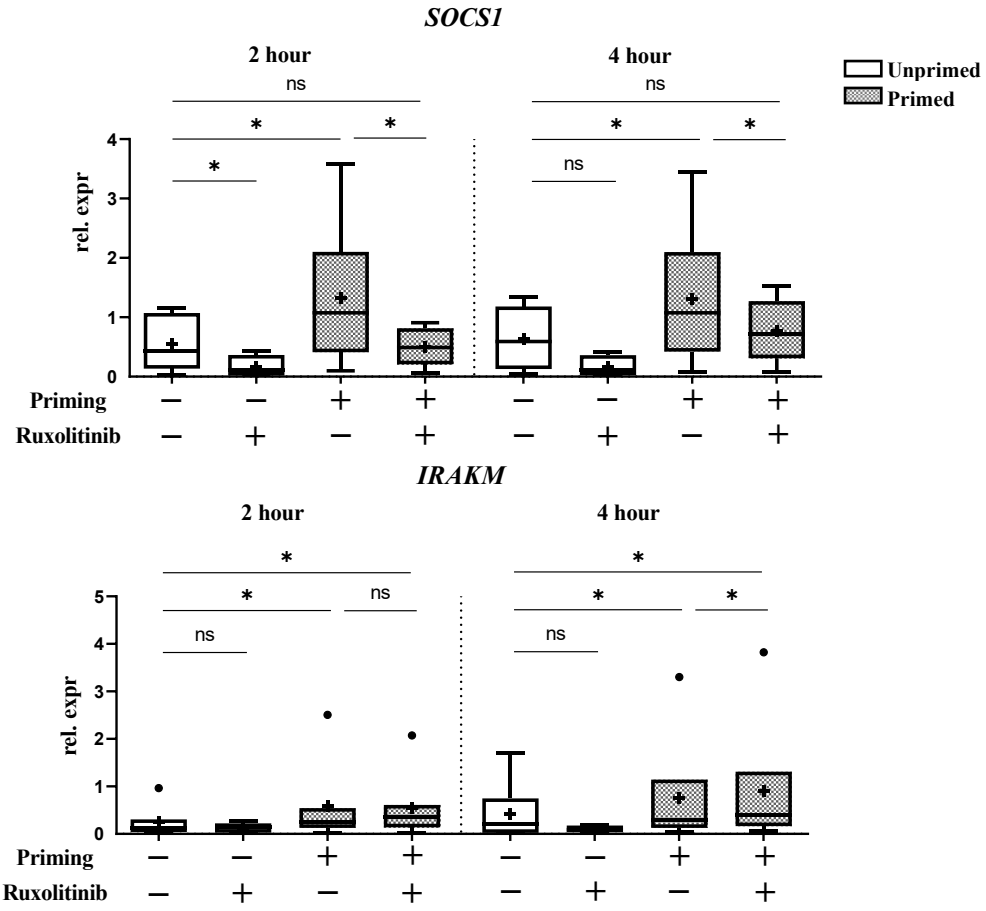

Figure. 22: Negative regulators of TLR2-NF-κB signaling pathway on maturation of tolerization LC following the JAK inhibitor Ruxolitinib. CD34LC were generated *in vitro* as described above. Cells exposure to either the priming treatment (Primed) or were left untreated (Unprimed). For primed cells, JAK inhibitors Ruxolitinib, was applied at a concentration of 1 µmol/L (µM) for a duration of indicated time, or left untreated. The qPCR was conducted by sorting CD1a-positive cell sorting via magnetic separation, followed by mRNA quantification, normalization to a housekeeping gene, and fold change presentation. Results are displayed as boxplots (n = 5-7), with the mean represented by "+", and outliers indicated as "●". Statistical significance was determined using the Wilcoxon Signed Ranks Test in SPSS. *p < .05; **p < .01; ns indicates non-significant (p > .05).

3.6 Summary of the results.

This study explored the mechanisms underlying the tolerization of human LC in an *in vitro* approach using an established model of CD34 stem cell-derived LC (CD34LC) exhibiting the phenotype of freshly isolated epidermal LC. To mimic persistent microbial pathogen stimulation in AD skin lesions, CD34LC were subjected to repeated exposure to low doses of TLR ligands, leading to the development of tolerized LC. Tolerization ot TLR2 signals in CD34LC is characterized by impaired maturation phenotypes upon activating doses of TLR ligand, reduced expression of maturation-related migratory molecules, and diminished migratory capacity. Furthermore, there is a decrease in inflammatory cytokines, including IL-6, IL-8, IL-10, and IL-23, while an upregulation of IL-1β and IL-18 release was observed. For investigation of potential mechanisms in tolerized LC, this study analyzed individual components of the TLR2-NF-κB signaling pathway, showing unresponsiveness of key signaling molecules to activating doses of TLR2-ligand. At the same time, negative regulators SOCS1 and IRAK-M were significantly increased by tolerization process. This study showed that a JAK inhibitor, specifically a JAK1/2 inhibitor, partially restored the activated phenotype of tolerized LC in response to Pam3Cys, achieved by inhibitory SOCS1. This underscores the crucial role of SOCS1 in tolerized LC and suggests a novel mechanism underlying the therapeutical effect of JAK inhibitors in AD.

4. Discussion

Based on our previous hypothesis, the hyporesponsiveness of LC in AD skin towards TLR2-mediated activation may be due to repeated TLR2 engagement *in situ*, as *S. a.* constantly trigger the immune cells in AD skin. This study explored the molecular and functional properties of LC in the context of the TLR2 signaling pathway in AD, shedding light on the associated underlying mechanisms governing these cells.

4.1 The priming induced tolerization of LC.

AD skin is characterized by a disrupted skin barrier and dysbiosis in the microbiome, with a distinct overgrowth and colonization of *S. a.*(Hülpüsch et al., 2021). LC have demonstrated their ability to breach the compromised skin barrier and tight junctions within AD lesions, enabling them to uptake antigens and contribute to AD's pathogenesis(Yoshida et al., 2014).

LC isolated from AD skin exhibit a diminished response to TLR2-mediated activation, potentially due to the prolonged but moderate activation of LC by microorganisms like *S. a.* in AD lesions. This way contribute to their adapted tolerized state instead of the notion of potent stimulation(Iwamoto et al., 2018). Building upon these insights, the approach of this study involved a repeated exposure of CD34LC to low-dose Pam3Cys, a TLR2 ligand, to replicate the AD skin environment. This induced tolerization in LC towards subsequent TLR2 stimulation. Similar observations have been shown in immune cell subsets, macrophages, monocytes, and moDC, which, when repetitively exposed to TLR ligands, displayed induced tolerance(Albrecht et al., 2008; Fekete et al., 2012; Ferlito et al., 2001; Kreutz et al., 1997; Murphy et al., 2015; Sato et al., 2000; Wang et al., 2002). CD83 has been established as a prominent marker for mature DC(Banchereau and Steinman, 1998; Lechmann et al., 2002; Zhou et al., 1992). Its expression is notably modest or absent in immature CD34LC but becomes markedly elevated upon maturation induced by TLR2 ligands Pam3Cys(Herrmann et al., 2021; Staudacher et al., 2015). Accordingly, the surface expression of CD83 served as a sensitive indicator of maturation in CD34LC in response to TLR2-driven activation. The tolerized LC through priming treatment exhibited a noteworthy suppression in CD83 expression upon TLR2 stimulation. This outcome was consistent with the behavior of LC derived from the AD skin(Iwamoto et al., 2018).

I. Impaired maturation of tolerized LC

The data demonstrated that tolerized LC display impaired maturation towards TLR2- and TLR4-mediated activation, as shown by the significantly inhibited expression of CD80, CD86, and MHC II on the primed cells. Consistent with previous findings that LC from AD skin were deficient in TLR2 expression and lacked phenotypic maturation responses to TLR2 ligation(Albrecht et al., 2008; Iwamoto et al., 2018; Wang et al., 2002). Moreover, it has been established that cells, including monocytes, macrophages, and moDC, repeatedly exposed to TLR2 or TLR4 ligands induce impaired maturation upon subsequent or final TLR-driven stimulation(Albrecht et al., 2008; Fekete et al., 2012; Geisel et al., 2007).

Furthermore, the data showed that priming treatment with heterologous TLR2 and TLR4 ligands induced impaired maturation. This is consistent with the existence of the crosstalk mechanism within the TLR pathway family[22–24]. In this way, immune responses are more effective in the TLR family between different kinds of pathogen[22–24]. Cross-tolerized LC may broaden the range of antigens, potentially increasing the risk of AD patients developing various types of infections(Coveney et al., 2015; Kawai and Akira, 2011; Koch et al., 2017b; Maglione et al., 2015; Saturnino et al., 2010), not limited to *S. a.* but also encompassing other pathogens in milieus and epidermis[16 24,29–31]. Indeed, AD manifests with symptoms of multiple pathogenic infections, including herpes simplex virus, *Molluscum contagiosum*, and the fungus *Malassezia sympodialis*(Weidinger and Novak, 2016). Considering the mechanism of tolerization in LC and their hyposensitivity to heterologous ligands, there is speculation on their potential role in cutaneous infections in AD.

Additionally, this study has confirmed that CD34LC exhibit different levels of activation in response to the TLR2 ligand Pam3Cys and the TLR4 ligand LPS. This demonstrates distinct activation behaviors of CD34LC when exposed to TLR2, representative of Gram-positive bacteria, and TLR4, representative of Gram-negative bacteria. This implied that within the complex microbial milieu on the skin surface, microbial pathogens with distinct attributes would induce varied response patterns in LC, particularly in *S. a.*-colonized AD.

II. Impaired migration of tolerized LC

Tolerized LC showed a diminished migratory capability as evidenced by the expression of migratory molecules CCR6 and CCR7, as well as the migration capacity. The downregulation of CCR7 expression in tolerized LC following TLR2 stimulation aligns with observations in tolerogenic DC induced by other activators, which also displayed reduced CCR7 expression(Domogalla et al., 2017). Interestingly, in AD skin, CCR6 expression is significantly lower in individuals with AD compared to healthy controls, and CCR7 expression is comparably low in both AD and healthy skin(Nümm, n.d.).These observations in AD are consistent with the expression patterns of these molecules in tolerized LC.

In this study, tolerized LC exhibited diminished migratory capability, which seems to be contrast with previous reports of high spontaneous migratory activity in LC from AD skin(Iwamoto et al., 2018) at the first glance. However, this discrepancy arises from differences in experimental setup: AD LCs were analyzed *ex vivo* using skin and cultured tissue, assessing spontaneous migration by the percentage of LC in the migrated cell population. In contrast, primed LCs were analyzed *in vitro* using a CCR7 ligand (Mip-3/CCL19) as the attractor, focusing on maturation-associated migration. This suggests that the high spontaneous migration of AD LCs is influenced by external factors in skin tissue, rather than by properties of the LC alone. Furthermore, CCR6 is a molecule responsible for maintaining LC localization in the epidermis through interaction with E-cadherin on keratinocytes(Deckers et al., 2018; Doebel et al., 2017; Gros et al., 2009; Merad et al., 2008). The downregulation of CCR6 in primed LC suggests that tolerized LC are more prone to detaching from keratinocytes and spontaneously migrating out of the epidermis, in contrast to unprimed or healthy LC. This observation is indeed in line with the increased spontaneous migration capacity of LC observed in cultured AD skin.

Despite the different setups, the number of migrated LC in AD skin studies also showed a lack of response to TLR2-driven stimulus(Iwamoto et al., 2018), consistent with tolerized LC. These observations highlight the influence of various factors on LC migratory ability in AD, contributing to the plastic immunological profile of LC.

III. Distinct cytokines profile of tolerized LC

The tolerized LC exhibited hyporesponsiveness and a distinct cytokine profile upon TLR2-driven activation. Although this finding may seem surprising given the well-established knowledge about LC releasing cytokines in response to TLR-mediated activation(Aliahmadi et al., 2009; Kashem et al., 2017), it aligns with the functional features of LC in response to antigens during immune processing(Deckers et al., 2018; Doebel et al., 2017). The reduced cytokine production of IL-6, IL-8, IL-10, IL-12, and IL-23 by the hyporesponsive DC upon TLR ligation is consistent with previous studies on tolerance and tolerogenic DC(Kashem et al., 2017; Mbongue et al., 2017; Morelli and Thomson, 2007). Also, IL-6(Iwamoto et al., 2018), IL-10(Iwamoto et al., 2018), and IL-12(Nümm, n.d.) were unresponsive to subsequent TLR2 stimulation in the *ex vivo* skin, as shown in previous results.

Studies have reported that reduced IL-1β production during TLR or other stimulus-induced hyporesponsiveness in macrophages and moDC(Biswas and Lopez-Collazo, 2009; Liu et al., 2019; Morelli and Thomson, 2007; Seeley and Ghosh, 2017), whereas IL-18 exhibited increased production upon re-stimulation(Rayhane et al., 1999; Verweyen et al., 2020). Tshis study revealed a significant increase in the release of IL-1β and IL-18 following TLR2 stimulation in tolerized LC. This observed elevation may be attributed to the priming-induced tolerization of LC, triggering NLRP3 inflammasome activation. This process involves two-step signals: the priming signal induced by TLR, TNFR, or IL-1R, and the activation signals mediated by various irritants(Kelley et al., 2019; Seok et al., 2021). Interestingly, while a direct link between LC and inflammasome activation in AD has not been definitively established, their crucial inflammatory role in AD development has been recognized(Tang and Zhou, 2020). This observation also aligns with the elevated levels of IL-1β and IL-18 found in the supernatant of *in ex vivo* AD skin(Iwamoto et al., 2018). AD is well-established as a Th2-driven inflammatory disease. IL-1β and IL-18, recognized as pathogen-associated alarmin cytokines, activate skin-resident group 2 innate lymphoid cells (ILC2) and trigger Th2 cell-mediated immune responses, which plays an important part in the early stage AD(Bernard et al., 2017; Clausen et al., 2020; Dai et al., 2011; Guttman-Yassky et al., 2023; Honda and Kabashima, 2020; Kortekaas Krohn et al., 2022; Kou et al., 2012; Murphy et al., 2000; Sun et al., 2021; Weidinger et al., 2018). LC perform different functions during AD pathogenesis, while they are traditionally not been considered as a source of IL-1β and IL-18. However, the findings showed that tolerized

LC produce IL-1β and IL-18. This finding may potentially implicate that under certain conditions such as a constitutive exposure to TLR ligands, like in AD skin condition, LC may represent a source of IL-1 and IL-18, influencing neighbor skin cells such as keratinocytes and ILC2s and thereby contributing to subsequent response.

Additionally, TNF-α production is significantly elevated in AD(Danso et al., 2014; Peng and Novak, 2015; Werfel et al., 2016) and remains strongly responsive to TLR2 stimulation in *ex vivo* AD skin(Nümm, n.d.). This aligns with the findings of this study which shows that TNF-α production by tolerized LC is not affected by the priming treatment and is still induced by TLR2 stimulation. This contrasts studies on tolerogenic LC and DC, where TNF-α production was significantly suppressed upon restimulation(Albrecht et al., 2008; Fekete et al., 2012; Mbongue et al., 2017; Morelli and Thomson, 2007). The discrepancies in high IL-1β and IL-18 levels and the unsuppressed TNF-α production in response to TLR2-driven activation between this tolerized LC and known tolerogenic DC highlight the distinct features of these two cell states.

Taken together, in AD, LC play a significant role as APC participating in infection-related processes by driving Th17 immune responses to bacterial pathogens and facilitating the elimination of *S.a.*, which impacts disease development(Aliahmadi et al., 2009; Igyártó et al., 2011; Kashem et al., 2015; Mathers et al., 2009). The characteristic tolerization of primed CD34LC is associated with impaired maturation and migration toward TLR2-driven stimuli, potentially affecting their antigen presentation ability. Additionally, the distinct cytokine profile of tolerized LC, with reduced cytokines that impact on Th17 responses, could weaken immune reactions, while increased cytokines might contribute to AD local inflammation(Kashem et al., 2015; Kobayashi et al., 2015). These findings suggest that tolerized LC might influence AD pathogenesis due to their unique molecular and functional characteristics. Furthermore, our data showed that tolerization occurred for both homologous (TLR2 ligand) and heterologous (TLR4 ligand) stimulation approaches. Given the mechanism of tolerization in LC and its potential role in cutaneous infections in AD, it is speculated that cross-tolerized LC may elevate the risk of AD patients developing various types of infections(Coveney et al., 2015; Kawai and Akira, 2011; Koch et al., 2017b; Maglione et al., 2015; Saturnino et al., 2010).

4.2 Role of the TLR2-NF-kB signaling pathway in the development of tolerized LC.

I. Negative regulators as key players in the tolerization mechanism.

Pam3Cys engages the TLR2 receptor, subsequently activating the NF-κB signaling pathway, driving LC maturation, which has been demonstrated in CD34LC(Herrmann et al., 2021; Iwamoto et al., 2018). The findings showed a decrease in TLR2/1 and MyD88 expression, confirming the engagement of the Pam3Cys ligand on CD34LC at the mRNA level. Key signaling molecules were also shown to be influenced by Pam3Cys engagement. However, these signaling molecules showed no significant alterations in the tolerization of LC. These observations indicated that the priming treatment impaired the activation of the TLR2-NF-κB pathway.

On the other hand, the data showed that the priming treatment alone induces SOCS1 and IRAK-M, which are further upregulated in response to Pam3Cys stimulation. This is in line with the fact that SOCS1 and IRAK-M were induced by recurrent exposure to TLR ligands in DC and function during the second or continuous exposure to the stimulus, contributing to the poor response of DC(Cole et al., 2012; Kinjyo et al., 2002; Kobayashi et al., 2002; Nakagawa et al., 2002; Wenink et al., 2009). SOCS1 plays a crucial role in regulating TLR responses in DC and macrophages by targeting intracellular signaling of TLR pathways, as demonstrated in several studies[31,32,35–37]. It inhibits the release of TLR2-induced inflammatory cytokines such as IL-6, TNFα, IFN-γ, IL-12, and IL-10(Kinjyo et al., 2002; Mansell et al., 2006; Nakagawa et al., 2002). Additionally, SOCS1 has been shown to play an essential role in regulating TLR2 ligand-induced DC maturation. Overexpression of SOCS1 in DC leads to low levels of CD80, CD86, and MHC II upon TLR stimulation(Fu et al., 2009; Hanada et al., 2003; Kinjyo et al., 2002), while silenced or deficient SOCS1 significantly upregulates these maturation molecules in the presence of stimulus or spontaneously activated cells(Hanada et al., 2003; Hildebrand et al., 2019; Nakagawa et al., 2002). IRAK-M has also been identified as a negative regulator of the TLR signaling pathway. Inhibition of downstream signals and suppression of TNFα, IL-6, IL-12p40, and IL-10 induced by TLR-mediated in DC(Cole et al., 2012; Kobayashi et al., 2002; Maldifassi et al., 2014; Nakayama et al., 2004; Zhou et al., 2013). When LPS was used to re-stimulate IRAK-M−/− BM-DC, MHC II and CD80 expression was up-regulated(Cole et al., 2012). These results are consistent with this studies on the molecular and functional features of tolerized LC induced by priming treatment followed by TLR2-mediated stimulation, except for the unaffected production of TNF-α. Thus, the priming-induced

SOCS1 and IRAKM might contribute to the tolerization of LC, similar to reports for other DC subtypes.

II. The role of SOCS1 in tolerized LC.

While SOCS1 is recognized as a negative regulator of the TLR signaling pathway and is induced by various TLR ligands on DC(Posselt et al., 2011, 2011; Wu et al., 2015), the precise induction of SOCS1 transcription by the TLR pathway remains debated. Currently, no clear evidence is established whether TLR2 directly or indirectly triggers SOCS1 transcription. Some studies have shown that TLR2-mediated engagement induces STAT1 phosphorylation in murine RAW264.7 macrophages(Luu et al., 2014), a known factor in SOCS1 expression induction. Additionally, in peritoneal macrophages, the TLR2 ligand LTA-induced SOCS1 mRNA expression depends on MyD88(Rhee et al., 2003). Conversely, the activation of the JAK-STAT pathway is acknowledged to prompt SOCS1 expression by acting as transcription factors for STAT1 and STAT3, establishing a negative feedback loop in signaling regulation(Baker et al., 2009; Krebs and Hilton, 2001; Morris et al., 2018; O'Shea et al., 2002). The investigations showed that a JAK inhibitor targeting the JAK-STAT signaling pathway downregulated heightened SOCS1 expression but had no impact on IRAKM, a member of the IRAK family involved in activating the TLR-NF-κB signaling pathway(Fukao and Koyasu, 2003; Liew et al., 2005). This suggests that the restoration of tolerized LC maturation by the JAK inhibitor does not involve the negative regulator induced by the TLR2-NF-κB pathway. Thus, it indicates that the induction of SOCS1 due to repeated exposure to the TLR2 ligand may, at least partly, occur through an indirect mechanism.

The induction of SOCS1 through the JAK-STAT pathway is a well-established phenomenon, although the impact of JAK inhibitors on SOCS1 remains incompletely understood. Previous studies have demonstrated that pretreatment of moDC with the JAK2 inhibitor TG101348 effectively blocks IL-6-induced pSTAT3(Betts et al., 2011). Additionally, Martino et al. reported that pretreatment with ruxolitinib, a JAK1/2 inhibitor, inhibits LPS-induced STAT1/3 phosphorylation and the subsequent increase in SOCS3 expression in human umbilical vein endothelial cells (HUVECs)(Martino et al., 2022). Consistent with these findings, this study indicated that the JAK1/2 inhibitor ruxolitinib significantly downregulates SOCS1 mRNA expression. This downregulation is associated with the restoration of maturation in tolerized CD34LC upon TLR2-mediated stimulation.

However, it should be noted that other unexplored mechanisms may contribute to how JAK1/2 inhibitors induce hypersensitive LC maturation.

This study showed that SOCS1 diminished by JAK inhibitors restoring maturation of the tolerized LC. It implied that SOCS1 plays a crucial role in developing these tolerization LC. Additionally, SOCS1 has been demonstrated to be expressed in the epidermis of chronic AD skin but not in non-lesional skin, whereas its expression is restricted to certain areas of faint positivity(Federici et al., 2002). This observation further validates the role of SOCS1 and supports the notion that tolerized LC generated in the *in vitro* experiments are comparable to LC isolated from AD skin.

4.3 JAK inhibitors restore the activation of tolerized LC, potentially through the inhibition of SOCS1.

I. Impact of JAK inhibitors on tolerized LC maturation.

This study showed that JAK inhibitors partially restored the response of tolerized LC to TLR2-mediated maturation and that CD83, CD86, and MHC II significantly upregulated primed CD34LC toward Pam3Cys. This is in contrast to other studies showing JAK inhibitors impairing DC maturation and activation by downregulating TLR-induced expression of CD80, CD86, and CD83(Heine et al., 2013; Shi et al., 2017; Stickel et al., 2017; Vogel et al., 2022) or altering the phenotypic differentiation of DC(Betts et al., 2011; Klaeschen et al., 2021; Marzaioli et al., 2020; Shi et al., 2017). The discrepancy could potentially be attributed to the utilization of IL-4 during the generation of DC. IL-4 is known to contribute to the promotion of DC differentiation(Hiasa et al., 2009; Holla et al., 2014; Rosenzwajg et al., 1998), and the IL-4-STAT pathway is also involved in this process. The utilization of JAK inhibitors could disrupt the generation of these cells. Furthermore, prolonged exposure of precursor cells to JAK inhibitors has also been demonstrated to affect the proportion of CD1a cells during DC generation(Heine et al., 2013; Klaeschen et al., 2021). A previous study has reported similar results, showing that JAK2 inhibitor induced a significant increase in CD40, CD83, and CD86 in DC without stimulation(Nefedova et al., 2005). Thus, JAK inhibitors can regulate the immunological behaviour of DC and have an impact on their maturation under certain conditions.

Additionally, JAK inhibitors enhanced the expression of CD86 on tolerized LC while having no impact on CD80 expression, potentially restoring at least in part their stimulatory ability towards T cells (Borriello et al., 1997; Subauste et al., 1998). Recent studies have identified the differences between CD80 and CD86 in influencing T-cell immune responses. CD86 has been proposed as the more important and dominant costimulatory ligand on DC for T cell stimulation and regulation involving CD28 and CTLA-4(Caux et al., 1994; Collins et al., 2002; Halliday et al., 2020; Zheng et al., 2004). The discrepancy of restored between CD80 and CD86 would differ from the response of healthy LC to T-cell stimulation.

II. The crosstalk mechanisms between the TLR2 and JAK-STAT signaling pathways.

Studies on DC have shown that SOCS1 can be induced by TLR-associated cytokines, such as type I and II interferons and IL-6, via the JAK/STAT signaling pathway(Baker et al., 2009; Huang et al., 2020; Morris et al., 2018; Steyn et al., 2019; Yoshimura et al., 2007; Zhang et al., 2012). However, Pam3Cys did not induce IFN-α or IFN-γ in either LC or tolerized LC. Moreover, blocking IL-6 and other potential JAK-associated cytokines (IL-3, IL-13, IL-31, IL-5, IL-15, IL-25, and TSLP) with additional antibodies did not prevent the development of LC into a tolerized state in response to Pam3Cys stimulation (data not shown). This implied that tolerized LC may not be induced by these specific cytokines.

SOCS1 exerts distinct inhibitory functions in the JAKs-STAT and TLR2-NF-κB signaling pathways. Structurally, SOCS1 comprises three conserved domains: N-terminal, SH2, and SOCS box(Sharma and Larkin, 2019; Trengove and Ward, 2013). The N-terminal domain, housing the kinase inhibitory region (KIR), specifically inhibits JAKs. The SH2 domain, with an extended SH2 sequence (ESS), prevents STAT binding by facilitating substrate binding to phosphotyrosine residues, thus blocking signaling. With Elongin B/C and Cullin5 sub-domains, the SOCS box recruits E3 ligase components for ubiquitination and subsequent proteasomal degradation of target proteins(Sharma and Larkin, 2019; Trengove and Ward, 2013). However, SOCS1 modulates the TLR2-NF-κB pathway by leveraging the E3 ubiquitin ligase, interacting with key signal transduction elements, including MAL/TIRAP, TRAF6, and the p65 subunit of NF-κB, leading to ubiquitin-mediated proteasomal degradation(Huang et al., 2020; Sharma and Larkin, 2019).

4.4 Restoration of TLR2 responsiveness in AD lesional skin.

In recent *ex vivo* study on AD skin(Philipp et al., 2024), LC isolated from lesional skin of both treated (topical steroids or tacrolimus for 2 days) and non-treated AD patients, as well as healthy controls (HC). These findings revealed that after treatment, LC from treated AD patients showed restored responsiveness to TLR2 stimulation, as evidenced by increased expression of CD83, CD80, and CD86, as well as enhanced production of IL-6 and IL-10, while IL-18 levels were reduced. Additionally, levels of IL-1ß, IL-18, TNF-a, and IL-23 were lower in treated AD compared to untreated AD. These results suggest that anti-inflammatory treatment promptly restores TLR2 activity in the lesion, preceding observable physical changes. However, the present study shows that the anti-inflammatory compounds hydrocortisone and tacrolimus do not restore TLR2 activation in tolerized LC, suggesting that the reactivity of LC from treated AD is not directly influenced by these drugs but in a secondary step. Therefore, based on our comprehensive findings, we speculate that reduced responsiveness of tolerized LC and AD LC to TLR2 may be attributed to exposure to the high-inflammatory cytokine environment of AD lesion. Application of anti-inflammatory drugs or JAK inhibitors may reduce exposure to inflammatory cytokines, thereby restoring activation responses to TLR2 ligands, thought at least partly SOCS1 regulation.

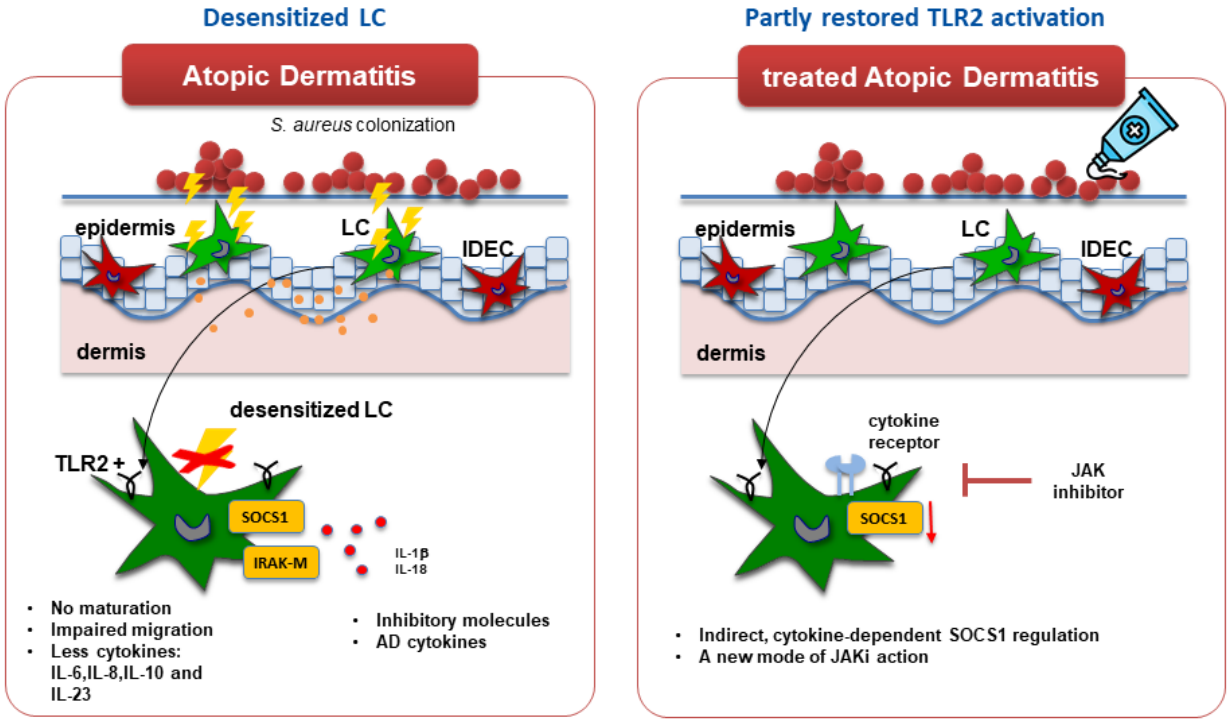

Figure. 23: Restoration of TLR2 responsiveness in AD lesional skin

Conclusion：

Taken together, this study sheds light on the involvement of hyporesponsive LC in the pathogenesis of AD by investigating the molecules and functions of tolerized LC. Results indicate that the tolerization of LC is associated to the induction of negative regulators of the TLR2 pathway, SOCS1, and IRKAM due to repetitive exposure to pathogens. These findings provide novel insights into the role of LC in the pathogenesis of AD and the control of the microbial composition on the ksin. Moreover, this study demonstrate that the JAK1/2 inhibitor can restore the maturation of hyporesponsive LC, potentially via downregulation of elevated SOCS1. These findings suggest a new mode of action of JAK1/2 inhibitors in AD therapy.

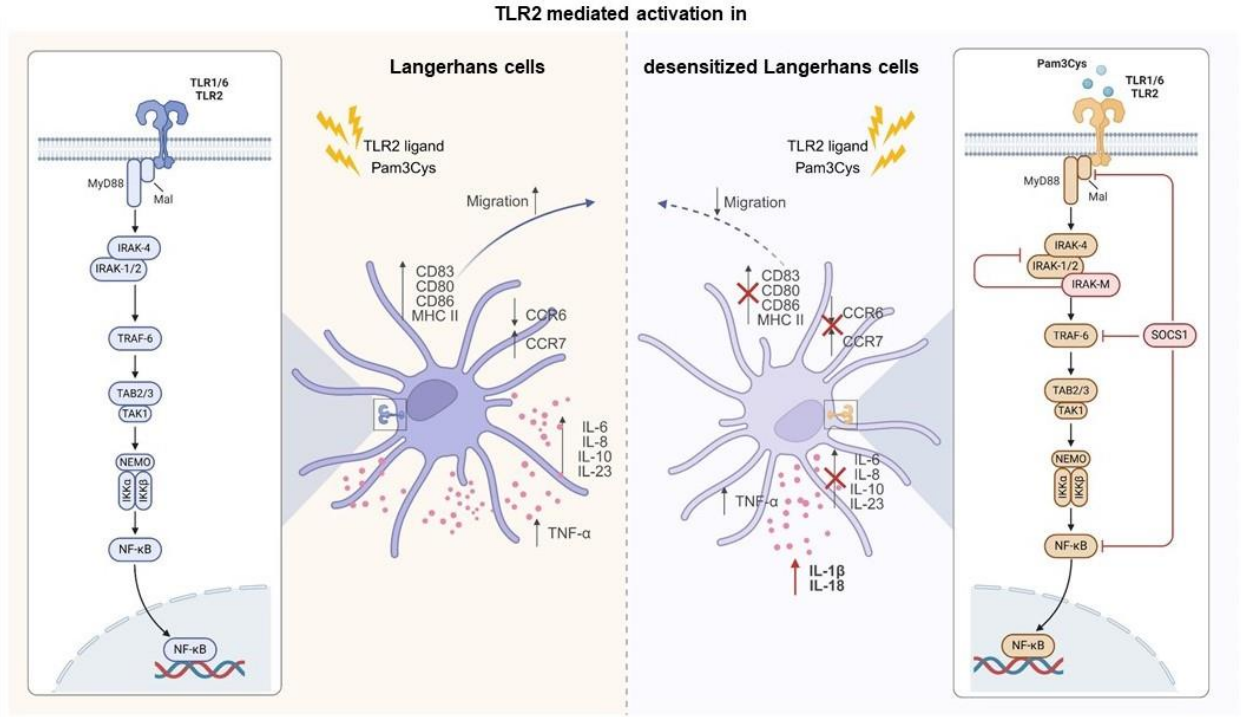

Figure. 24: TLR2 mediated activation in LC and tolerized LC

5. Abstract

Atopic dermatitis (AD) represents the most common chronic, inflammatory, and recurrent disease intricately influenced by genetic and immune factors, with environmental interactions playing a pivotal role. Epidermal Langerhans cells (LC), as primary antigen-presenting dendritic cells (APC) in the epidermis, serve as indispensable intermediaries bridging the innate and adaptive immune systems. Recognizing microbial signals through various pattern recognition receptors (PRRs) like Toll-like receptors (TLR) on APC triggers LC activation, cytokine production, and subsequent T-cell responses. Notably, TLR2 is implicated to sense *Staphylococcus aureus* (*S. a.*) from the skin´s microbiota and has a high prevalence in AD skin. Thus *S. a.* contributes to the pathogenesis of the disease.

This study investigated the molecular and functional properties of LC within the TLR2 signaling pathway in AD, shedding light on the underlying mechanisms governing these cells. Previous findings revealed TLR2 signaling tolerance in LC isolated from AD lesions, indicating an impaired *S. a.* sensing. The hypothesis of this study is that LC tolerization results from persistent TLR2 stimulation in AD lesions, attributable to increased *S. a.* colonization. The objective was to replicate tolerized LC observed in AD *in vitro*, comprehensively study their molecular and functional characteristics and explore strategies to restore TLR2-induced activation.

To address this, an *in vitro* model was established as part of this work. LC were generated from CD34 hematopoetic stem cells (CD34LC) and persistent microbial pathogen stimulation in AD skin lesions was mimicked by repetitive TLR2 triggering. Tolerization of CD34LC was characterized by impaired maturation, reduced expression of migratory molecules, and diminished migratory capacity upon stimulation. Thus, the model mirrored hallmarks of skin LC in AD. Additionally, there was an altered cytokine profile, including a lack of IL-6, IL-8, IL-10, and IL-23 release, confirming the impaired LC response. Surprisingly IL-1β and IL-18 levels were increased upon TLR2 stimulation in these cells. This does not only show LC to be a source of these factors under certain conditions, but again shows a parallel to primary skin culture results from AD donors. Taken together, the herein newly established model successfully represents LC from AD skin.

Exploring potential mechanisms in tolerized LC, the signaling molecules of the TLR downstream signal pathway were addressed. The unresponsiveness of LC was accompanied by elevated negative regulators SOCS1 and IRAK-M, while the molecules

of the activatory line were hardly affected. In order to restore the functionality, several agents were addressed. JAK1/2 inhibitors partially restored the activated phenotype of tolerized LC via a SOCS1 downregulation.

In conclusion, this study sheds light on the involvement of hyporesponsive LC in AD pathogenesis by dissecting the functions and underlying molecular mechanisms of tolerized LC. The central role for negative regulators including SOCS1 and the potential of JAK1/2 inhibitors to decrease SOCS1 and to restore maturation in these cells offers novel insights into the mode of action of JAK inhibitors in AD therapy.

6. List of figures

7. List of tables

8. References

van der Aar AMG, Sylva-Steenland RMR, Bos JD, et al. Cutting Edge: Loss of TLR2, TLR4, and TLR5 on Langerhans Cells Abolishes Bacterial Recognition1. The Journal of Immunology 2007;178(4):1986–1990

Agüero MG de, Vocanson M, Hacini-Rachinel F, et al. Langerhans Cells Protect from Allergic Contact Dermatitis in Mice by Tolerizing $CD8^+$ T Cells and Activating $Foxp3^+$ Regulatory T Cells. J Clin Invest 2012;122(5):1700–1711

Albrecht V, Hofer TP, Foxwell B, et al. Tolerance Induced via TLR2 and TLR4 in Human Dendritic Cells: Role of IRAK-1. Bmc Immunol 2008;9(1):69

Aliahmadi E, Gramlich R, Grützkau A, et al. TLR2-Activated Human Langerhans Cells Promote Th17 Polarization via IL-1β, TGF-β and IL-23. Eur J Immunol 2009;39(5):1221–1230

Atmatzidis D h., Lambert W c. and Lambert M w. Langerhans Cell: Exciting Developments in Health and Disease. J Eur Acad Dermatol Venereol 2017;31(11):1817–1824

Baker BJ, Akhtar LN and Benveniste EN. SOCS1 and SOCS3 in the Control of CNS Immunity. Trends Immunol 2009;30(8):392–400

Banchereau J and Steinman RM. Dendritic Cells and the Control of Immunity. Nature 1998;392(6673):245–252

Baratin M, Foray C, Demaria O, et al. Homeostatic NF-κB Signaling in Steady-State Migratory Dendritic Cells Regulates Immune Homeostasis and Tolerance. Immunity 2015;42(4):627–639

Barton GM and Medzhitov R. Toll-Like Receptor Signaling Pathways. Science 2003;300(5625):1524–1525

Bernard M, Carrasco C, Laoubi L, et al. IL-1β Induces Thymic Stromal Lymphopoietin and an Atopic Dermatitis-like Phenotype in Reconstructed Healthy Human Epidermis: IL-1β Induces AD-like Epidermal Phenotype. J Pathol 2017;242(2):234–245

Betts BC, Abdel-Wahab O, Curran SA, et al. Janus Kinase-2 Inhibition Induces Durable Tolerance to Alloantigen by Dendritic Cell-Stimulated Human T Cells, Yet Preserves Immunity to Recall Antigen. Blood 2011;118(21):1903

Bieber T. Atopic Dermatitis: An Expanding Therapeutic Pipeline for a Complex Disease. Nat Rev Drug Discovery 2022;21(1):21–40

Bieber T, Novak N, Herrman N, et al. Role of Dendritic Cells in Atopic Dermatitis: An Update. Clin Rev Allerg Immu 2011;41(3):254–258

Bieber T, Paller AS, Kabashima K, et al. Atopic Dermatitis: Pathomechanisms and Lessons Learned from Novel Systemic Therapeutic Options. J Eur Acad Dermatol Venereol 2022;36(9):1432–1449

Biswas SK and Lopez-Collazo E. Endotoxin Tolerance: New Mechanisms, Molecules and Clinical Significance. Trends Immunol 2009;30(10):475–487

Borriello F, Sethna MP, Boyd SD, et al. B7-1 and B7-2 Have Overlapping, Critical Roles in Immunoglobulin Class Switching and Germinal Center Formation. Immunity 1997;6(3):303–313

Bruynzeel-Koomen C, van Wichen DF, Toonstra J, et al. The Presence of IgE Molecules on Epidermal Langerhans Cells in Patients with Atopic Dermatitis. Arch Dermatol Res 1986;278(3):199–205

Cabeza-Cabrerizo M, Cardoso A, Minutti CM, et al. Dendritic Cells Revisited. Annu Rev Immunol 2021;39(1):131–166

Caux C, Vanbervliet B, Massacrier C, et al. B70/B7-2 Is Identical to CD86 and Is the Major Functional Ligand for CD28 Expressed on Human Dendritic Cells. J Exp Med 1994;180(5):1841–1847

Chovatiya R and Paller AS. JAK Inhibitors in the Treatment of Atopic Dermatitis. J Allergy Clin Immunol 2021;148(4):927–940

Clausen M-L, Kezic S, Olesen CM, et al. Cytokine Concentration across the Stratum Corneum in Atopic Dermatitis and Healthy Controls. Sci Rep 2020;10(1):21895

Cole TS, Zhang M, Standiford TJ, et al. IRAK-M Modulates Expression of IL-10 and Cell Surface Markers CD80 and MHC II after Bacterial Re-Stimulation of Tolerized Dendritic Cells. Immunol Lett 2012;144(1–2):49–59

Colleselli K, Stierschneider A and Wiesner C. An Update on Toll-like Receptor 2, Its Function and Dimerization in Pro- and Anti-Inflammatory Processes. International Journal of Molecular Sciences 2023;24(15):12464

Collins AV, Brodie DW, Gilbert RJC, et al. The Interaction Properties of Costimulatory Molecules Revisited. Immunity 2002;17(2):201–210

Coveney AP, Wang W, Kelly J, et al. Myeloid-Related Protein 8 Induces Self-Tolerance and Cross-Tolerance to Bacterial Infection via TLR4- and TLR2-Mediated Signal Pathways. Sci Rep 2015;5(1):13694

Dai X, Sayama K, Tohyama M, et al. Mite Allergen Is a Danger Signal for the Skin via Activation of Inflammasome in Keratinocytes. J Allergy Clin Immun 2011;127(3):806-814.e4

Damsky W and King BA. JAK Inhibitors in Dermatology: The Promise of a New Drug Class. Journal of the American Academy of Dermatology 2017;76(4):736–744

Danso MO, van Drongelen V, Mulder A, et al. TNF-α and Th2 Cytokines Induce Atopic Dermatitis–Like Features on Epidermal Differentiation Proteins and Stratum Corneum Lipids in Human Skin Equivalents. J Invest Dermatol 2014;134(7):1941–1950

Deckers J, Hammad H and Hoste E. Langerhans Cells: Sensing the Environment in Health and Disease. Front Immunol 2018;9:93

Doebel T, Voisin B and Nagao K. Langerhans Cells – The Macrophage in Dendritic Cell Clothing. Trends in Immunology 2017;38(11):817–828

Domogalla MP, Rostan PV, Raker VK, et al. Tolerance through Education: How Tolerogenic Dendritic Cells Shape Immunity. Front Immunol 2017;8

Federici M, Giustizieri ML, Scarponi C, et al. Impaired IFN-γ-Dependent Inflammatory Responses in Human Keratinocytes Overexpressing the Suppressor of Cytokine Signaling 1. J Immunol 2002;169(1):434–442

Fekete T, Szabo A, Beltrame L, et al. Constraints for Monocyte-Derived Dendritic Cell Functions under Inflammatory Conditions. Eur J Immunol 2012;42(2):458–469

Ferlito M, Romanenko OG, Ashton S, et al. Effect of Cross-Tolerance between Endotoxin and TNF-α or IL-1β on Cellular Signaling and Mediator Production. J Leukocyte Biol 2001;70(5):821–829

Fu H, Song S, Liu F, et al. Dendritic Cells Transduced with SOCS1 Gene Exhibit Regulatory DC Properties and Prolong Allograft Survival. Cell Mol Immunol 2009;6(2):87–95

Fucikova J, Palova-Jelinkova L, Bartunkova J, et al. Induction of Tolerance and Immunity by Dendritic Cells: Mechanisms and Clinical Applications. Front Immunol 2019;10

Fukao T and Koyasu S. PI3K and Negative Regulation of TLR Signaling. Trends in Immunology 2003;24(7):358–363

Gardner A, de Mingo Pulido Á and Ruffell B. Dendritic Cells and Their Role in Immunotherapy. Front Immunol 2020;11

Geisel J, Kahl F, Müller M, et al. IL-6 and Maturation Govern TLR2 and TLR4 Induced TLR Agonist Tolerance and Cross-Tolerance in Dendritic Cells. J Immunol 2007;179(9):5811–5818

Gros E, Bussmann C, Bieber T, et al. Expression of Chemokines and Chemokine Receptors in Lesional and Nonlesional Upper Skin of Patients with Atopic Dermatitis. J Allergy Clin Immun 2009;124(4):753-760.e1

Guttman-Yassky E, Irvine AD, Brunner PM, et al. The Role of Janus Kinase Signaling in the Pathology of Atopic Dermatitis. J Allergy Clin Immunol 2023

Halliday N, Williams C, Kennedy A, et al. CD86 Is a Selective CD28 Ligand Supporting FoxP3+ Regulatory T Cell Homeostasis in the Presence of High Levels of CTLA-4. Front Immunol 2020;11

Hanada T, Yoshida H, Kato S, et al. Suppressor of Cytokine Signaling-1 Is Essential for Suppressing Dendritic Cell Activation and Systemic Autoimmunity. Immunity 2003;19(3):437–450

He H and Guttman-Yassky E. JAK Inhibitors for Atopic Dermatitis: An Update. Am J Clin Dermatol 2019;20(2):181–192

Heine A, Held SAE, Daecke SN, et al. The JAK-Inhibitor Ruxolitinib Impairs Dendritic Cell Function in Vitro and in Vivo. Blood 2013;122(7):1192–1202

Hennessy EJ, Parker AE and O'Neill LAJ. Targeting Toll-like Receptors: Emerging Therapeutics? Nat Rev Drug Discov 2010;9(4):293–307

Herrmann N, Nümm TJ, Iwamoto K, et al. Vitamin D3–Induced Promotor Dissociation of PU.1 and YY1 Results in FcεRI Reduction on Dendritic Cells in Atopic Dermatitis. J Immunol 2021;206(3):531–539

Hiasa M, Abe M, Nakano A, et al. GM-CSF and IL-4 Induce Dendritic Cell Differentiation and Disrupt Osteoclastogenesis through M-CSF Receptor Shedding by up-Regulation of TNF-Alpha Converting Enzyme (TACE). Blood 2009;114(20):4517–4526

Hildebrand D, Metz-Zumaran C, Jaschkowitz G, et al. Silencing SOCS1 via Liposome-Packed siRNA Sustains TLR4-Ligand Adjuvant. Front Immunol 2019;10:1279

Holla S, Sharma M, Vani J, et al. GM-CSF along with IL-4 but Not Alone Is Indispensable for the Differentiation of Human Dendritic Cells from Monocytes. J Allergy Clin Immun 2014;133(5):1500-1502.e1

Honda T and Kabashima K. Reconciling Innate and Acquired Immunity in Atopic Dermatitis. Journal of Allergy and Clinical Immunology 2020;145(4):1136–1137

Hu W and Spaink HP. The Role of TLR2 in Infectious Diseases Caused by Mycobacteria: From Cell Biology to Therapeutic Target. Biology 2022;11(2):246

Hu X, Li J, Fu M, et al. The JAK/STAT Signaling Pathway: From Bench to Clinic. Signal Transduct Tar 2021;6(1):1–33

Huang S, Liu K, Cheng A, et al. SOCS Proteins Participate in the Regulation of Innate Immune Response Caused by Viruses. Front Immunol 2020;11:558341

Hülpüsch C, Weins AB, Traidl-Hoffmann C, et al. A New Era of Atopic Eczema Research: Advances and Highlights. Allergy 2021;76(11):3408–3421

Igyártó BZ, Haley K, Ortner D, et al. Skin-Resident Murine Dendritic Cell Subsets Promote Distinct and Opposing Antigen-Specific T Helper Cell Responses. Immunity 2011;35(2):260–272

Iwamoto K, Nümm TJ, Koch S, et al. Langerhans and Inflammatory Dendritic Epidermal Cells in Atopic Dermatitis Are Tolerized toward TLR2 Activation. Allergy 2018;73(11):2205–2213

Iwasaki A and Medzhitov R. Toll-like Receptor Control of the Adaptive Immune Responses. Nat Immunol 2004;5(10):987–995

Jasani B, Navabi H and Adams M. Ampligen: A Potential Toll-like 3 Receptor Adjuvant for Immunotherapy of Cancer. Vaccine 2009;27(25):3401–3404

Jiang A, Bloom O, Ono S, et al. Disruption of E-Cadherin-Mediated Adhesion Induces a Functionally Distinct Pathway of Dendritic Cell Maturation. Immunity 2007;27(4):610–624

Jin MS and Lee J-O. Structures of the Toll-like Receptor Family and Its Ligand Complexes. Immunity 2008;29(2):182–191

Kashem SW, Haniffa M and Kaplan DH. Antigen-Presenting Cells in the Skin. Annu Rev Immunol 2017;35(1):469–499

Kashem SW, Igyártó BZ, Gerami-Nejad M, et al. Candida Albicans Morphology and Dendritic Cell Subsets Determine T Helper Cell Differentiation. Immunity 2015;42(2):356–366

Kawai T and Akira S. Toll-like Receptors and Their Crosstalk with Other Innate Receptors in Infection and Immunity. Immunity 2011;34(5):637–650

Kawasaki T and Kawai T. Toll-Like Receptor Signaling Pathways. Front Immunol 2014;5

Kelley N, Jeltema D, Duan Y, et al. The NLRP3 Inflammasome: An Overview of Mechanisms of Activation and Regulation. Int J Mol Sci 2019;20(13):3328

Kinjyo I, Hanada T, Inagaki-Ohara K, et al. SOCS1/JAB Is a Negative Regulator of LPS-Induced Macrophage Activation. Immunity 2002;17(5):583–591

Klaeschen AS, Nümm TJ, Herrmann N, et al. JAK1/2 Inhibition Impairs the Development and Function of Inflammatory Dendritic Epidermal Cells in Atopic Dermatitis. Journal of Allergy and Clinical Immunology 2021;147(6):2202-2212.e8

Kobayashi K, Hernandez LD, Galán JE, et al. IRAK-M Is a Negative Regulator of Toll-like Receptor Signaling. Cell 2002;110(2):191–202

Kobayashi T, Glatz M, Horiuchi K, et al. Dysbiosis and Staphylococcus Aureus Colonization Drives Inflammation in Atopic Dermatitis. Immunity 2015;42(4):756–766

Koch S, Stroisch TJ, Vorac J, et al. AhR Mediates an Anti-Inflammatory Feedback Mechanism in Human Langerhans Cells Involving FcεRI and IDO. Allergy 2017a;72(11):1686–1693

Koch SR, Lamb FS, Hellman J, et al. Potentiation and Tolerance of Toll-like Receptor Priming in Human Endothelial Cells. Transl Res 2017b;180:53-67.e4

Kondo T, Kawai T and Akira S. Dissecting Negative Regulation of Toll-like Receptor Signaling. Trends Immunol 2012;33(9):449–458

Korn T, Bettelli E, Oukka M, et al. IL-17 and Th17 Cells. Annu Rev Immunol 2009;27(1):485–517

Kortekaas Krohn I, Aerts JL, Breckpot K, et al. T-Cell Subsets in the Skin and Their Role in Inflammatory Skin Disorders. Allergy 2022;77(3):827–842

Kou K, Aihara M, Matsunaga T, et al. Association of Serum Interleukin-18 and Other Biomarkers with Disease Severity in Adults with Atopic Dermatitis. Arch Dermatol Res 2012;304(4):305–312

Krebs DL and Hilton DJ. SOCS Proteins: Negative Regulators of Cytokine Signaling. STEM CELLS 2001;19(5):378–387

Kreutz M, Ackermann U, Hauschildt S, et al. A Comparative Analysis of Cytokine Production and Tolerance Induction by Bacterial Lipopeptides, Lipopolysaccharides and Staphyloccocus Aureus in Human Monocytes. Immunology 1997;92(3):396–401

Kuo I-H, Carpenter-Mendini A, Yoshida T, et al. Activation of Epidermal Toll-like Receptor 2 Enhances Tight Junction Function: Implications for Atopic Dermatitis and Skin Barrier Repair. J Invest Dermatol 2013;133(4):988–998

Kushwah R and Hu J. Role of Dendritic Cells in the Induction of Regulatory T Cells. Cell & Bioscience 2011;1(1):20

Kwiek B, Leśniewska A, Kowalewski C, et al. Langerhans Cells Are Predominant High Affinity Immunoglobulin E Receptor Bearing Cells in the Epidermis of Bullous Pemphigoid Skin. Journal of Dermatological Science 2017;85(1):60–63

Langan SM, Irvine AD and Weidinger S. Atopic Dermatitis. The Lancet 2020;396(10247):345–360

Lechmann M, Berchtold S, Steinkasserer A, et al. CD83 on Dendritic Cells: More than Just a Marker for Maturation. Trends Immunol 2002;23(6):273–275

Leung DYM. New Insights into Atopic Dermatitis: Role of Skin Barrier and Immune Dysregulation. Allergol Int 2013;62(2):151–161

Li D and Wu M. Pattern Recognition Receptors in Health and Diseases. Signal Transduct Tar 2021;6(1):1–24

Liew FY, Xu D, Brint EK, et al. Negative Regulation of Toll-like Receptor-Mediated Immune Responses. Nat Rev Immunol 2005;5(6):446–458

Liu D, Cao S, Zhou Y, et al. Recent Advances in Endotoxin Tolerance. J of Cellular Biochemistry 2019;120(1):56–70

Liu J, Zhang X, Cheng Y, et al. Dendritic Cell Migration in Inflammation and Immunity. Cell Mol Immunol 2021;18(11):2461–2471

Liu K and Nussenzweig MC. Origin and Development of Dendritic Cells. Immunological Reviews 2010;234(1):45–54

Luu K, Greenhill CJ, Majoros A, et al. STAT1 Plays a Role in TLR Signal Transduction and Inflammatory Responses. Immunol Cell Biol 2014;92(9):761–769

Maglione PJ, Simchoni N and Cunningham-Rundles C. Toll-like Receptor Signaling in Primary Immune Deficiencies: TLR Signaling in Primary Immune Deficiencies. Ann Ny Acad Sci 2015;1356(1):1–21

Maldifassi MC, Atienza G, Arnalich F, et al. A New IRAK-M-Mediated Mechanism Implicated in the Anti-Inflammatory Effect of Nicotine via A7 Nicotinic Receptors in Human Macrophages. Ho Y-S. ed. PLoS ONE 2014;9(9):e108397

Mansell A, Smith R, Doyle SL, et al. Suppressor of Cytokine Signaling 1 Negatively Regulates Toll-like Receptor Signaling by Mediating Mal Degradation. Nat Immunol 2006;7(2):148–155

Martino N, Bossardi Ramos R, Chuy D, et al. SOCS3 Limits TNF and Endotoxin-Induced Endothelial Dysfunction by Blocking a Required Autocrine Interleukin-6 Signal in Human Endothelial Cells. American Journal of Physiology-Cell Physiology 2022;323(2):C556–C569

Marzaioli V, Canavan M, Floudas A, et al. Monocyte-Derived Dendritic Cell Differentiation in Inflammatory Arthritis Is Regulated by the JAK/STAT Axis via NADPH Oxidase Regulation. Front Immunol 2020;11:1406

Mathers AR, Janelsins BM, Rubin JP, et al. Differential Capability of Human Cutaneous Dendritic Cell Subsets to Initiate Th17 Responses1. The Journal of Immunology 2009;182(2):921–933

Mbongue JC, Nieves HA, Torrez TW, et al. The Role of Dendritic Cell Maturation in the Induction of Insulin-Dependent Diabetes Mellitus. Front Immunol 2017;8

McLornan DP, Pope JE, Gotlib J, et al. Current and Future Status of JAK Inhibitors. The Lancet 2021;398(10302):803–816

Merad M, Ginhoux F and Collin M. Origin, Homeostasis and Function of Langerhans Cells and Other Langerin-Expressing Dendritic Cells. Nat Rev Immunol 2008;8(12):935–947

Merad M, Sathe P, Helft J, et al. The Dendritic Cell Lineage: Ontogeny and Function of Dendritic Cells and Their Subsets in the Steady State and the Inflamed Setting. Annu Rev Immunol 2013;31(1):563–604

Morelli AE and Thomson AW. Tolerogenic Dendritic Cells and the Quest for Transplant Tolerance. Nat Rev Immunol 2007;7(8):610–621

Morris R, Kershaw NJ and Babon JJ. The Molecular Details of Cytokine Signaling via the JAK/STAT Pathway: Cytokine Signaling via the JAK/STAT Pathway. Protein Sci 2018;27(12):1984–2009

Murphy J-E, Robert C and Kupper TS. Interleukin-1 and Cutaneous Inflammation: A Crucial Link Between Innate and Acquired Immunity. J Invest Dermatol 2000;114(3):602–608

Murphy MB, Xiong Y, Pattabiraman G, et al. Pellino-3 Promotes Endotoxin Tolerance and Acts as a Negative Regulator of TLR2 and TLR4 Signaling. J Leukocyte Biol 2015;98(6):963–974

Nakagawa R, Naka T, Tsutsui H, et al. SOCS-1 Participates in Negative Regulation of LPS Responses. Immunity 2002;17(5):677–687

Nakayama K, Okugawa S, Yanagimoto S, et al. Involvement of IRAK-M in Peptidoglycan-Induced Tolerance in Macrophages. Journal of Biological Chemistry 2004;279(8):6629–6634

Nefedova Y, Cheng P, Gilkes D, et al. Activation of Dendritic Cells via Inhibition of Jak2/STAT3 Signaling. Journal of immunology (Baltimore, Md : 1950) 2005;175(7):4338–4346.

Niebuhr M, Langnickel J, Draing C, et al. Dysregulation of Toll-like Receptor-2 (TLR-2)-Induced Effects in Monocytes from Patients with Atopic Dermatitis: Impact of the TLR-2 R753Q Polymorphism. Allergy 2008;63(6):728–734

Niebuhr M, Lutat C, Sigel S, et al. Impaired TLR-2 Expression and TLR-2-Mediated Cytokine Secretion in Macrophages from Patients with Atopic Dermatitis. Allergy 2009;64(11):1580–1587

Novak N. An Update on the Role of Human Dendritic Cells in Patients with Atopic Dermatitis. Journal of Allergy and Clinical Immunology 2012;129(4):879–886

Novak N, Koch S, Allam J-P, et al. Dendritic Cells: Bridging Innate and Adaptive Immunity in Atopic Dermatitis. J Allergy Clin Immunol 2010;125(1):50–59

Novak N, Kraft S and Bieber T. Unraveling the Mission of FcεRI on Antigen-Presenting Cells. J Allergy Clin Immun 2003;111(1):38–44

Nümm TJ, Langerhans and Inflammatory Dendritic Epidermal Cells in Atopic Dermatitis Tolerate Toll-like Receptor 2-Specific Activation. PhD Thesis, University of Bonn, German, 2021

Ohl L, Mohaupt M, Czeloth N, et al. CCR7 Governs Skin Dendritic Cell Migration under Inflammatory and Steady-State Conditions. Immunity 2004;21(2):279–288

de Oliviera Nascimento L, Massari P and Wetzler L. The Role of TLR2 in Infection and Immunity. Front Immunol 2012;3.

O'Neill LAJ. When Signaling Pathways Collide: Positive and Negative Regulation of Toll-like Receptor Signal Transduction. Immunity 2008;29(1):12–20

O'Neill LAJ and Bowie AG. The Family of Five: TIR-Domain-Containing Adaptors in Toll-like Receptor Signalling. Nat Rev Immunol 2007;7(5):353–364

O'Shea JJ, Gadina M and Schreiber RD. Cytokine Signaling in 2002. Cell 2002;109(2):S121–S131

Otsuka M, Egawa G and Kabashima K. Uncovering the Mysteries of Langerhans Cells, Inflammatory Dendritic Epidermal Cells, and Monocyte-Derived Langerhans Cell-Like Cells in the Epidermis. Front Immunol 2018;9:1768

Peiser M, Koeck J, Kirschning CJ, et al. Human Langerhans Cells Selectively Activated via Toll-like Receptor 2 Agonists Acquire Migratory and CD4+T Cell Stimulatory Capacity. J Leukocyte Biol 2008;83(5):1118–1127

Peng W and Novak N. Pathogenesis of Atopic Dermatitis. Clin Exp Allergy 2015;45(3):566–574

Philipp M-S, Nümm TJ, Deng Y, et al. Evidence for a Restoration of TLR2 Response in Epidermal Dendritic Cells in Atopic Dermatitis by Topical Anti-Inflammatory Therapy. Allergy 2024;79(1):249–252

Posselt G, Schwarz H, Duschl A, et al. Suppressor of Cytokine Signaling 2 Is a Feedback Inhibitor of TLR-Induced Activation in Human Monocyte-Derived Dendritic Cells. J Immunol 2011;187(6):2875–2884

Ratzinger G, Baggers J, de Cos MA, et al. Mature Human Langerhans Cells Derived from CD34+ Hematopoietic Progenitors Stimulate Greater Cytolytic T Lymphocyte Activity in the Absence of Bioactive IL-12p70, by Either Single Peptide Presentation or Cross-Priming, Than Do Dermal-Interstitial or Monocyte-Derived Dendritic Cells1. J Immunol 2004;173(4):2780–2791

Rayhane N, Fitting C and Cavaillon J-M. Dissociation of IFN-γ from IL-12 and IL-18 Production during Endotoxin Tolerance. Journal of Endotoxin Research 1999;5(5–6):319–324

Reid SD, Penna G and Adorini L. The Control of T Cell Responses by Dendritic Cell Subsets. Curr Opin Immunol 2000;12(1):114–121

Renn CN, Sanchez DJ, Ochoa MT, et al. TLR Activation of Langerhans Cell-Like Dendritic Cells Triggers an Antiviral Immune Response1. The Journal of Immunology 2006;177(1):298–305

Rhee SH, Jones BW, Toshchakov V, et al. Toll-like Receptors 2 and 4 Activate STAT1 Serine Phosphorylation by Distinct Mechanisms in Macrophages. Journal of Biological Chemistry 2003;278(25):22506–22512

Romani N, Brunner PM and Stingl G. Changing Views of the Role of Langerhans Cells. J Invest Dermatol 2012;132(3):872–881

Rosenzwajg M, Camus S, Guigon M, et al. The Influence of Interleukin (IL)-4, IL-13, and Flt3 Ligand on Human Dendritic Cell Differentiation from Cord Blood CD34+ Progenitor Cells. Exp Hematol 1998;26(1):63–72.

Said A and Weindl G. Regulation of Dendritic Cell Function in Inflammation. J Immunol Res 2015;2015:1–15

Sato S, Nomura F, Kawai T, et al. Synergy and Cross-Tolerance Between Toll-Like Receptor (TLR) 2- and TLR4-Mediated Signaling Pathways1. The Journal of Immunology 2000;165(12):7096–7101

Saturnino SF, Prado RO, Cunha-Melo JR, et al. Endotoxin Tolerance and Cross-Tolerance in Mast Cells Involves TLR4, TLR2 and FcεR1 Interactions and SOCS Expression: Perspectives on Immunomodulation in Infectious and Allergic Diseases. BMC Infect Dis 2010;10(1):240

Schwartz DM, Kanno Y, Villarino A, et al. JAK Inhibition as a Therapeutic Strategy for Immune and Inflammatory Diseases. Nat Rev Drug Discov 2017;16(12):843–862

Seeley JJ and Ghosh S. Molecular Mechanisms of Innate Memory and Tolerance to LPS. J Leukocyte Biol 2017;101(1):107–119

Seneschal J, Clark RA, Gehad A, et al. Human Epidermal Langerhans Cells Maintain Immune Homeostasis in Skin by Activating Skin Resident Regulatory T Cells. Immunity 2012;36(5):873–884

Seok JK, Kang HC, Cho Y-Y, et al. Therapeutic Regulation of the NLRP3 Inflammasome in Chronic Inflammatory Diseases. Arch Pharm Res 2021;44(1):16–35

Sharma J and Larkin J. Therapeutic Implication of SOCS1 Modulation in the Treatment of Autoimmunity and Cancer. Front Pharmacol 2019;10:324

Shi Z, Jiang W, Wang M, et al. Inhibition of JAK/STAT Pathway Restrains TSLP-Activated Dendritic Cells Mediated Inflammatory T Helper Type 2 Cell Response in Allergic Rhinitis. Mol Cell Biochem 2017;430(1–2):161–169

Simpson ME and Petri WA. TLR2 as a Therapeutic Target in Bacterial Infection. Trends in molecular medicine 2020;26(8):715–717

Solano-Gálvez SG, Tovar-Torres SM, Tron-Gómez MS, et al. Human Dendritic Cells: Ontogeny and Their Subsets in Health and Disease. Medical Sciences 2018;6(4):88

Ständer S. Atopic Dermatitis. Ropper AH. ed. N Engl J Med 2021;384(12):1136–1143

Staudacher A, Hinz T, Novak N, et al. Exaggerated IDO1 Expression and Activity in Langerhans Cells from Patients with Atopic Dermatitis upon Viral Stimulation: A Potential Predictive Biomarker for High Risk of Eczema Herpeticum. Allergy 2015;70(11):1432–1439

Steyn PJ, Dzobo K, Smith RI, et al. Interleukin-6 Induces Myogenic Differentiation via JAK2-STAT3 Signaling in Mouse C2C12 Myoblast Cell Line and Primary Human Myoblasts. Int J Mol Sci 2019;20(21):5273

Stickel N, Hanke K, Marschner D, et al. MicroRNA-146a Reduces MHC-II Expression via Targeting JAK/STAT Signaling in Dendritic Cells after Stem Cell Transplantation. Leukemia 2017;31(12):2732–2741

Subauste CS, De Waal Malefyt R and Fuh F. Role of CD80 (B7.1) and CD86 (B7.2) in the Immune Response to an Intracellular Pathogen. The Journal of Immunology 1998;160(4):1831–1840

Sun L, Liu W and Zhang L. The Role of Toll-Like Receptors in Skin Host Defense, Psoriasis, and Atopic Dermatitis. J Immunol Res 2019;2019:1–13

Sun Z, Vattepu R and Zhang S. Chemokines and Innate Lymphoid Cells in Skin Inflammation. Cells-basel 2021;10(11):3074

Tang L and Zhou F. Inflammasomes in Common Immune-Related Skin Diseases. Front Immunol 2020;11:882

Terhune J, Berk E and Czerniecki BJ. Dendritic Cell-Induced Th1 and Th17 Cell Differentiation for Cancer Therapy. Vaccines-basel 2013;1(4):527–549

Trengove MC and Ward AC. SOCS Proteins in Development and Disease. American journal of clinical and experimental immunology 2013;2(1):1–29.

Van Dalen R, De La Cruz Diaz JS, Rumpret M, et al. Langerhans Cells Sense *Staphylococcus Aureus* Wall Teichoic Acid through Langerin To Induce Inflammatory Responses. Gründling A and Msadek T. eds. mBio 2019;10(3):e00330-19

Verweyen E, Holzinger D, Weinhage T, et al. Synergistic Signaling of TLR and IFNα/β Facilitates Escape of IL-18 Expression from Endotoxin Tolerance. Am J Resp Crit Care 2020;201(5):526–539

Vogel A, Martin K, Soukup K, et al. JAK1 Signaling in Dendritic Cells Promotes Peripheral Tolerance in Autoimmunity through PD-L1-Mediated Regulatory T Cell Induction. Cell Rep 2022;38(8):110420

Vu AT, Baba T, Chen X, et al. Staphylococcus Aureus Membrane and Diacylated Lipopeptide Induce Thymic Stromal Lymphopoietin in Keratinocytes through the Toll-like Receptor 2–Toll-like Receptor 6 Pathway. J Allergy Clin Immun 2010;126(5):985-993.e3

Vulcano M, Albanesi C, Stoppacciaro A, et al. Dendritic Cells as a Major Source of Macrophage-Derived Chemokine/CCL22 in Vitro and in Vivo. Eur J Immunol 2001;31(3):812–822

Wang JH, Doyle M, Manning BJ, et al. Induction of Bacterial Lipoprotein Tolerance Is Associated with Suppression of Toll-like Receptor 2 Expression. J Biol Chem 2002;277(39):36068–36075

Weidinger S, Beck LA, Bieber T, et al. Atopic Dermatitis. Nature Reviews Disease Primers 2018;4(1):1

Weidinger S and Novak N. Atopic Dermatitis. Lancet 2016;387(10023):1109–1122

Wenink MH, Santegoets KCM, Broen JCA, et al. TLR2 Promotes Th2/Th17 Responses via TLR4 and TLR7/8 by Abrogating the Type I IFN Amplification Loop. J Immunol 2009;183(11):6960–6970

Werfel T, Allam J-P, Biedermann T, et al. Cellular and Molecular Immunologic Mechanisms in Patients with Atopic Dermatitis. J Allergy Clin Immun 2016;138(2):336–349

West HC and Bennett CL. Redefining the Role of Langerhans Cells As Immune Regulators within the Skin. Front Immunol 2018;8:1941

Wu J, Ma C, Wang H, et al. A MyD88-JAK1-STAT1 Complex Directly Induces SOCS-1 Expression in Macrophages Infected with Group A Streptococcus. Cell Mol Immunol 2015;12(3):373–383

Yin X, Chen S and Eisenbarth SC. Dendritic Cell Regulation of T Helper Cells. Annu Rev Immunol 2021;39(1):759–790

Yoshida K, Kubo A, Fujita H, et al. Distinct Behavior of Human Langerhans Cells and Inflammatory Dendritic Epidermal Cells at Tight Junctions in Patients with Atopic Dermatitis. J Allergy Clin Immun 2014;134(4):856–864

Yoshimura A, Naka T and Kubo M. SOCS Proteins, Cytokine Signalling and Immune Regulation. Nat Rev Immunol 2007;7(6):454–465

Yu Y, Zhang Y, Zhang J, et al. Impaired Toll-like Receptor 2-Mediated Th1 and Th17/22 Cytokines Secretion in Human Peripheral Blood Mononuclear Cells from Patients with Atopic Dermatitis. J Transl Med 2015;13(1):384

Zhang J, Li H, Yu J-P, et al. Role of SOCS1 in Tumor Progression and Therapeutic Application. Int J Cancer 2012;130(9):1971–1980

Zheng Y, Manzotti CN, Liu M, et al. CD86 and CD80 Differentially Modulate the Suppressive Function of Human Regulatory T Cells1. The Journal of Immunology 2004;172(5):2778–2784

Zhou H, Yu M, Fukuda K, et al. IRAK-M Mediates Toll-like Receptor/IL-1R-Induced NFκB Activation and Cytokine Production. Embo J 2013;32(4):583–596

Zhou LJ, Schwarting R, Smith HM, et al. A Novel Cell-Surface Molecule Expressed by Human Interdigitating Reticulum Cells, Langerhans Cells, and Activated Lymphocytes Is a New Member of the Ig Superfamily. Journal of Immunology (Baltimore, Md: 1950) 1992;149(2):735–742.

9. Acknowledgements

As I complete this PhD dissertation, I am reminded of the many individuals who have contributed to this achievement and to whom I owe my deepest gratitude.

I would like to start by thanking my supervisor, Prof. Dr. Dr. Thomas Bieber, for his exceptional guidance, insightful feedback, and unwavering support throughout my doctoral studies. His dedication to my success has been a source of inspiration. Additionally, his financial support and provision of resources were crucial in enabling this research.

I extend my heartfelt thanks to my group leader, Dr. Nadine Herrmann, for her practical guidance and daily supervision of my research work. Her hands-on approach, constructive critiques, and constant encouragement were vital in ensuring the progress and quality of my research.

I am also grateful to my dissertation committee members, Prof. Dr. Irmgard Förster, Prof. Dr. Natalio Garbi, and Prof. Dr. med. Jörg Wenzel for their valuable input and constructive critiques. Their diverse perspectives enriched my research and helped shape this dissertation.

I wish to acknowledge my colleagues and peers in the AG-Bierber at Department of Dermatology and Allergy, University Hospital Bonn/ Christine Kühne-Center for Allergy Research and Education (Davos), Switzerland. In particular, I would like to thank Dr. Jörg Weßendorf, Sylvia Schnautz, Said Benfadal and Wenming Peng for their camaraderie, collaboration, and the stimulating discussions that have been so beneficial to my work.

I gratefully acknowledge the financial support provided by China Scholarship Council (CSC), and , which made this research possible.

On a personal level, I am deeply grateful to my family. My parents, Wenhong Deng and Ying Li, have always provided me with unconditional support and encouragement. I also wish to thank my friends for their encouragement and understanding, particularly Lin Peng, and Yi Li who have been there for me through thick and thin.

Lastly, I also want to express my gratitude to myself. The perseverance, dedication, and hard work that I put into this journey were essential to its completion. This achievement is a testament to my commitment and resilience.

Thank you all for your unwavering support and belief in my potential.

10. Academic publications

Deng Y, Leib N, Schnautz S, et al. Langerhans cell modulation in atopic dermatitis is TLR2/SOCS1-dependent and JAK inhibitor-sensitive. Allergy 2025;80(9): 2586-2599 https://doi.org/10.1111/all.16641

Philipp M-S, Nümm TJ, Deng Y, et al. Evidence for a Restoration of TLR2 Response in Epidermal Dendritic Cells in Atopic Dermatitis by Topical Anti-Inflammatory Therapy. Allergy 2024;79(1):249–252 https://doi.org/10.1111/all.15899